Dynamic Effect of Thermal Bridges on the Energy Performance of Residential Buildings

Fuad Baba

A Thesis in

The Department of

Building, Civil, and Environmental Engineering

Presented in Partial Fulfillment of the Requirements

For the Degree of Master of Applied Science (Building Engineering) at

Concordia University

Montréal, Québec, Canada

October 2015

CONCORDIA UNIVERSITY

SCHOOL OF GRADUATE STUDIES

This is to certify that the thesis prepared

By: Fuad Baba

Entitled: "Dynamic Effect of Thermal Bridges on the Energy Performance of Residential Buildings"

and submitted in partial fulfillment of the requirements for the degree of

Master of Applied Science (Building Engineering)

Complies with the regulations of this University and meets the accepted standards with respect to originality and quality.

Signed by the final examining committee:

_____ Chair

Dr. Z. Chen

_____ Examiner, External

Dr. M. Y. Chen, MIE

_____ Examiner

Dr. L. Wang

_____ Examiner

Dr. Z. Chen

_____ Supervisor

Dr. H. Ge

Approved by: _____

Chair of Department or Graduate Program Director

October 2015

_____

Dean of Faculty

ABSTRACT

Dynamic Effect of Thermal Bridges on the Energy Performance of Residential Buildings

Fuad Baba

The existence of thermal bridges in building envelopes affects the energy performance of buildings, their durability and occupants' thermal comfort. Typically the effect of thermal bridges on the energy performance is taken into account by implementing an equivalent U-value in 1D whole building energy simulation program. This treatment accounts for the effect of thermal bridges on the overall thermal resistance, while their thermal inertia effect is ignored.

This thesis investigates the dynamic effect of thermal bridges on the energy performance of residential buildings, surface temperatures and condensation risk through simulations. Three case studies, with different construction types, insulation levels and under different climatic zones, are used for the investigation. Simulation results show that the equivalent wall method and equivalent U-value method may considerably underestimate the heating load for cold climate and the cooling loads for the hot climate comparing with 3D dynamic modelling method, however, the equivalent wall method performs better than the equivalent U-value method.. With improving building envelope details, such as increasing of insulation level or implementation of thermal break in balcony slab, or with reduction of buildings' thermal mass, i.e. by using the wood construction instead of concrete construction, the significance of 3D dynamic method decreases. The milder of the climate, the greater the 3D dynamic effect is. In addition the 3D dynamic simulation increase the surface temperatures of junction comparing with that modelled using 3D steady state simulation, and then the condensation risk is lower.

Keywords: Thermal bridges, building envelope, whole building energy simulations, equivalent wall method, dynamic effect of thermal bridges; condensation risk

ACKNOWLEDGEMENTS

It is with sincere gratitude that I thank my supervision Dr. Hua Ge for positively believing in my work and her considerations during my research. It would not be possible for me to accomplish my research goals without her academic support.

I want to thank my father Dr. Mutasim Baba, who introduced me to profession of Building Engineering and helped me being innovative in this path. Finally, I dedicate this thesis to my mother, my wife, my son, and my brother and sisters that without whom nothing would be possible.

Table of Contents

Table of Figures

Table of Tables

Nomenclature

$\varphi_{ii}, \varphi_{ie}, \varphi_{ee}$	Structure factors of equivalent wall (-)
C_t	Thermal capacity of wall (KJ/K)
C	Total thermal capacity per unit area for the elements with thermal bridges. ($kJ/m^2 \cdot K$)
C_m	Thermal capacity of the m-th layer ($kJ/m^2 \cdot K$)
c_p	Specific heat capacity ($kJ/kg \cdot K$)
dTB	2D thermal bridge effect distance (mm)
dV	Differential volume of region (m^3)
e	Equivalent wall layer thickness (m)
E	Total energy stored in thermal bridge (kJ)
E_u, E_l	Energy stored in the upper and lower region of the thermal bridge (kJ)
T	Amplitude temperature (^oC)
F_l, F_u	Lower and upper heat flow fraction through thermal bridge
H_f	Vertical distance from the adiabatic plane to the façade wall (mm)
H_s	Vertical distance from the base of the thermal bridge to the adiabatic plane (mm)
k	Thermal conductivity (W/m K)
q_{in}, q_{out}	Heat flux that across the inside and outside boundary (W/m^2)
Q_l, Q_u	Heat flow across lower and upper slab surface (W)

R	Total thermal resistance ($m^2 \cdot K/W$)
R_i, R_o	Surface film resistance ($m^2 \cdot K/W$)
R_{i-m}, R_{m-e}	Thermal resistance between the internal surface and the m-th layer; and thermal resistance between the m-th layer and the external surface (m^2 K/W)
R_m	Thermal resistance of the m-th layer ($m^2 \cdot K/W$)
S_i , S_o	Interior and exterior boundaries of thermal bridges
t	Time (hr)
T_i, T_o	Inside and outside temperature (^oC)
U	Overall thermal transmittance ($W/m^2 \cdot K$)
θ	Dimensionless temperature through the thermal bridge (-)
ρ	Density (kg/m^3)

1 INTRODUCTION

1.1 BACKGROUND

The world tends to minimize the energy consumption of buildings and maximize its durability, occupants' comfort and indoor air quality. Building energy use including residential and commercial, consumes 17% to 32% of Canada energy consumption (NRCan, 2008). Building envelops' design, thermal insulation properties and location, and optimum thermal mass design are major factors to improve the energy performance of buildings.

Thermal bridges created by the discontinuity of thermal insulations as parts of the building envelope have a major effect on the thermal performance, e.g. increased heat loss in the winter and heat gain in the summer; reduced interior surface temperature, thus, increased risk of condensation and mold growth in the wintertime. Studies have shown that in some buildings up to 50% of the elevation area consists of three-dimensional envelope structural details (Kosny and Desjarlais, 1994) and up to 30% of heating energy can be lost through thermal bridges for well-insulated residential buildings adopting high performance windows and highly insulated walls and roofs (Theodosiou and Papadopoulous ,2008 and Erhorn et al., 2010). Therefore, it is critical to properly address thermal bridges in building envelope to achieve high performing low-energy buildings.

There are two typical categories of thermal bridges in the building envelope assemblies, one is the thermal bridges created by the repetitive structural members within the building envelope such as studs and joists, and the other is junctions such as connection between external walls and roofs, foundations, and floors, balconies, etc. The impact of thermal bridges is typically taken into account in the energy performance regulation by imposing a limit on the linear or point thermal transmittances (ψ) of thermal bridges within the building envelope in European countries, such as EN ISO 14683 (EN ISO 14683, 2007), or by mandating a maximum effective thermal transmittance (U-value) in North America, such as the National Energy Code of Buildings in Canada (NEBC, 2011) or ASHRAE 90.1 (ASHRAE 90.1, 2013). The linear or point or the effective thermal transmittances are calculated under steady-state conditions. The

dynamic effect of 2D junctions can also be accounted for by calculating a linear thermal transmittance under periodic conditions as suggested by EN ISO 13786 (EN ISO 13786, 2007), however, this method is not commonly used in North America and not included in this study.

The effect of thermal bridges on the energy performance of buildings is typically evaluated through whole building energy modeling using the equivalent U-value method. The equivalent U-value method is to adjust the insulation level of the one-dimensional multi-layered envelope component such that its thermal transmittance is equal to the effective overall U-value of the envelope detail with thermal bridges, while the material properties of the multi-layered component are kept unchanged. Therefore, the effect of thermal bridges on the overall thermal resistance is taken into account, while the thermal inertia effect of the thermal bridges is ignored. The presence of thermal bridges not only reduces the overall thermal resistance but also changes the dynamic characteristics of the opaque walls (Mao and Johannesson, 1997). A study by Mao and Johannesson (Mao and Johannesson, 1997) using frequency response method indicated that depending on the structures, the presence of thermal bridges such as metal steel studs and heavy weight wall-floor junction modified the amplitude and phase lag of admittance and transmittance. Therefore, the application of equivalent U-value method in energy modeling may lead to errors in energy performance evaluation. An improvement on the equivalent U-value method is the Combined Thermal Properties (CTP) method introduced by Purdy and Beausoleil Morrison (Purdy and Beausoleil, 2001). The CTP method involves adjusting the thermal conductivity of the composite layer (insulation with frame) to match the total thermal resistance of the structure with thermal bridges. The density and specific heat of this composite layer is also adjusted to match the thermal mass of the frame and insulation to account for the thermal mass effect although it may not represent the actual dynamic thermal behaviour. This method is only applicable to thermal bridges created by repetitive structural members within the building envelope assemblies.

To account for the dynamic effect of thermal bridges in energy modeling, the equivalent wall method was developed by Kossecka and Kosny (Kossecka and Kosny, 1997 and 1998) and used to generate conduction transfer functions for 20 common wall assemblies with connection details, which are included in EnergyPlus (Kossecka and Kosny, 2001). The equivalent wall method is to represent the thermal bridges by a 1-D multi-layered structure, which has the same

dynamic thermal characteristics as the complex wall systems with thermal bridges; therefore, the thermal inertia effect can also be taken into account. The equivalent wall method was modified by Aguilar et al. (Aguilar et al., 2013) for 2D junctions and their study showed that the equivalent wall method can accurately represent the dynamic effect of 2D junctions with high thermal mass on the transient heat flow. Martin et al. (Martin et. Al, 2011 and 2012) developed a methodology to generate 1-D equivalent walls and compared the transient heat flow with 2D modeling for a number of thermal bridge geometries. Mahattanataw et al. (Mahattanataw et al., 2006) compared the effect of using different methods to implement steel-stud and wood-frame in walls on the energy performance of a two-storey house using EnergyPlus. The equivalent wall method was used as the reference and they found that the Combined Thermal Properties (CTP) method achieved similar results as the equivalent wall method for cooling loads.

The direct 2-D or 3-D modeling of thermal bridges in whole building energy simulation programs requires greater computing capacity and increases the complexity. Gao et al. (Gao et al., 2008) attempted to develop a low-order three-dimensional heat transfer model using state model reduction techniques. The accuracy of the model was verified with frequency response and time-domain outputs. Some software tools have the capability to simulate two and three-dimensional conduction such as WUFI Plus, ESP-r programs, however, there are very limited studies reporting the effect of direct 2D or 3D modeling of thermal bridges on the energy performance of whole buildings. Déqué et al. (Déqué et al., 2001) used a two-stage approach to firstly model two types of 2D thermal bridge geometries using the state space technique and then the reduced dynamic wall models were implemented in an energy modeling program.

Despite the significant impact of thermal bridges on building energy consumption, the Canadian building codes do not have elaborate requirements of thermal bridges. The 2011 National Energy Code of Canada for Buildings (NEBC, 2011) requires that the thermal bridging effect of repetitive structural members such as studs and joists, and of ancillary members such as lintels, sills and plates, to be accounted for in the calculation of effective thermal resistance of assemblies. However, minor penetration or minor structural members, and major structural penetrations, such as balconies, with a cross-sectional area less than 2% of the penetrated wall area need not be taken into account in the calculation of the effective thermal

resistance of the penetrated wall area. A study by Ge et al. (Ge et al., 2013) showed that for a typical high-rise Multi-unit residential building, a balcony cross-section area representing 4% of the total exterior wall may contribute up to 11% of the space heating energy consumption depending on the thermal performance of windows and the opaque walls. A recent study on thermal bridges of typical constructions in the region of British Columbia showed that improved building envelope details minimizing thermal bridges can result in up to 10% energy savings, which is comparable to increasing insulation levels and using triple-glazing windows (BC Hydro Power Smart, 2014). In these studies, the equivalent U-value method was used to implement thermal bridges in whole building energy simulation programs. As discussed earlier, the presence of thermal bridges not only degrades the effectiveness of thermal insulations but also changes the dynamic thermal characteristics of the envelope; therefore, the application of equivalent U-value method in energy modeling may lead to errors in energy performance evaluation.

1.1 RESEARCH OBJECTIVES

The objective of this research is to investigate the dynamic effect of thermal bridges on the energy performance of residential buildings, surface temperature and hence the condensation risk. Three methods, namely equivalent U-value method, equivalent wall method, and direct 3D modeling method, are implemented in WUFI Plus, a whole building Heat, Air and Moisture (HAM) modeling program. The results obtained from direct 3D thermal bridge modeling using WUFI Plus are used as the reference for comparison.

1.2 OUTLINE OF THE THESIS

This thesis includes five chapters as follows:

- Chapter 1 describes the importance of the effect thermal bridges on buildings and its occupants as well as brief explanation of the dynamic effect of thermal ridges. Also, the objectives of the research are described.
- Chapter 2 contains greater details of previous literature regarding the impact of thermal bridges, building standards and codes, dynamic effect and thermal bridge modeling methods.

- Chapter 3 explains the methodology employed the different case studies and the methods which were performed to implement the thermal bridge in a whole energy building program.
- Chapter 4 summarizes and discusses the results from simulations.
- Chapter 5 contains the conclusion of this study with some recommendation and contribution.

2 LITERATURE REVIEW

2.1 INTRODUCTION

A literature survey was conducted to incorporate the existing studies that have performed a similar analysis or developed methods to assist in describing the importance and the dynamic effect of thermal bridges as well as to find out how the building codes and standards deal with thermal bridges. In addition, this chapter includes a detailed explanation of the methods used to represent the thermal bridges in whole building energy simulation programs.

2.2 IMPORTANCE OF STUDYING THERMAL BRIDGES

It is necessary to know the effect of thermal bridges on energy performance of buildings and on building envelopes. Thermal bridges, and the subsequent damage, can be avoided by several strategies starting from proper evaluation of thermal bridges effects on building performance during the design phase to optimal implementation of solutions during construction phase. Therefore, this section studies the effect of thermal bridges on building, occupants and global environment.

2.2.1 Waste of energy

The importance of the thermal bridges strongly rises today particularly in low energy constructions such as passive houses. Many researchers have investigated the effect of different thermal bridges on the heat transmittance of building components and then on the building energy performance.

Building standards and codes impose strict requirements on the thermal transmittance values of the building envelope components. Many designers are working to meet these requirements through the improvement and increasing the thickness of the insulation in 1-D analysis and are neglecting the effect of thermal bridges in building envelope. Discontinuity of thermal insulation can be considered the major reason to create thermal bridges. Previous studies have shown that thermal bridges have a significant impact on the thermal transmittance value of the

building envelope components that may make it unable to meet the required specifications. Cappelletti found that the position of window insulation cavity could reduce the thermal bridge effect on the linear thermal transmittance of window by 70–75% (Cappelletti, Gasparella, Romagnoni, and Baggio, 2011). The mortars that cut the insulation wall increase transmission loads by 62% -103% depending on the thickness of the mortar (Al-Sanea, and Zedan, 2012). Ignoring metal profiles in external wall can lead to an overestimate of the thermal resistance by up to 50 % (Gorgolewski, 2007). To achieve the continuity of thermal insulation through the balcony slabs, the thermal break was created. This thermal break can reduce the overall U-value of the balcony 72–85% according to Ge et al. (Ge et al., 2013).

The thermal bridges not only affect the thermal transmittance values for all components of the building envelope, but also affect the overall energy performance of the building and comfort of the occupants. Gomes and et al. investigated the impact of steel framing in the wall on the thermal load and annual energy consumption of building. They concluded that the implementation of steel studs increase the peak thermal load and annual energy consumption by 10% and 5%, respectively (Gomes, Souza, Tribess, 2013). Moreover, Ge, et al. found that including thermal break in the balcony slab reduces the annual space heating consumption by 5–11% using U-value method (Ge et al., 2013).

2.2.2 Risk of frost damage and mold formation and condensation

Thermal bridges not only increase the heat loss of building components, but also decrease surface temperatures. With the drop of surface temperature below the dew-point of ambient air, the risk of mould formation increases. Sedlbauer, et al (2007) described the boundary conditions for mold growth. They stated that there are four important factors including temperature, humidity, time and substrate that affect the probability of mold growth. These factors indicate that the thermal bridges remarkably affect this issue (Sedlbauer et al., 2007).

In winter-season, thermal bridges create the local warm spots on the exterior surface of the building that lead to wall wetting by melting of wind-driven snow and then freezing damage, unexpected expansion or contraction, and possible health and safety issues (Brown, Wilson. 1963). Thermal bridges cause 40% of the wall damages and aesthetic problems (Corvacho, 1996).

Figure 2.1 Mould formation caused by thermal bridges

(Reprinted from indoor climate experts. 2014, Retrieved from June. 1, 2015, from http://www.indoorclimateexperts.com Copyright © 2014)

2.2.3 Ice dam formation

The ice dam forms by refreezing melt-water at the building roof and along the eaves. These ice dams increase the likelihood of leaking melt-water under and through the roofing, especially shingles and decking of roof. In addition, large ice dams along the eaves may cause damage or injury to people if they fall down. Ice dams occur when part of a roof becomes warm enough to melt snow. Therefore, the major cause of creating ice dams is the variation in temperature on the surface of roof. According to Straube, one of the main reasons is the thermal bridges (Straube, 2006). As shown in Figure 2.2, the discontinuity of insulation through wall/ roof junction leaks significant amounts of heat to the bottom of the sheathing, which increases the roof-snow temperature until the melting point (Straube, 2006).

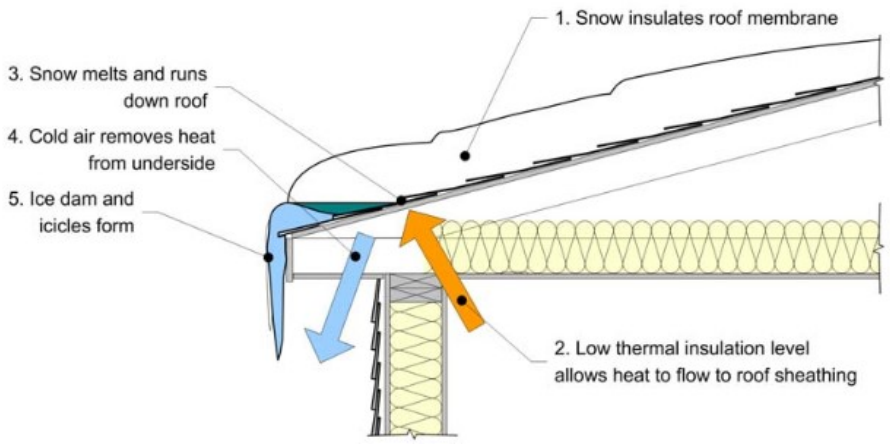

Figure 2.2 The process of ice dam formation caused by poor insulation (Straube, 2006)

To solve this problem, Straube describes two solutions: the first is to eliminate the thermal bridge through improving and keeping the continuity of insulation; and the other is to maintain the sheathing cool through natural ventilation in the roof system (Straube, 2006).

2.2.4 Health hazards

Mould which is formed around thermal bridges releases spores into rooms. Those spores can cause a variety of health problems; from minor allergic reactions like irritated eyes, nose, and throat to severe asthma symptoms. That is because mould spores are allergens and can cause sinusitis, rhinitis and asthma. As indoor exposure is usually prolonged, there is a risk that these allergic reactions develop into chronic conditions. It is estimated that 10% of the population in the U.S. is allergic to house dust and 70% of these people are specifically allergic to mite allergen (Bates et al. 1993). Moreover, Thermal bridges increase the carbon dioxide emissions around 27% on an annual basis. Thus, thermal bridges affect negatively the global environment (Theodosiou and Papadopoulos, 2008).

2.3 BUILDING STANDARDS AND CODES

Since 1995, the European standards had been developed for dealing with thermal bridge effects such as EN ISO 10211-1(EN ISO 10211-1, 1995) that deals with the aspects of thermal performance of building constructions. After that, the EN ISO 10211:2007 (EN ISO 10211,

2007); "Thermal bridges in building construction heat flows and surface temperatures detailed calculations" was improved to show further development of the standardization. For that, EN ISO 10211:2007 (EN ISO 10211, 2007) was used as a reference by most of building codes for energy performance in the European member states for linear thermal transmittance of thermal bridge calculations. EN ISO 10211:2007 (EN ISO 10211, 2007) illustrated the methodology of modelling thermal bridges and the validation test cases. The modelling rules start from defining the distance of thermal bridging, which is called cut off plane. In general, this distance from a thermal bridge is 1 meter. The other rule that is necessary to analyze the thermal bridges is the selection of the thermal conductivity of the building materials according to standard EN ISO 10456 (EN ISO 10456, 2007) or national conventions, but the air layers can be chosen according to different standards (EN 673 (EN 673, 1997), EN ISO 6946 (EN ISO 6946, 2007) and EN ISO 10077 (EN ISO 10077, 2012)). In addition, EN ISO 10211(EN ISO 10211, 2007) provides the calculation for:

1. The minimum (lowest) surface temperatures in order to assess the risk of surface condensation,
2. The heat flows in order to predict overall heat loss from a building (for the constant, steady state flow case; i.e. time independent temperature distribution) and
3. Linear and point thermal transmittance and surface temperature coefficients (of thermal bridges).

Also, EN ISO 10211 (EN ISO 10211, 2007) provides the possibility to validate the different programs by four different test cases under steady state. Antretter et al. (Antretter et al., 2013) used those cases to validate the steady state 3D of WUFI Plus program.

Further standard that deals with this subject is EN ISO 14683 (EN ISO 14683, 2007) "Thermal bridges in building construction - Linear thermal transmittance - Simplified methods and default values". This standard concerns the thermal bridges with two separate environments only, such as wall/floor junction. It gives the default linear thermal transmittance values of 2D geometric model of thermal bridges under steady state condition.

In Canada, the National Energy Code of Canada for Buildings (NECB, 2011) requires the continuity of insulation to reduce thermal bridges and it provides solutions to keep the

continuity of insulation through beams, balcony slabs, and ground floors, but without any heat flow or temperature distribution calculations. Also, it requires taking into account the effect of repetitive structural members only such as stud and joists on effective thermal resistance of assemblies. However, it is neglecting the minor penetration or minor structural members, and major structural penetrations, such as balconies with a cross-sectional area less than 2% of the penetrated wall.

ANSI/ASHRAE/IES Standard 90.1 (ASHRAE Standard 90.1, 2013) incorporates the concept of thermal bridging by introducing the concept of continuous insulation. Its definition of continuous insulation (CI) states: "Insulation that is continuous across all structural members without thermal bridges other than fasteners and service openings. It is installed on the interior or exterior or is integral to any opaque surface of the building envelope (enclosure)." Also, ASHRAE 90.1 provides the maximum of the U-values for different building envelope components with metal studs and wood frame only.

ASHRAE 1365 RP (ASHRAE 1365 RP, 2011) "Thermal Performance of Building Envelope Details for Mid- and High-Rise Buildings" analyzed the thermal transmittance data for high- and mid- rise common building envelope details construction by creating a catalogue that contains significant information regarding thermal bridges for designers. This catalogue contains the 40 common building assemblies with thermal bridges in North American with focus on 3D thermal bridges details. Siemens PLM, FEMAP and NX heat transfer programs, hot box test measurements and ISO standards were used to calculate the heat transfer for building assemblies.

2.4 DYNAMIC EFFECT OF THERMAL BRIDGES

In the past a few decades, with the increased requirements for building energy efficiency, it became necessary to study the whole building with all assemblies under dynamic conditions that represent the reality. For that, the energy simulation programs have been created to design, develop and estimate the energy consumption of buildings during the design period. Most of these programs simulate the whole building through 1D heat flow which may lead to neglect three-dimensional envelope structural details that represent up to 50% from the total elevation

area of building (Kosny and Desjarlais, 1994). This ratio contains the two- and three-dimensional building envelope details as the thermal bridges, which makes it necessary to account a multi-dimensional heat flow in the whole building simulation. There are typically two main approaches to implement the effect of 2D and 3D thermal bridges in whole building energy simulation programs which are illustrated and described in more details in section 2.5. The first approach is to create a model in 1D heat flow, which has the same effect of 2D or 3D heat flow in energy performance program. The second one is to develop the energy simulation programs with the capability to model dynamic 2D and 3D heat transfer.

The first approach includes simplified and complex methods that are used to implement the thermal bridges in the 1D energy performance programs. One of the commonly used simple methods is the equivalent U- value method that represents the steady state method. Most of the studies have used this method to represent thermal bridges in 1D whole building energy modeling programs because it only needs 2D steady state heat transfer program to obtain an equivalent U-value for the thermal bridges. From such studies, the French project (Lahmidi and Leguillon, 2010) that analyzed the impact of corrective techniques such as thermal rupture and thermal break on nine different types of thermal bridges in a new single-family home with concrete construction. This French study (Lahmidi and Leguillon, 2010) showed that the improvement of joints can lead to major energy savings of more than 18 kWh/m^{2}a, and this is more than 15% of the primary energy for heating. In the "Influence of thermal bridge details on the energy performance of houses with different energy quality" study (Šubrt, 2007), the impact of thermal bridges on a residential building with brick construction were analysed using equivalent U-value method. They concluded that the impact of the thermal bridges on the energy demand is 7 % higher than the energy demand without thermal bridges at low thermal building quality case, while the effect of thermal bridges on the energy demand increased by 28% with improved quality (Šubrt, 2007).

Trying to represent the dynamic effect of thermal bridge in 1D, the equivalent U-value method has been modified to consider the thermal mass effect by calculating the equivalent density and specific heat. This method was called Combine Thermal Properties (CTP). Gomes et al. (Gomes et al., 2013) used the CTP method to implement partially the dynamic effect of steel framing in EnergyPlus program with two scenarios. In the first scenario, the goal was to

investigate the effect of steel framing on the peak thermal loads of a small two-story commercial building. In the second scenario, the objective was to study the effects of steel framing on the annual energy consumption of a ten-story building. The results showed that the inclusion of steel framing has led to an increase in peak thermal load by about 10% in the first scenario and an increase of the annual energy use by 5% in the second scenario (Gomes et al., 2013).

The equivalent wall method was developed to represent the 3D dynamic effect in 1D as shown in section 2.5.5. Mahattanataw et al. (2006) used the equivalent wall method as the reference to compare the effects of using different methods to implement steel-studs and wood-frames in external walls on the energy performance of a two-storey house using EnergyPlus. They found that the Combined Thermal Properties (CTP) method produced similar results as the equivalent wall method for cooling loads with a difference of 0.34% and 0.44% for wood frame and steel studs, respectively.

For the second approach to implement thermal bridges, two methods were used to develop the energy simulation programs. The first is creating 3D thermal bridges outside of the whole building energy modeling program and then implementing this characteristic in the whole building energy modeling program. This method is called state space method and it is discussed in more details in section 2.5.6. In 2001, Déqué et al. (Déqué et al., 2001) used the state space method to implement the T and L-shape thermal bridges in the Matisse apartment through a whole building energy modeling program Clim 2000. Sisley program was used to generate the meshing, state space model and model reduction for the two thermal bridges. The reduction models of thermal bridges, which have been done by Sisley program, were stored in a Unix Tree structure for simulation and then were created in Clim 2000 to calculate the energy demand. They found the 2D model from T-and L-shape using state space method increased the annual energy consumption by 5-7% comparing with the simplified model results that was created from the statutory tabulated values in the K77:1977 standard “Rules for calculating the useful thermal characteristics of building walls" CSTB. The second method is directly incorporating the thermal bridges as 2D and 3D objects in the whole building energy modeling program, such as WUFI Plus.

2.5 THERMAL BRIDGE MODELING METHODS

Energy simulation programs are increasingly used for analysis of energy performance of buildings and thermal comfort of their occupants. Today, there are many building performance simulation programs with different user interfaces and different simulation engines that are capable of these analyses.

The majority of whole building energy simulation programs use one dimensional conduction and dynamic calculations to model heat transfers through various construction elements. For that, the steady state calculation is becoming obsolete and does not consider realistic conditions. As mentioned, 1D dynamic simulation programs are not enough to account for the effects of structural elements (thermal bridges). Several methods have been developed to implement the effect of thermal bridge in the energy simulation programs. These include a simplified method which disregards the effect of thermal bridge to methods that include the dynamic effect of thermal bridges. The following section provides an introduction of these methods.

2.5.1 Neglecting thermal bridges

This method depends on neglecting thermal bridges that are created by the repetitive structural members within the building envelope or that created by junctions. Figure 2.3 shows a typical wall in reality with wood frame and the wall that is implemented in whole building energy simulation programs. This disregard of thermal bridges results in large errors in energy performance calculation (Al-Sanea and Zedan, 2012).

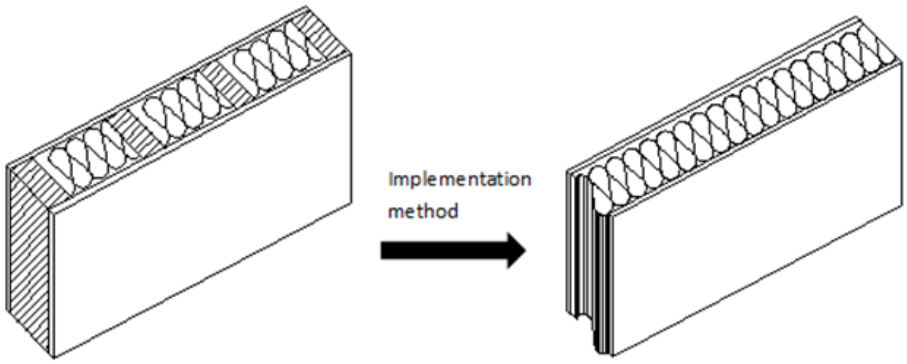

a) b)

Figure 2.3 Neglecting thermal bridge: a) typical wall with studs; b) wall as implemented in energy programs

2.5.2 Implementation of two surfaces with two materials

This method can be used for thermal bridges that are created by the repetitive structural members only. Two surfaces will be modeled to represent the typical wall as shown in Figure 2.4. The first surface represents a center of the wall without studs. The second surface represents the total area of studs in the wall. This method is still complex to use if we have a complex model due to the doubling of the input surface numbers. Also, this method cannot be used for other thermal bridges such as junctions.

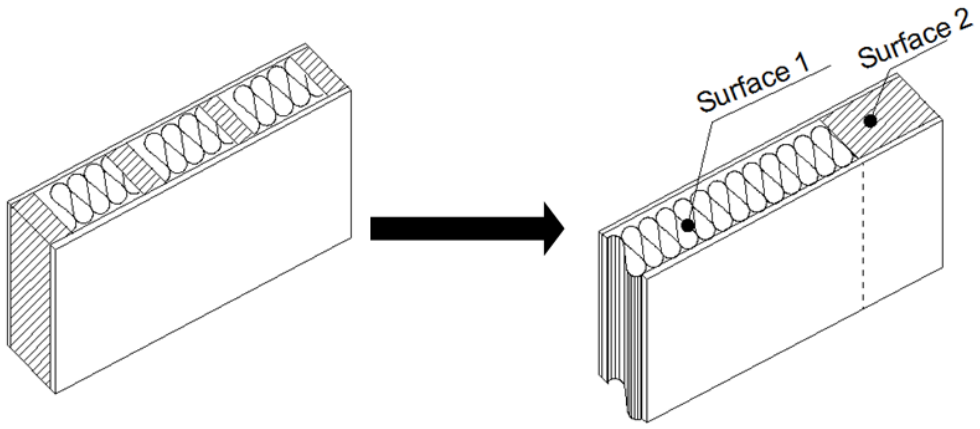

a) b)

Surface1 is an insulation part, surface2 is a stud part

Figure 2.4 With and without stud method: a) typical wall with studs; b) wall as implemented in energy programs with two sub-surfaces

2.5.3 Equivalent U-value method

A two-dimensional conduction heat-transfer analysis program is needed to calculate the effective U-value for thermal bridges under steady state conditions. The sub-surfaces that have the same component layers as the 1-D building envelope component are added in whole building energy simulation programs to represent the junctions. In these sub-surfaces, the thickness of insulation is adjusted to represent the equivalent U-value of junctions that obtained from two-dimensional conduction heat-transfer analysis program, while the thickness of the other two layers and the physical properties of all three layers will be kept the same as in the 1-D multi-layer structure, as shown in Figure 2.5.

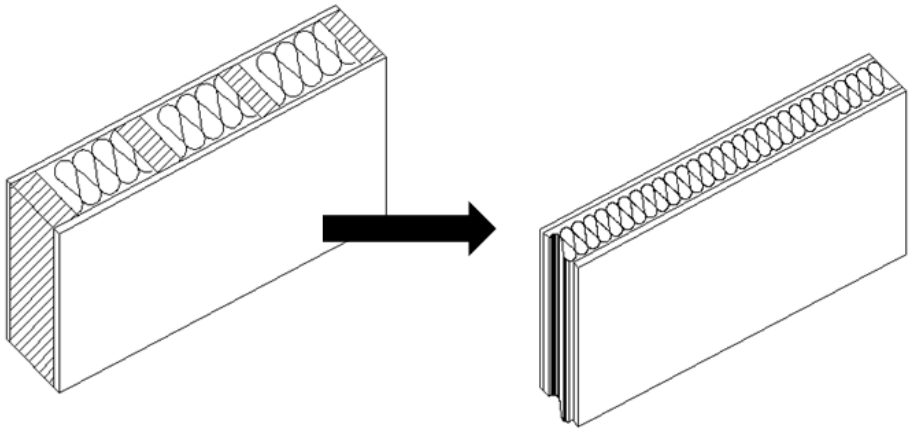

a) b)

Figure 2.5 Equivalent U-value: a) typical wall with studs; b) wall as is implemented in energy programs after insulation thickness was adjusted

2.5.4 Combined thermal properties (CTP)

Purdy and Beausoleil (Purdy and Beausoleil, 2001) introduced the combine thermal properties (CTP) method as a single-layer structure that has the same thermal properties of original wall as shown in Figure 2.6. In the 2013 publication, Gomes et.al (Gomes et.al, 2013) illustrated the mathematical sequence to adjust and to calculate the thermal conductivity, density and specific heat of a single-layer structure to achieve the thermal properties of the original wall.

- Adjustment of the thermal conductivity: A 2-D heat transfer program is required to calculate the overall heat transfer coefficient of the original wall and then adjust the thermal conductivity of the one-layer structure to match the U-value.
- Adjustments of a single-layer density (ρ_s) and specific heat (c_s) are done by the following equations [2.1 and 2.2]:

$$\rho_s = \sum_{i=1}^{n} C_i \, \rho_i$$ Equation [2.1]

$$\sum_{i=1}^{n} V_i \, \rho_i \, C_i \; = \sum_{i=1}^{n} V_s \; \rho_s C_s$$ Equation [2.2]

Where:

V_i is the volume of the material i in the original wall (m^3),

ρ_i is the density of the material i in the original wall (Kg/m^3),

Ci is the specific heat of the material i in the original wall (KJ/(kg K)),

V_s is the volume of a single-layer structure (m^3),

ρ_s is the density of a single-layer structure (Kg/m^3),

C_s is the specific heat of a single-layer structure (KJ/(kg K)).

The effects of thermal bridge on the thermal resistance and thermal mass of the wall are taken into account although it may not represent the actual real one because it neglects structure factors that are determined by thermal capacity, resistance and dimensionless temperature along its thickness. According to that, this method is not applicable to thermal bridges created by junctions between building envelope components.

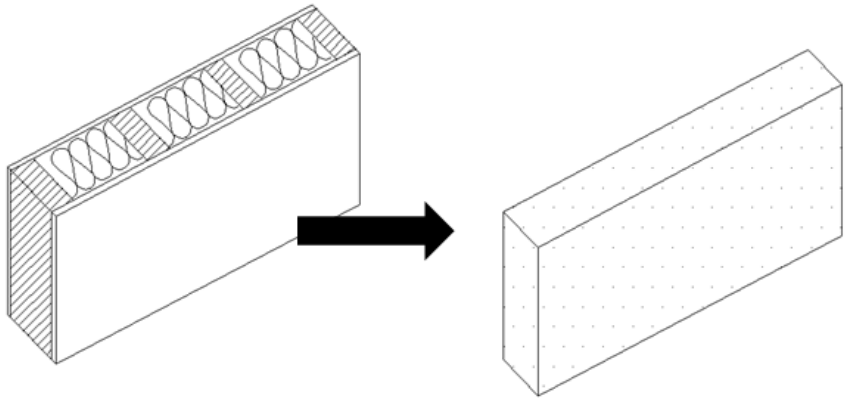

a) b)

Figure 2.6 Combine thermal properties (CTP) method: a) typical wall with studs; b) a single-layer structure as it is implemented in energy programs

2.5.5 Equivalent wall method

Kossecka and Kosny described the equivalent wall method in compilation of papers (1996; 1997; 2002) as a method to represent thermal bridges by a 1-D multi-layered structure. This structure has the same dynamic thermal characteristics as the complex wall systems with thermal bridges as shown in Figure 2.7 (Kossecka and Kosny, 1996).

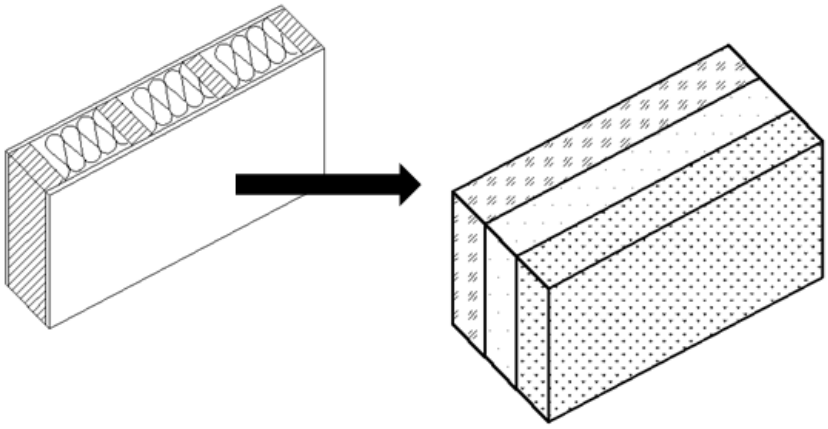

a) b)

Figure 2.7 Equivalent wall method: a) typical wall with studs; b) a multi-layered structure as it is implemented in energy programs

In the 1997 paper, they explained the mathematical methodology of equivalent wall method starting from the Fourier heat conduction equation to three terms called structure factors. Structure factors, the dimensionless quantities, represent the fraction of heat storage in the wall components volume. They are not determined by density and specific heat only, but also by temperature distribution through elements volume using the following equations.

$$\varphi_{ii} = \frac{1}{C_t} \int_V \rho \ c_p \ (1-\theta)^2 dV \qquad \text{Equation [2.3]}$$

$$\varphi_{ie} = \frac{1}{C_t} \int_V \rho \ c_p \ (1-\theta)\theta \ dV \qquad \text{Equation [2.4]}$$

$$\varphi_{ee} = \frac{1}{C_t} \int_V \rho \ \ c_p \, \theta^2 \, dV$$ Equation [2.5]

$$\varphi_{ii} + 2\varphi_{ie} + \varphi_{ee} = 1$$ Equation [2.6]

Where C_t is the total thermal capacity of the wall elements V (kJ/ K), and it can be calculated using the following equation:

$$C_t = \int_V \rho * c_p * dV$$ Equation [2.7]

Where,

ρ is the density of each element in the assembly(kg/m^3)

c_p is a specific heat capacity (J/kg·K)

θ is the reduced temperature, the dimensionless solution of the steady-state heat conduction equation for the ambient temperatures T_i=0 ^oC and T_e=1^oC. These values are obtained from 2D-heat transfer programs.

dV is a differential volume (m^3)

The structure factors, φ_{ii} and φ_{ie}, for a wall consisting of n plane homogenous multilayers numbered from 1 to n (with layer 1 at the interior surface), are given by (Kossecka and Kosny, 1997):

$$\varphi_{ii} + \varphi_{ie} = \frac{1}{RC} \sum_{m=1}^{n} C_m \left(\frac{R_m}{2} + R_{m-e} \right)$$ Equation [2.8]

$$\varphi_{ie} = \frac{1}{R^2 \, C} \sum_{m=1}^{n} C_m \left(-\frac{{R_m}^2}{3} + \frac{R_m R}{2} + R_{m-e} R_{i-m} \right)$$ Equation [2.9]

$$C = \sum_{m=1}^{n} C_m$$ Equation [2.10]

Where

R is the total thermal resistance of the wall ($m^2 \cdot K/W$) and C is total thermal capacity per unit area for the elements with thermal bridges ($kJ/m^2 \cdot K$).

$$R = \sum_{k=1}^{n} R_k$$ Equation [2.11]

R_m and C_m is the thermal resistance and heat capacity of the m^{th} layer, respectively;

$$R_{i-m} = R_i + \sum_{k=1}^{m-1} R_k$$ Equation [2.12]

$$R_{m-e} = \sum_{k=m+1}^{n} R_k + R_e$$ Equation [2.13]

In the 1996, 1997 and 1998 publications, the Kosny and Kossecka illustrated the mathematical relationship between structure factors and response factors. This relation confirms the effect of structure factors on the dynamic characteristics of a wall (Kossecka and Kosny, 1996, 1997 and 1998). In the 2002, Kosny and Kossecka (Kossecka and Kosny, 2002) tested the validation of equivalent wall method through the comparison between the heat flows that resulted from 1D multi-layer equivalent wall and practical results using a hot-box test. The comparison results indicated that a good agreement with a little deviation was found between equivalent wall method and hot-box test results (Kossecka and Kosny, 2002).

The procedure developed by Kossecka and Kosny (Kossecka and Kosny, 1996 and 1997) can be easily used to generate equivalent walls for thermal bridges created by repetitive structural elements such as studs. Modification is required to generate equivalent walls for 2D or 3D junctions such as wall/slab or wall/ground floor junctions. Aguilar et al. (Aguilar et al., 2013), developed a modified equivalent wall procedure and the validity of this method was verified by comparing the heat flux through these 2D junctions with direct transient 2D heat transfer modeling. This procedure involves identifying the adiabatic plane of the 2D thermal bridge geometries and determining thermal properties of equivalent walls to represent the dynamic

characteristics of the 2D junctions. The adiabatic plane is defined as a plane that divides the intersecting mass of the thermal bridge proportionally to its influence over the two spaces surrounding the enclosure, which can be determined based on heat flow distribution obtained from the 2D steady-state heat transfer analysis. One-dimensional heat conduction can be assumed for regions above the cut-off plane. Cut-off plane is the plane dividing the 2D and 1D region, since these regions are not affected by the 2D effect of thermal bridges. In this thesis, the procedure outlined above is followed to generate the thermal properties of the equivalent walls to represent the 2D thermal bridge junctions that are described in more detail in section 3.1.5.

2.5.6 State space method

Some programs, such as EnergyPlus and BLAST program, use the Conduction Transfer Function (CTF) solution method to model the one-dimensional transient conduction through all building elements instead of finite difference, finite element or finite volume methods. There are two methods to calculate the CTF coefficients in the CTF method. The first one is called Older Laplace Transform method and second one is called the State Space method. In a completion publication, Ceylan and Myers (1980), Seem (1987), and Ouyang and Haghighat (1991) illustrated the mathematical sequence to calculate the CTF coefficients using the State Space method. The following linear matrix equations define the basic state space system:

$$\begin{cases} [\dot{X}] = [A][X] + [B][U] \\ [Y] = [C][X] + [D][U] \end{cases} \qquad \text{Equation [2.14]}$$

Where:

$\dot{X}$ is a derivative array of X.

X is a vector of state variables.

The matrix U contains the values of the system inputs.

Y is the system output.

A, B, C and D are arrays that are coefficient matrices

These matrices in equation [2.14] can be used to calculate the transient heat conduction equation. In this case the equations become:

$$\frac{d[T]}{dt} = [A][T] + B[U] \qquad \text{Equation [2.15]}$$

$$[q] = [C][T] + [D][U] \qquad \text{Equation [2.16]}$$

Where:

T is a temperature at mesh nodes.

A, B, C and D are arrays that characterize of building configurations, such as thermal conductivity, specific heat and density

U is the outside air temperature and inside air temperature.

q is the heat flux through the configuration.

According to the engineering reference document (EnergyPlus, 2013), the EnergyPlus uses the state space method to solve the CTF coefficients instead the Laplace transform method for two obvious advantages. These advantages are the short time steps to calculate the CTF coefficients and the capability to obtain 2D and 3D conduction transfer functions.

EnergyPlus Articles from the Building Energy Simulation User New (EnergyPlus, 2003) described the mathematical calculation to introduce thermal bridge in the state space method of EnergyPlus program. Figure 2.8 shows the methodology for implementing thermal bridges in the EnergyPlus program using state space method. The first step in this method is to use another specific program, such as Sisley program, to model each thermal bridge configuration using finite difference, finite element, or finite volume method, and to create a regression process to generate gray boxes. The second step is to calculate the CTF coefficients for 1D building components using state space method in the Energy Plus. After that, the heat flux from thermal bridges is calculated and is stored in the EnergyPlus using a special computer code. However, this method is very complicated and limited to only one program such as EnergyPlus program (EnergyPlus, 2003).

Figure 2.8 Methodology of implementation thermal bridges in EnergyPlus program (EnergyPlus, 2003)

In this article, the authors tested the methodology of implementing thermal bridges in EnergyPlus program (EnergyPlus, 2003). Figure 2.9 shows the Matisse Apartment that was selected to make the simulation test. It is a hypothetical apartment and it was developed by Electricité de France (EdF) to compare the results obtained from different energy programs (EnergyPlus, 2003). This apartment includes two different types of thermal bridges, namely T-shaped and L-shaped as shown in Figure 2.10, which represents 10% of the total apartment walls area (EnergyPlus, 2003). T and L-shape thermal bridges are formed where the roof meets the corridor wall and external wall, respectively. These two thermal bridges were modeled in Sisley Software, a 2D heat transfer program, to calculate the state space equations and to generate the gray box, and then to create the model reduction black box. The model reduction results were stored in the EnergyPlus laboratory using a special computer code to be used in the simulation. The results showed that the heating load of the apartment with thermal bridges is 14% higher than the apartment without including thermal bridges (EnergyPlus, 2003).

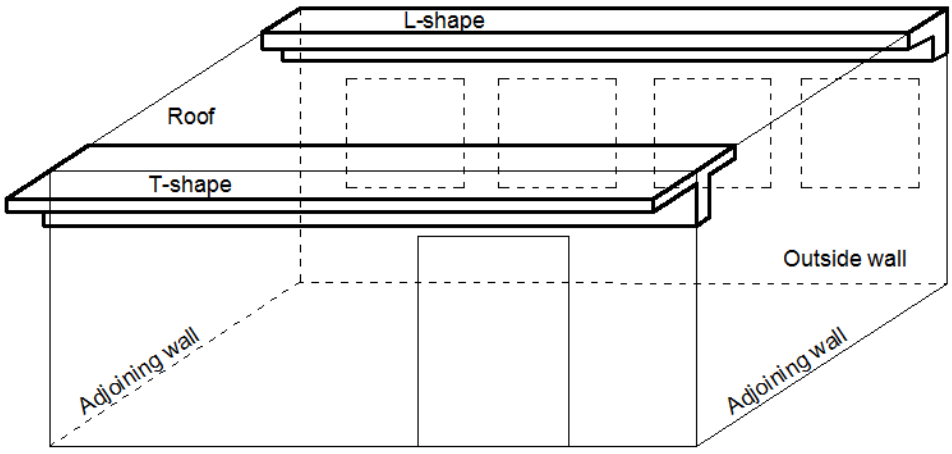

Figure 2.9 The Matisse apartment (EnergyPlus, 2003)

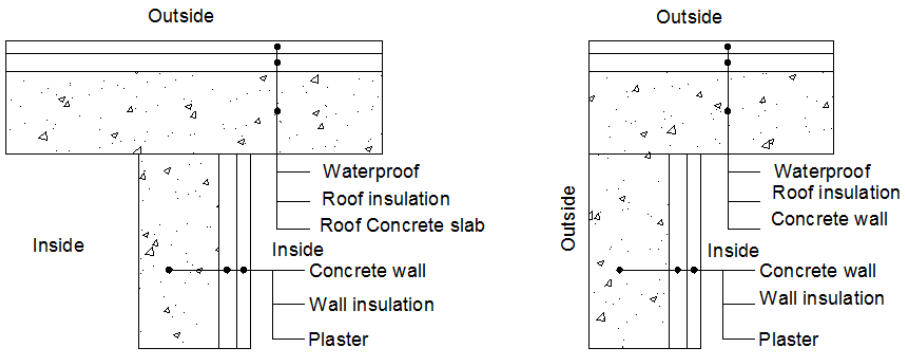

Figure 2.10 T and L-shaped thermal bridges (EnergyPlus, 2003)

Finally, the equivalent wall method can be applied in the EnergyPlus program through the mathematical relationship between structure factors and response factors that were described by Kossecka and Kosny (Kossecka and Kosny, 1996, 1997 and 1998). Since the CTF coefficients depend on the response factors, thus the structure factors relate to CTF coefficients.

2.5.7 Direct 2D/3D dynamic modeling method

This method is directly modeling the 2D and 3D thermal bridges within the same whole building energy simulation program under transient condition. WUFI Plus, a whole building Heat, Air and Moisture (HAM) program, was developed to simulate thermal, energy and moisture of buildings under steady state and transient climate conditions by Künzel (Künzel 1994). The WUFI Plus provides the possibility to compute the coupled heat and moisture 1D transfer for building components, and also has the capability to analyse the thermal bridges in 3D transfer by so called "3D objects". Figure 2.11 shows, as an example, the 3D junction between slab and external walls at the corner. Antretter et al. in 2011 (Antretter et al., 2011) evaluated the coupled heat 1D transfer in WUFI Plus program according to VDI Guideline 6020-2001 standard, and ANSI/ASHRAE standard 140-2007 for thermal and energy simulation evaluation, while they used the Moisture Buffer Experiment test to assess the 1D moisture transfer. They concluded that the validation of WUFI Plus showed good results compared to the VDI 6020 guideline and ASHRAE Standard140-2007 and Moisture Buffer Experiment (Antretter et al., 2011).

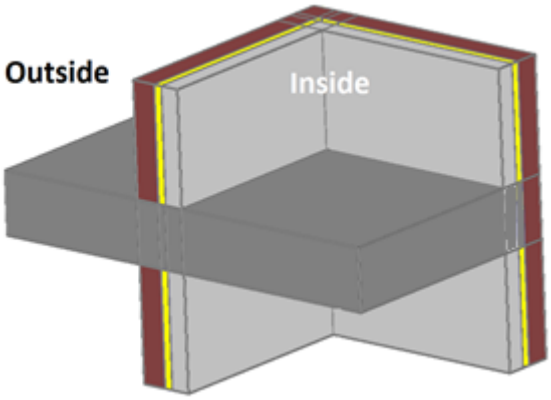

Figure 2.11 3D intermediate and balcony slab junction in WUFI Plus program

In 2013, Antretter and et al. (Antretter et al., 2013) validated 3D thermal bridge simulation in WUFI Plus program according to DIN EN ISO 10211 (DIN 2007) under steady state conditions.

WUFI Plus program uses the finite volume method to calculate 3D thermal bridging. The 3D thermal bridges can be modelled in WUFI Plus program by providing the right dimensions along x, y, and z axes with the right materials. After that, the 3D objects can be linked to the whole building by selecting the boundary conditions. The volume of the whole building needs to be calculated excluding the portion of the walls that have already been modelled in the 3D object; otherwise this portion of the wall will be counted.

2.6 SUMMARY

Most of building energy standards, codes and designers still deal with thermal bridges using steady state method, i.e. equivalent U-value method. This treatment accounts for the effect of thermal bridges on the overall thermal transmittance, while their thermal inertia effect is ignored. Some of researchers tried to find methods to take thermal inertia effect into account such as CTP method and equivalent wall method. However, the 3D dynamic method is still ignored and the question is: will the commonly used equivalent U-value method introduce errors in evaluating the energy performance.

The research presented here is motivated by the needs to understand the impact of 3D dynamic modelling method on energy loads by comparing its results with equivalent wall method and equivalent U-value method.

3 METHODOLOGY

3.1 INTRODUCTION

To investigate the dynamic effect of thermal bridges on the energy performance of buildings and the condensation risks, different building types with different construction materials, insulation levels and different climates will be considered. In general, three different thermal bridge modelling methods, namely equivalent U-value method, equivalent wall method, and direct 3D modeling method, will be used to represent thermal bridges in these buildings. The following sections describe case studies and thermal bridge modelling methods that will be used to study the effect of thermal bridges on thermal performance of buildings under dynamic and steady state conditions. Three case studies representing typical residential buildings are used in this study. Section 3.2 describes the case study of a low-rise residential building. This case study investigates the effect of different thermal bridge junctions on energy performance and surface temperatures of a low-rise residential building with different insulation levels and under different climate conditions. Section 3.3 describes a typical high-rise residential building. This case study investigates the dynamic and steady state effect of balcony slabs and thermal

break on energy demand of a high-rise residential building under different climate conditions. Section 3.4 describes a hypothetical tall wood building using Cross-Laminated Timber (CLT) as wall assembly. This case study investigates the effect of thermal mass on dynamic simulation by comparing CLT construction with concrete construction.

3.2 CASE STUDY 1: A LOW-RISE RESIDENTIAL BUILDING

3.2.1 Introduction

The low-rise residential building selected as a case study has two storeys with a window wall ratio of 30%. The plans of both floors of the building are illustrated in Figure 3.1. This building has a typical four junctions, namely wall/intermediate floor, wall/ground, wall/roof and balcony junctions. The typical construction details and thermal properties of these junctions' materials are shown in Figure 3.2 and Table 3.1, respectively. These details of the thermal bridges are implemented in the whole building HAM program WUFI Plus using equivalent U-value method, equivalent wall method and direct 3D modelling method. Figure 3.3 shows the model of the building in the WUFI Plus program with five thermal zones; namely south, north, east, west and middle, that divided the each floor.

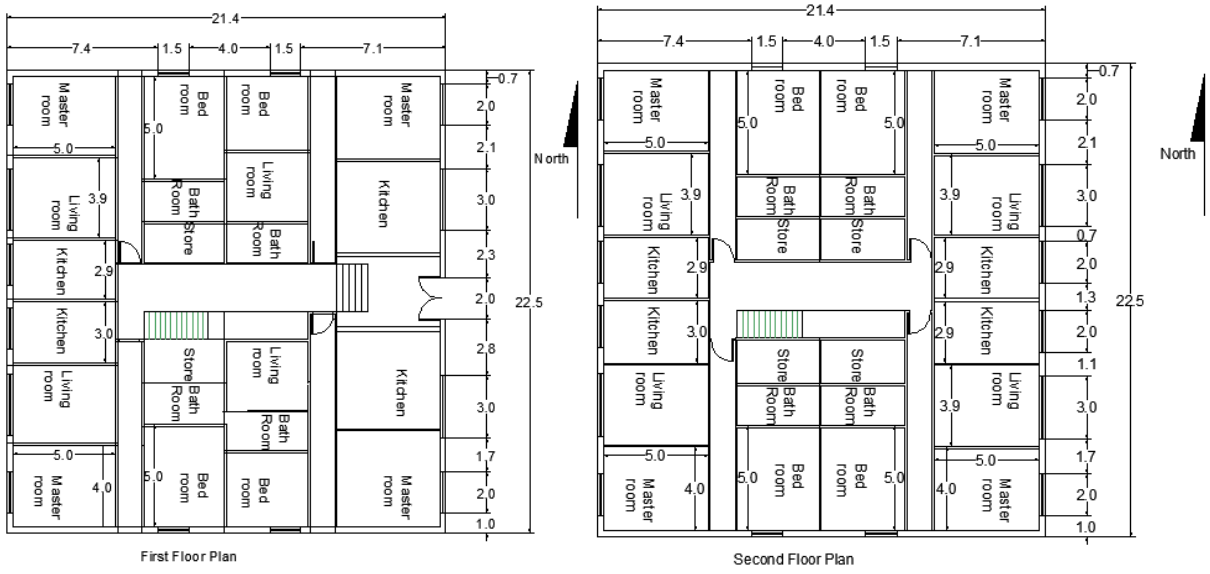

Figure 3.1 Floor plans of the low-rise residential building. All dimensions are in meter.

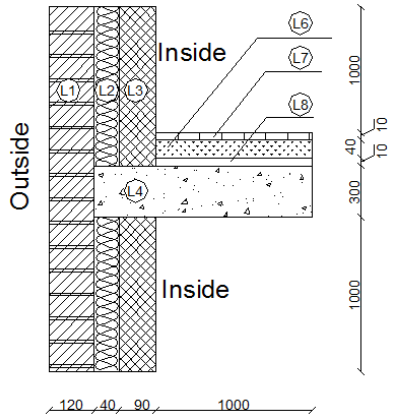

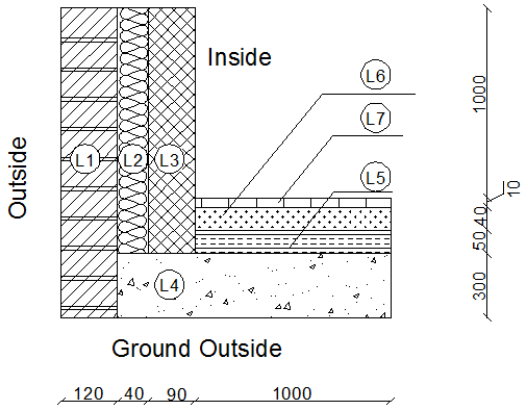

(a) External wall with intermediate floor junction. b) External wall with ground slab junction.

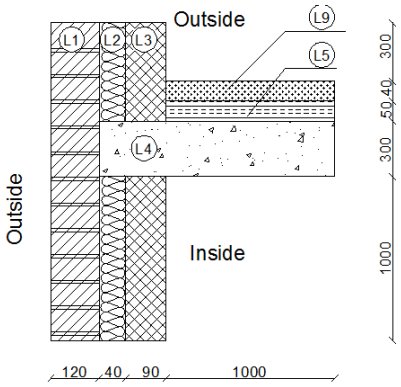

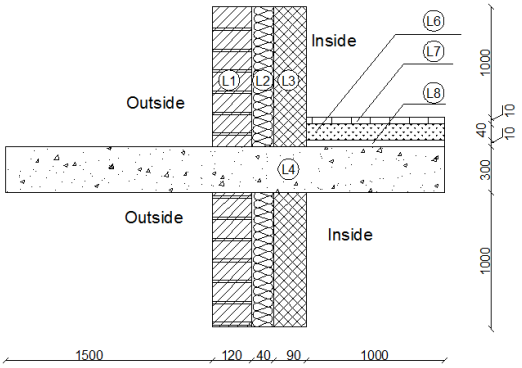

(c) External wall with roof slab junction d) Concrete balcony slab junction

Figure 3.2 Typical thermal bridge junctions implemented in the case study building. All dimensions in mm.

Table 3.1 Thermal and physical properties of the junctions materials

Layers	Material	K (m^2.k/W)	ρ (Kg/m^3)	C (J/Kg. K)
L1	Solid Brick	0.512	900	899

L2	Mineral Wool	0.041	40	800
L3	Double Hollow Brick	0.212	630	1000
L4	Reinforced Concrete Slab	1.220	1090	1000
L5	Extruded Polystyrene insulation	0.040	25	1500
L6	Reinforced Mortar	0.700	1350	1000
L7	Ceramic tiles	1.000	2000	903
L8	Acoustic insulation	0.032	40	850
L9	Stone Grit	2.000	1045	1950

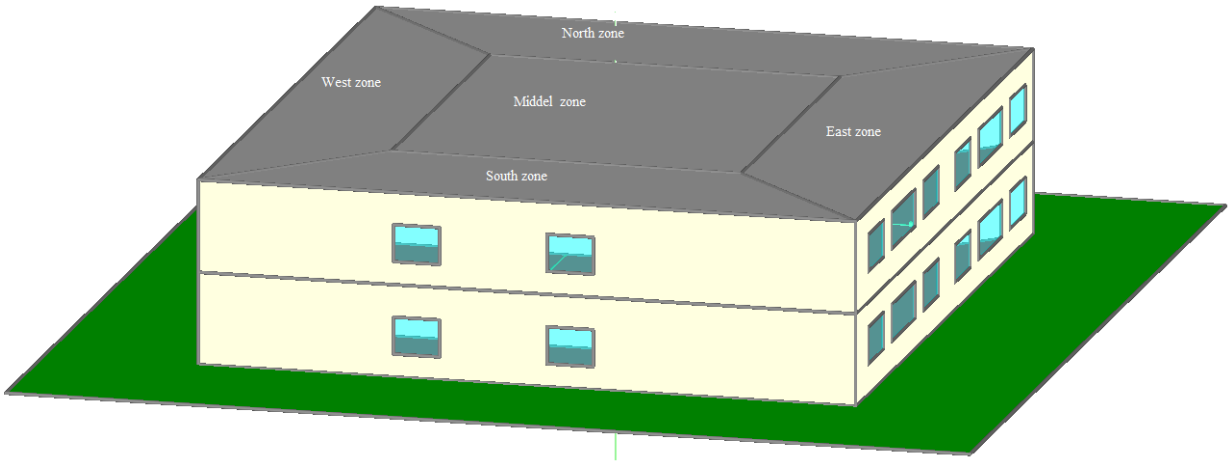

Figure 3.3 The Low rise building model with five zones in WUFI Plus program

3.2.2 Climatic conditions

Four climates are chosen for the whole building energy simulations. Three climates, i.e. Quebec City, Toronto and Vancouver locates in Canada, are chosen to represent a heating-dominated cold climate. The last one, i.e. Phoenix locates in USA, is chosen to represent a cooling-dominated hot climate.

Quebec City, Toronto and Vancouver located in Canada Building Energy Code Climate zone 7, 5 and 4, respectively. As example, Figure 3.4 shows the dynamic outer temperature of Quebec City and Table 3.2 shows the maximum temperatures in summer, minimum temperatures in winter and mean temperatures according to the WUFI Plus program that based on Oak Ridge National Laboratory, USA.

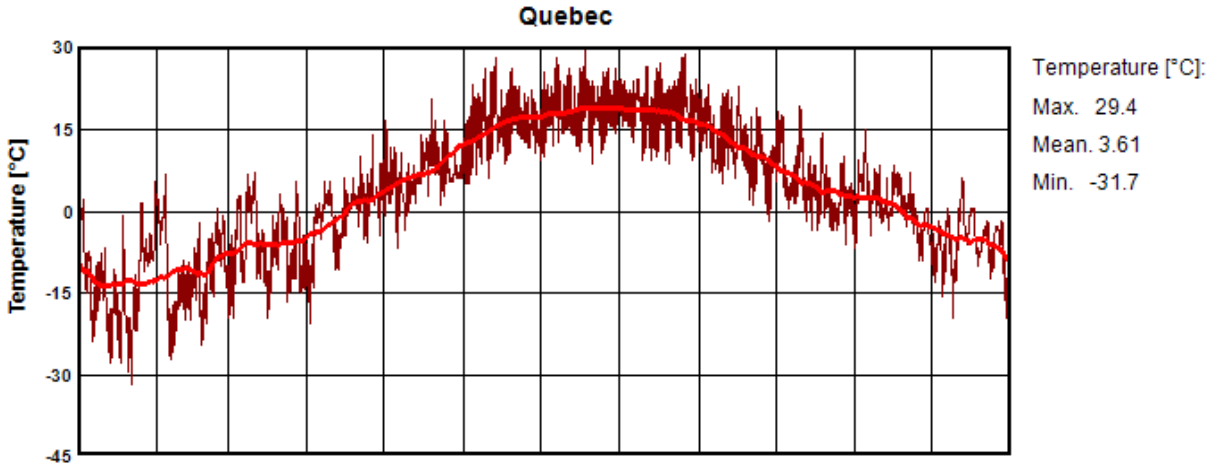

Figure 3.4 Exterior temperature profile for Quebec City climate in WUFI Plus program

Table 3.2 Maximum and minimum temperature of different location in Canada

Location	Max. temperature (^{o}C)	Mean temperature (^{o}C)	Min. temperature (^{o}C)
Quebec City	29.4	3.61	-31.7
Toronto	32.8	6.7	-23.3
Vancouver	27.2	9.06	-11.1

To model the junction of ground floor and the external wall, the ground condition is defined in WUFI Plus program according to Canadian Climate Normals 1971-2000 Station Data [23]. A sine-wave with a mean value and an amplitude temperature are assumed to represent the temperature profile of the ground at 50cm below the grade for each location, as shown in Figure 3.5. The mean values and an amplitudes are listed in Table 3.3.

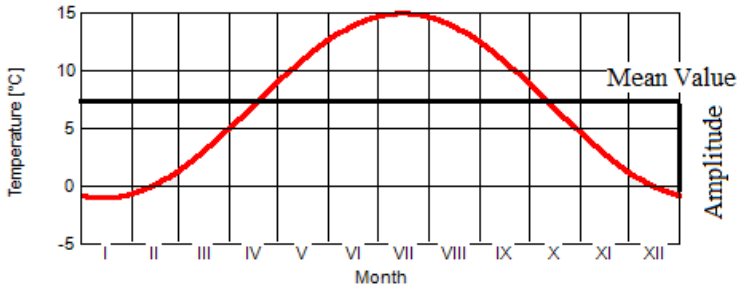

Figure 3.5 A sine-wave with a mean value and an amplitude temperature

Table 3.3 Mean value and amplitude temperature of ground at 50cm below the grade

Location	Mean value (^{o}C)	Amplitude (^{o}C)
Quebec City	7	8
Toronto	11	7
Vancouver	12	6

Phoenix, located in ASHRAE Climate zone 2B, is chosen to represent a cooling-dominated hot climate. The ground condition is defined in WUFI Plus program according to Hendricks [24]. A sine-wave with a mean value of 22^{o}C and an amplitude of 5^{o}C is assumed to represent the temperature profile of the ground at 50cm below the grade.

3.2.3 Thermal properties of junctions

These thermal bridge junctions shown in Fig. 3.2 are simulated with two insulation levels, namely low insulation and high insulation, under the Quebec City climate and with high insulation level under Toronto and Vancouver climates. The low insulation level is at the level of the existing building envelopes and the high insulation level meets the requirements by the latest National Energy Code of Canada for Buildings (NECB, 2011) for climate zone 7. For hot climate, i.e. phoenix, the insulation level meets the requirements by ASHRAE 90.1 (ASHRAE 90.1, 2013) for climate zone 2B. The higher insulation level in building envelope is achieved

by increasing the insulation thickness, therefore, in 3D direct modeling the higher insulation level is represented by an increase in insulation thickness only.

3.2.4 Equivalent U-values

The overall U-values of the 1D building envelope components are listed in Table 3.4 and the overall U-value of the 2D junctions obtained from THERM are listed in Table 3.5. The effective U-values obtained from THERM are used to determine the insulation thickness in the equivalent U-value method to represent these thermal bridge junctions. Figure 3.6 shows the different sub-surfaces that are added in WUFI Plus using both equivalent wall and equivalent U-value methods to represent different junctions.

Table 3.4 Overall thermal transmittance (U-value in $W/m^2 \cdot K$) of one-dimensional building components.

	Cold Climate		Hot Climate (Phoenix)
Building envelope components	Low insulation level	High insulation level	Insulation level in compliance with ASHRAE 90.1-2013
External walls	0.55	0.25	0.55
Ground floor	0.60	0.20	0.60
Roof slab	0.58	0.18	0.28

The overall U-value of windows is 1.96 $W/m^2.K$. Thermal bridges of windows and connection between windows and opaque walls are taken into account by the effective overall thermal transmittance of fenestration according to EN ISO 10077 (EN ISO 10077, 2012).

Table 3.5 Overall thermal transmittance (U-value in $W/m^2 \cdot K$) of thermal bridge junctions obtained from THERM.

Junctions	Cold Climate		Hot Climate (Phoenix)
	Low insulation level	High insulation level	Insulation level in compliance with ASHRAE 90.1-2013
Intermediate floor	1.14	0.88	1.14
Balcony	0.67	0.46	0.67
Ground wall	0.79	0.37	0.79
Roof wall	0.68	0.54	0.72
Roof slab	0.60	0.20	0.28

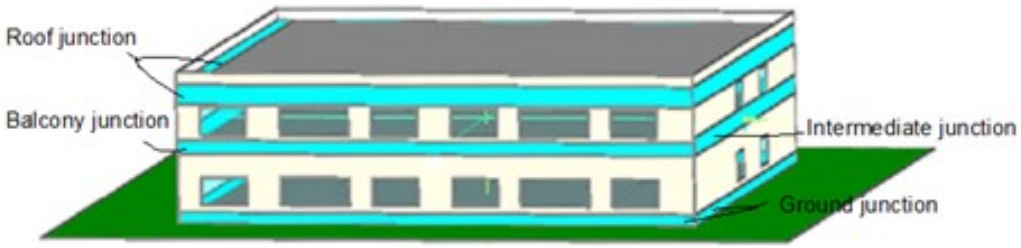

Figure 3.6 Sub-surfaces added in WUFI Plus to represent the different junctions.

3.2.5 Thermal properties of equivalent wall layers

As discussed in section 2.5.5, the first step for determination of the dynamic properties of equivalent wall layers is to identify the adiabatic plane. Different procedures are used for roof or ground slab junctions and intermediate slab or balcony slab junctions.

Roof and ground slab junctions

The heat flow generated through the 2D junctions by THERM is used to determine the adiabatic plane. At the adiabatic plane, the heat flow that enters the vertical wall from outside should be equal to the heat flow that leaves the vertical wall from inside, as is expressed by equation 3.1 (Aguilar et al., 2014):

Equation [3.1]

$$\int_{So} q_{out} ds = \int_{Si} q_{in}\, ds$$

Where S_o and S_i are the outside and inside surface boundaries of the thermal bridge, and q_{out} and q_{in} are the heat fluxes that across the thermal bridge boundary from outside and inside (W/m^2), respectively. As shown in Figure 3.7a, H_s is the vertical distance from the exterior layer of the roof slab to the adiabatic plane (360 mm), and H_f is the vertical distance from the adiabatic plane to the exterior facade (30 mm) The steady-state conduction analysis allows the identification of influencing region by the thermal bridge on the horizontal and vertical components of the 2D geometry, i.e. dTB wall and dTB slab, as shown in Figure 3.7b. The 2D thermal bridge effect (dTB slab) extends to 600 mm from the innermost surface of the vertical wall in the roof slab, while the 2D thermal bridge effect (dTB wall) extends to 400mm below the interior surface of the roof slab in the wall. As shown in Fig. 5c, the adiabatic plane divides the 2D roof junction into two thermal bridge regions, roof slab region and roof wall region. The roof slab region measures 850mm and the roof wall region measures 430mm. A three-layered equivalent wall is then generated for each region.

The temperature distribution obtained from THERM is used to calculate the structure factors using equations 2.3-2.5 for each region in the junction. The flow diagram shown in Figure 3.11 is used to solve equations 2.8-2.10 to generate the dynamic properties of the equivalent wall for each region. Three-layer structures (n=3) are assumed for the equivalent walls. Equations 2.8-2.9 represent three conditions, to be satisfied by six variables (2n), some of the variables need to be assigned with initial values and the remaining variables can then be solved. However, the solution obtained in this way may not be correct. For example, the first approximations of R_n may result in negative C_n values. Therefore, following the procedure suggested by Kossecka and Kosny (Kossecka, 1998), a flow chart (Fig. 3.11) is created to generate, with some logic, a set of R_n values to find admissible combinations of C_n values. The thermophysical properties of

the layers can then be established to match R_n and C_n values and total thickness of the wall. Two variables, A_{max} in the range of 5 to 10, and B_{max} in the range of 100 to 500, are assumed to assign initial values for R_1 and R_2. The ranges chosen for A_{max} and B_{max} are to ensure the total heat capacity of the second layer C_2 be positive but very close to zero since the middle layer is insulation with much lower density compared to other layers.

In THERM simulations, the exterior temperature for vertical wall and horizontal slab is set at 1 ^oC with a surface thermal resistance of 0.04 $m^2 \cdot K/W$. The interior temperature is set at 0^oC with surface thermal resistance of 0.13 $m^2 \cdot K/W$ for the vertical wall, 0.1 $m^2 \cdot K/W$ for the horizontal roof slab and 0.17 $m^2 \cdot K/W$ for horizontal ground slab. The structure factors and thermal properties of the equivalent wall are listed in Table 3.6 for the roof junction and Table 3.7 for the slab-on-grade junction. Figures 3.7-3.9 show the adiabatic plane, dTB distance, and the parameter of regions for high insulation roof junction, low and high insulation ground junction.

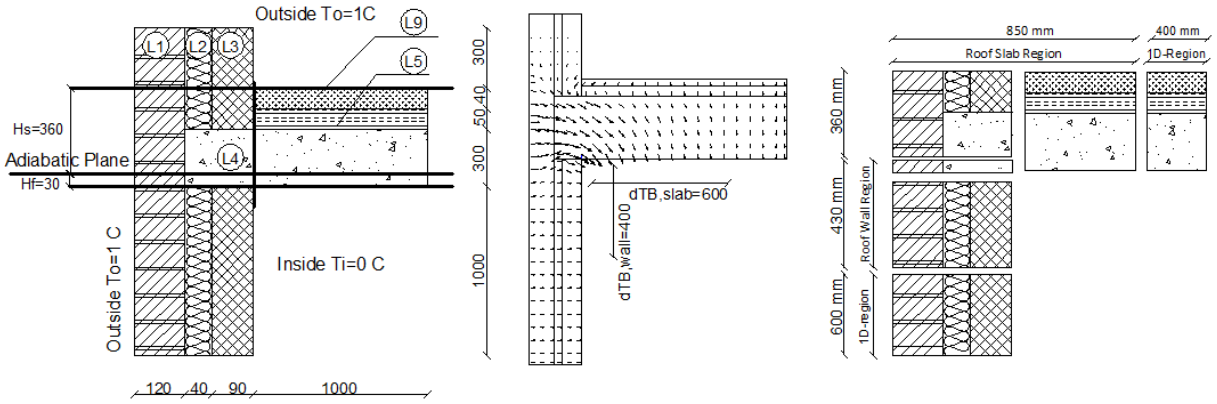

a) b) c)

Figure 3.7 Methodology to identify the adiabatic plane for the roof junction with low insulation level: a) geometry of the roof junction b) heat flux across the roof junction c) roof junction divided into two regions.

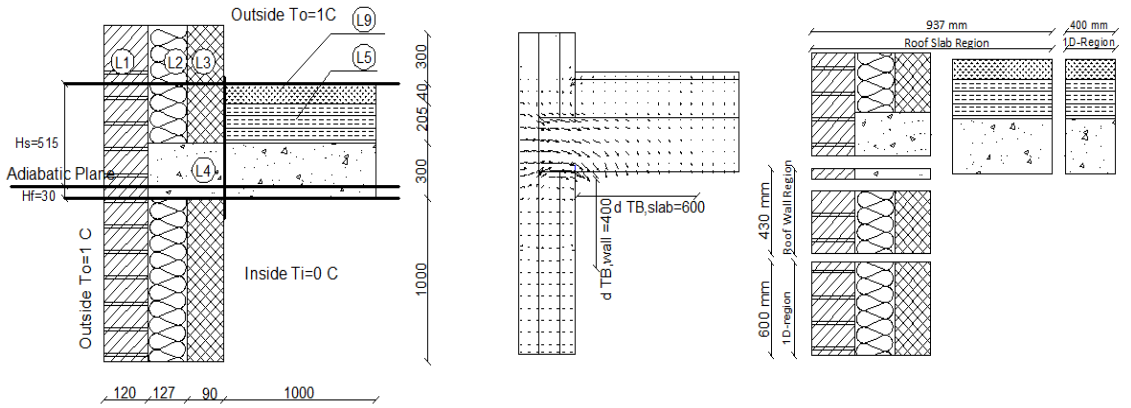

a) b) c)

Figure 3.8 Methodology to identify the adiabatic plane for the roof junction with high insulation level: a) geometry of the roof junction b) heat flux across the roof junction c) roof junction divided into two regions

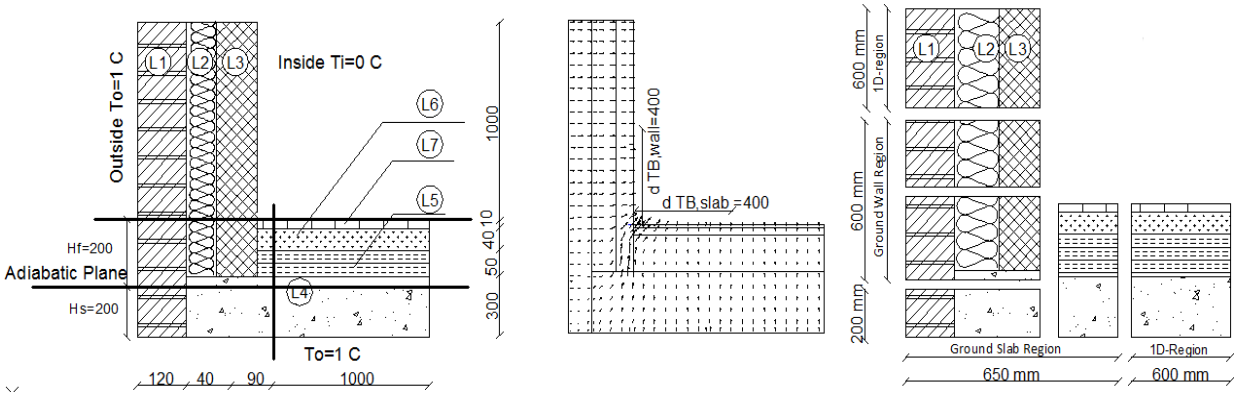

Figure 3.9 Methodology to identify the adiabatic plane for the ground junction with low insulation level: a) geometry of the ground junction b) heat flux across the ground junction c) ground junction divided into two regions

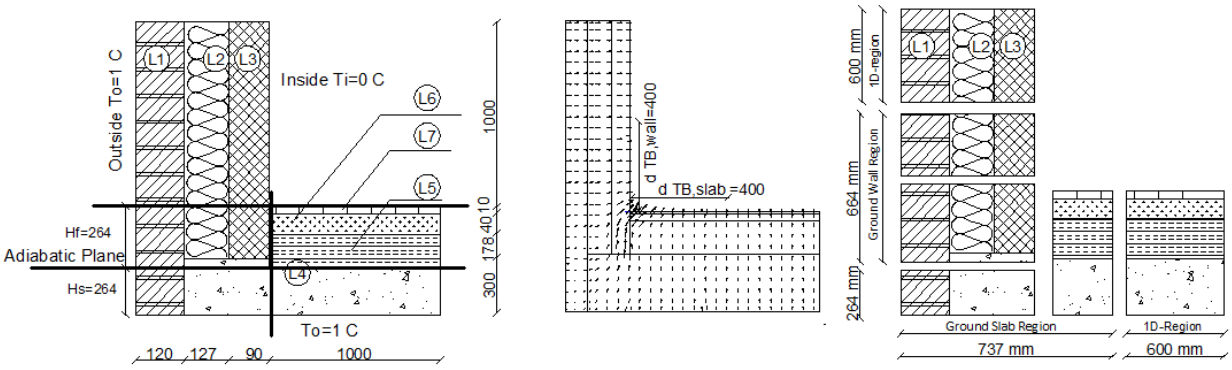

a) b) c)

Figure 3.10 Methodology to identify the adiabatic plane for the ground junction with high insulation level: a) geometry of the ground junction b) heat flux across the ground junction c) ground junction divided into two regions

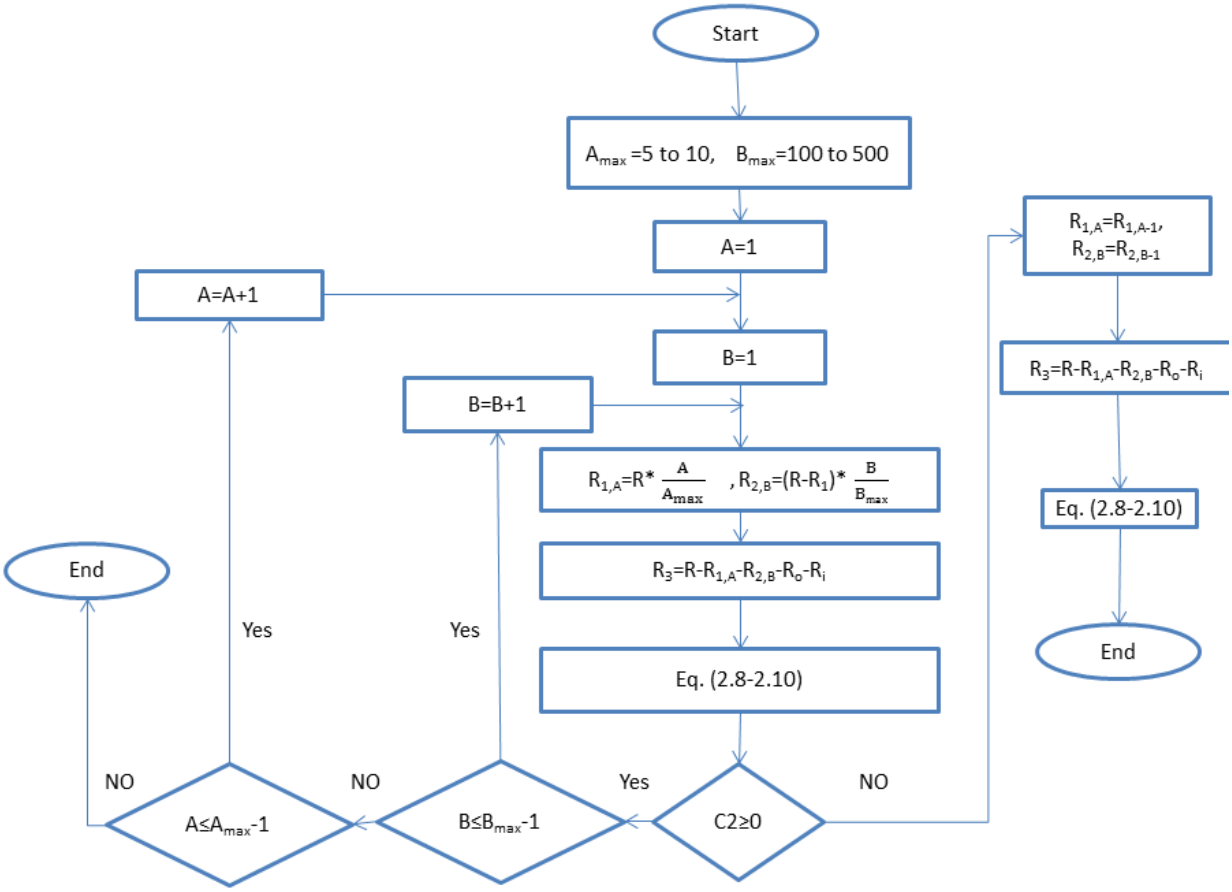

Figure 3.11 Flow diagram to determine the dynamic wall properties using the equivalent wall method.

Table 3.6 Overall thermal transmittance and structure factors for roof junction regions.

Regions	Cold climate								Hot climate (Phoenix)			
	Low insulation level				High insulation level							
	U ($W/m^2 \cdot K$)	φ_{ii}	φ_{ee}	φ_{ie}	U ($W/m^2 \cdot K$)	φ_{ii}	φ_{ee}	φ_{ie}	U ($W/m^2 \cdot K$)	φ_{ii}	φ_{ee}	φ_{ie}
Roof wall region	0.721	0.198	0.562	0.120	0.449	0.265	0.552	0.094	0.703	0.208	0.549	0.131
Roof slab region	1.311	0.341	0.330	0.164	0.895	0.406	0.335	0.129	1.064	0.414	0.324	0.119

Table 3.7.a Thermal properties of the equivalent wall layers of the roof wall region in the roof junction.

Layers	Cold climate								Hot climate				All cases	
	Low insulation level				High insulation level									
	R $m^2 \cdot K/W$	C $kJ/m^2 \cdot K$	K $W/m \cdot K$	ρ kg/m^3	R $m^2 \cdot K/W$	C $kJ/m^2 \cdot K$	K $W/m \cdot K$	ρ kg/m^3	R $m^2 \cdot K/W$	C $kJ/m^2 \cdot K$	K $W/m \cdot K$	ρ kg/m^3	e m	c_p $kJ/Kg \cdot K$
S_i	0.13	-	-	-	0.13	-	-	-	0.13	-	-	-	-	-

L_1	0.27	136.90	0.36	1369.2	0.32	133.54	0.31	1335.4	0.28	134.25	0.35	1342.5	0.1	1
L_2	0.67	0.64	0.15	6.4	1.39	0.15	0.07	1.5	0.69	0.63	0.14	6.27	0.1	1
L_3	0.27	53.90	0.38	539.2	0.35	68.38	0.29	683.9	0.27	56.60	0.37	566.0	0.1	1
S_o	0.04	-	-	-	0.04	-	-	-	0.04	-	-	-	-	-
Total	1.39	191.48			2.23	202.07			1.42	191.48			0.3	

Table 3.6b Thermal properties of the equivalent wall layers of the roof slab region in the roof junction.

	Cold climate (Quebec city)								Hot climate (Phoenix)				All cases	
	Low insulation level				High insulation level									
Layers	R	C	K	ρ	R	C	k	ρ	R	C	K	ρ	e	$c_{p,}$
	$m^2 \cdot K/W$	$kJ/m^2 \cdot K$	$W/m \cdot K$	kg/m^3	$m^2 \cdot K/W$	$kJ/m^2 \cdot K$	$W/m \cdot K$	kg/m^3	$m^2 \cdot K/W$	$kJ/m^2 \cdot K$	$W/m \cdot K$	kg/m^3	m	$kJ/kg \cdot K$
S_i	0.10	-	-	-	0.10	-	-	-	0.10	-	-	-	-	-
L_1	0.19	348.11	0.52	3481.1	0.19	371.90	0.54	3719.0	0.13	344.68	0.74	3446.8	0.1	1
L_2	0.26	1.00	0.38	10.0	0.57	0.65	0.17	6.5	0.51	0.01	0.20	0.1	0.1	1

L_3	0.17	244.24	0.58	2442.4	0.22	270.60	0.46	2706.0	0.16	230.01	0.63	2300.1	0.1	1
S_o	0.04	-	-	-	0.04	-	-	-	0.04	-	-	-	-	-
Total	0.76	593.34			1.12	643.15			0.94	574.70			0.3	

Table 3.7 Overall thermal transmittance and structure factors for ground regions with high insulation under cold climate.

Regions	Cold climate (Quebec city)							
	Low insulation level				High insulation level			
	U ($W/m^2 \cdot K$)	φ_{ii}	φ_{ee}	φ_{ie}	U ($W/m^2 \cdot K$)	φ_{ii}	φ_{ee}	φ_{ie}
Ground wall region	0.678	0.151	0.629	0.112	0.346	0.180	0.710	0.055
Ground slab region	0.719	0.112	0.724	0.079	0.323	0.095	0.844	0.031

Table 3.7a Thermal properties of the equivalent wall layers of the ground wall region in ground junction.

	Cold climate								All cases	
	Low insulation level				High insulation level					
Layers	R	C	K	ρ	R	C	k	ρ	E	c_p
	$m^2 \cdot K/W$	$kJ/m^2 \cdot K$	$W/m \cdot K$	kg/m^3	$m^2 \cdot K/W$	$kJ/m^2 \cdot K$	$W/m \cdot K$	kg/m^3	m	$kJ/kg \cdot K$
S_i	0.13				0.13	-	-	-	-	-
L_1	0.30	218.93	0.34	2189.3	0.24	241.75	0.42	2417.5	0.1	1
L_2	0.79	0.47	0.13	4.7	2.27	1.04	0.04	10.4	0.1	1
L_3	0.22	59.90	0.46	599.0	0.21	64.73	0.47	647.3	0.1	1
S_o	0.04				0.04	-	-	-	-	-

Total	1.48	279.30	2.89	307.52	0.3	

Table 3.7b Thermal properties of the equivalent wall layers of the ground slab region in ground junction.

	Cold climate								All cases	
	Low insulation level				High insulation level					
Layers	R	C	K	ρ	R	C	k	ρ	E	c_p
	$m^2 \cdot K/W$	$kJ/m^2.K$	$W/m \cdot K$	kg/m^3	$m^2 \cdot K/W$	$kJ/m^2 \cdot K$	$W/m \cdot K$	kg/m^3	m	$kJ/kg \cdot K$
S_i	0.17				0.17	-	-	-	-	-
L_1	0.08	445.88	1.22	4458.8	0.19	466.91	0.53	4669.1	0.1	1
L_2	0.99	0.28	0.10	2.8	2.46	0.52	0.04	5.2	0.1	1
L_3	0.05	73.14	1.90	731.4	0.18	51.87	0.56	518.7	0.1	1
S_o	0.10				0.10	-	-	-	-	-
Total	1.32	519.30			3.10	519.30			0.3	

Balcony and intermediate floor junctions

Balcony and intermediate floor junctions are created by the external wall and the intermediate slab that separates two levels of indoor spaces. In this case, the calculation method is based on the analysis of energy stored in the thermal bridge and heat flow across the upper and lower slab surfaces. The fraction of heat flow across each surface with respect to the total amount of energy that enters the slab is interpreted as the influence of the thermal bridge over the lower and upper indoor spaces (Aguilar et al., 2014).

The fraction of the heat flow across upper and lower slab surfaces can be calculated using the following equations:

$$F_u = \frac{Q_u}{Q_u + Q_l}$$ Equation [3.2]

$$F_l = \frac{Q_l}{Q_u + Q_l}$$ Equation [3.3]

Where F_u and F_l are the upper and lower fraction, respectively, and the Q_u and Q_l are the heat flow across upper and lower slab surfaces, respectively. The total energy stored in the thermal bridge is

$$E = \int_V \rho\, c_p\, \theta\, dv$$ Equation [3.4]

The adiabatic plane is determined as such that the energy stored in the upper region of the thermal bridge is equal to that stored in the lower region. The energy stored in each region can be calculated using equations 3.5 and 3.6:

$$E_l = F_l * \int_{y0}^{y1} \rho\, c_p \theta\, dV$$ Equation [3.5]

$$E_u = F_u * \int_{y1}^{y2} \rho\, c_p \theta\, dV$$ Equation [3.6]

Where y_0 is the bottom surface of the slab, y_1 is the adiabatic plane, and y_2 is the top surface of the slab.

Figures 3.12-3.15 show the procedure to identify the regions for the balcony and intermediate floor junctions with high and low insulation levels. Following the same procedure used for the roof junction, the temperature distribution obtained from THERM is used to calculate the structure factors for each region in the junction using equations 2.3-2.5. The flow diagram shown in Figure 3.11 is used to solve equations 2.8-2.10 to generate the dynamic properties of the equivalent wall junctions. The structure factors and thermal properties of equivalent wall layers are listed in Table 3.8 for the balcony junction and Table 3.9 for the intermediate floor junction. The properties of balcony and intermediate floor junction for the hot climate are the

same as the case with low insulation level for the cold climate since the overall U-values of these geometrical thermal bridges are the same as shown in Table 3.5.

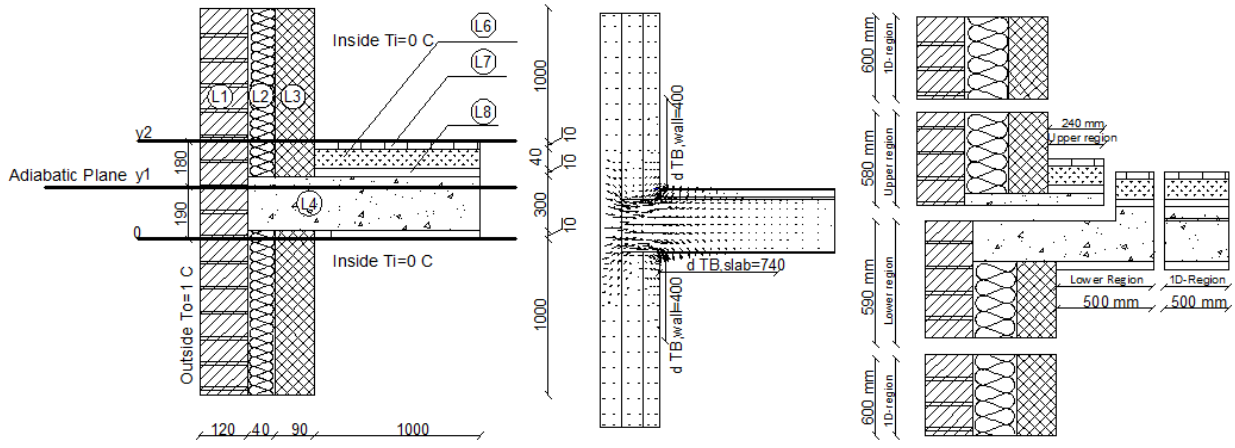

a) b) c)

Figure 3.12 Methodology to identify the adiabatic plane for the intermediate junction with low insulation level: a) geometry of the intermediate junction b) heat flux across the intermediate junction c) balcony junction divided into two regions.

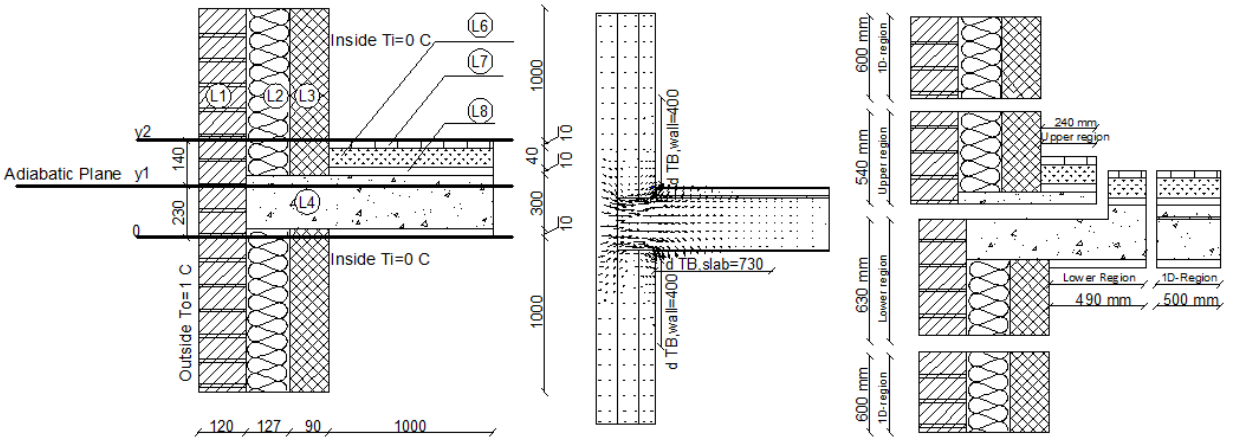

a) b) c)

Figure 3.13 Methodology to identify the adiabatic plane for the intermediate junction with high insulation level: a) geometry of the intermediate junction b) heat flux across the intermediate junction c) intermediate junction divided into two regions

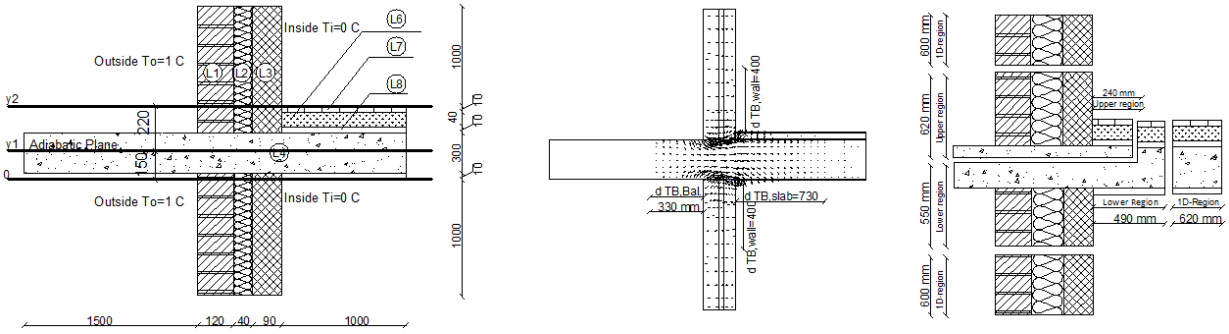

b) b) c)

Figure 3.14 Methodology to identify the adiabatic plane for the balcony slab with low insulation level: a) geometry of the balcony junction b) heat flux across the balcony junction c) balcony junction divided into two regions.

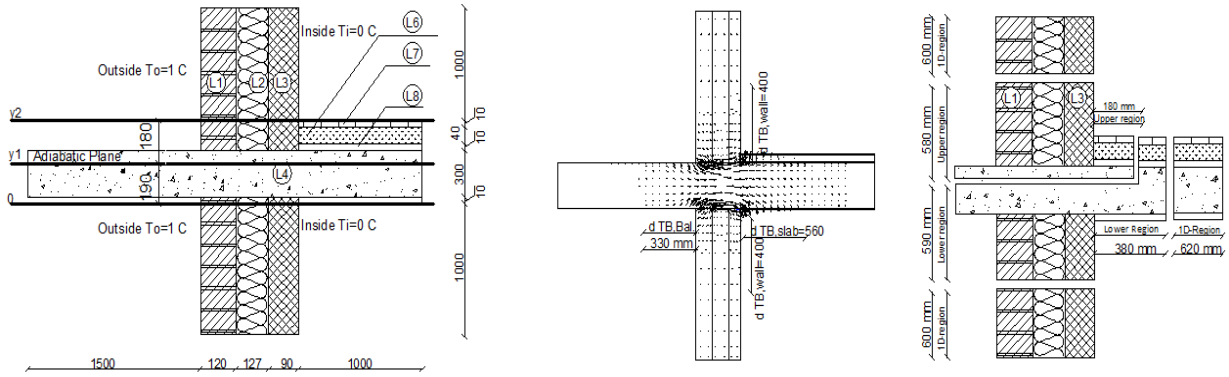

a) b) c)

Figure 3.15 Methodology to identify the adiabatic plane for the balcony slab with high insulation level: a) geometry of the balcony junction b) heat flux across the balcony junction c) balcony junction divided into two regions.

Table 3.8 Overall thermal transmittance and structure factors for the balcony junction.

Regions	Cold climate							
	Low insulation level				High insulation level			
	U ($W/m^2 \cdot K$)	φ_{ii}	φ_{ee}	φ_{ie}	U ($W/m^2 \cdot K$)	φ_{ii}	φ_{ee}	φ_{ie}
Upper region	0.734	0.274	0.490	0.117	0.424	0.264	0.528	0.103
Lower Region	1.107	0.413	0.368	0.110	0.820	0.394	0.394	0.104

Table 3.8aThermal properties of the equivalent wall layers of the upper region in the balcony junction.

Layers	Cold climate								All cases	
	Low insulation level				High insulation level					
	R $m^2 \cdot K/W$	C $kJ/m^2 \cdot K$	k $W/m \cdot K$	ρ kg/m^3	R $m^2 \cdot K/W$	C $kJ/m^2 \cdot K$	k $W/m \cdot K$	ρ kg/m^3	e m	c_p kJ/kg·K
S_i	0.13	-	-	-	0.13	-	-	-	-	-
L_1	0.19	197.53	0.51	1975.3	0.39	233.65	0.25	2336.5	0.1	1
L_2	0.75	0.62	0.13	6.2	1.35	0.16	0.07	1.6	0.1	1
L_3	0.25	119.97	0.40	1199.7	0.44	120.86	0.23	1208.6	0.1	1
S_o	0.04	-	-	-	0.04	-	-	-	-	-
Total	1.36	318.12			2.36	354.67			0.3	

Table 3.8b Thermal properties of the equivalent wall layers of the lower region in the balcony junction.

	Cold climate								All cases	
	Low insulation level				High insulation level					
Layers	R	C	k	ρ	R	C	k	ρ	e	$c_{p,}$
	$m^2 \cdot K/W$	$kJ/m^2 \cdot K$	$W/m \cdot K$	kg/m^3	$m^2 \cdot K/W$	$kJ/m^2 \cdot K$	$W/m \cdot K$	kg/m^3	m	$kJ/kg \cdot K$
S_i	0.13	-	-	-	0.13	-	-	-	-	-
L_1	0.18	302.45	0.55	3024.5	0.09	287.96	1.07	2879.6	0.1	1
L_2	0.34	0.57	0.29	5.7	0.81	0.07	0.12	0.7	0.1	1
L_3	0.21	280.25	0.48	2802.5	0.15	253.01	0.69	2530.1	0.1	1
S_o	0.04	-	-	-	0.04	-	-	-	-	-
Total	0.90	583.27			1.22	541.04			0.3	

Table 3.9 Overall thermal transmittance and structure factors for the intermediate floor junction.

	Cold climate							
	Low insulation level				High insulation level			
Regions	U $(W/m^2 \cdot K)$	φ_{ii}	φ_{ee}	φ_{ie}	U $(W/m^2 \cdot K)$	φ_{ii}	φ_{ee}	φ_{ie}
Upper region	0.647	0.472	0.288	0.117	0.450	0.394	0.369	0.120
Lower Region	1.066	0.497	0.246	0.126	0.735	0.572	0.225	0.102

Table 3.9aThermal properties of the equivalent wall layers of the upper region in the intermediate floor junction.

	Cold climate								All cases	
	Low insulation level				High insulation level					
Layers	R $m^2 \cdot K/W$	C $kJ/m^2 \cdot K$	k $W/m \cdot K$	ρ kg/m^3	R $m^2 \cdot K/W$	C $kJ/m^2 \cdot K$	k $W/m \cdot K$	ρ kg/m^3	e m	c_p kJ/kg·K
S_i	0.13				0.13	-	-	-	-	-
L_1	0.23	174.19	0.44	1741.9	0.44	172.57	0.22	1725.7	0.1	1
L_2	0.96	1.02	0.10	10.2	1.12	0.48	0.09	4.8	0.1	1
L_3	0.19	92.59	0.53	925.9	0.49	146.65	0.20	1466.5	0.1	1
S_o	0.04				0.04	-	-	-	-	-
Total	1.55	267.80			2.22	319.70			0.3	

Table 3.9b Thermal properties of the equivalent wall layers of the lower region in the intermediate floor junction.

	Cold climate								All cases	
	Low insulation level				High insulation level					
Layers	R $m^2 \cdot K/W$	C $kJ/m^2 \cdot K$	k $W/m \cdot K$	ρ kg/m^3	R $m^2 \cdot K/W$	C $kJ/m^2 \cdot K$	k $W/m \cdot K$	ρ kg/m^3	e m	c_p kJ/kg·K
S_i	0.13				0.13	-	-	-	-	-

L_1	0.10	331.38	1.03	3313.8	0.10	346.19	0.10	3461.9	0.1	1
L_2	0.57	2.58	0.17	25.8	0.99	0.07	0.10	0.7	0.1	1
L_3	0.10	114.34	1.03	1143.4	0.09	108.50	0.10	1085.0	0.1	1
S_o	0.04				0.04	-	-	-	-	-
Total	0.94	448.30			1.36	454.76	0.30		0.3	

Verification of the equivalent wall method

Transient modeling of the thermal bridge junctions is carried out in WUFI Plus and the results are used for the verification of the equivalent wall method. The outdoor temperature is defined by $T_o = T * \sin\left(\frac{2\pi}{24}t\right)$, where T is an amplitude temperature of 5 ^oC and t is time, hr, and the interior temperature is set at $T_i = 20^oC$. Comparisons in terms of heat flow are made for all thermal bridge junctions considered in this study. As examples, Figure 3.16 and 3.17 show the comparison in terms of heat flow for the intermediate floor/wall junction and roof junction, respectively. Similar trend is found for other cases. Among all the cases, the maximum difference in heat flow between the 2D junctions and the equivalent wall is within 0-4% over the 24-hour period.

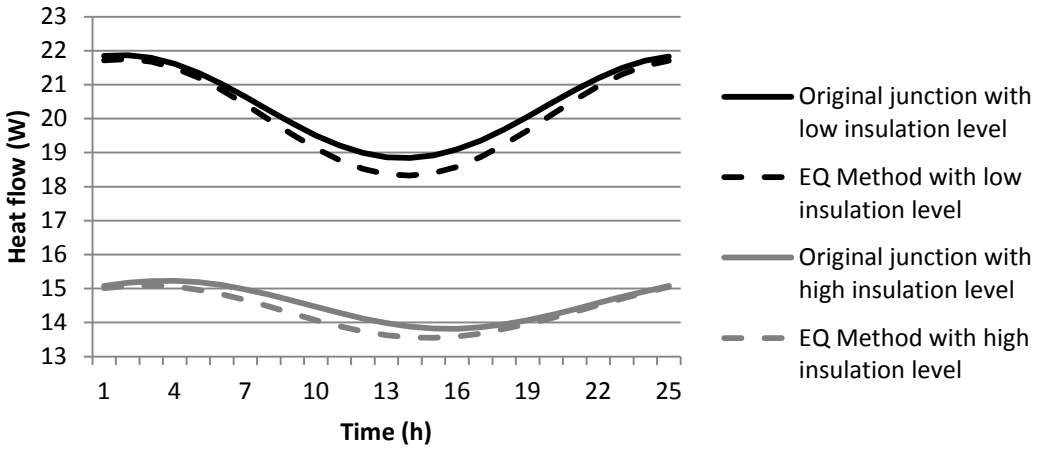

Figure 3.16 Comparison between the original 2D junction and the equivalent wall for the intermediate floor/wall junction.

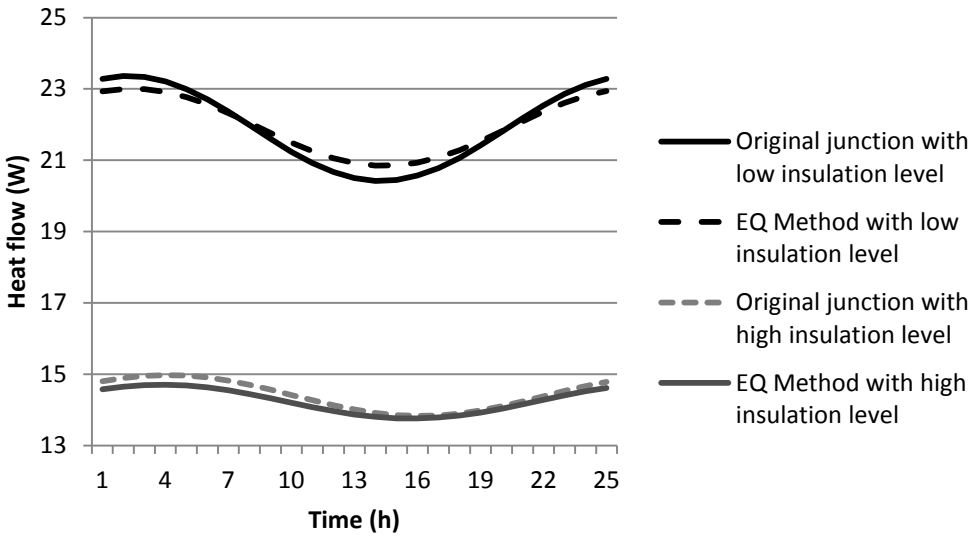

Figure 3.17 Comparison between the original 2D junction and the equivalent wall for the roof junction.

3.2.6 Direct 3D modelling

As discussed in section 2.5.7, the WUFI Plus has the capability to draw 3D thermal bridges and insertion them in the whole building energy simulation directly. Figure 3.18 illustrates the steps to model the four different junctions in this case. The first step is to identify three thermal bridges in 3D-Objects list, namely intermediate and balcony junction, roof junction and ground junction. The second step is to determine the dimensions of each junction by X, Y and Z axis to draw the bridges and then select the materials for each junction. The fourth step is to link the thermal bridges with the zones in the whole building by determining the interior and exterior boundary conditions. To avoid double counting the portion of the walls that have already been modelled in the 3D object , the net volume of the whole building needs to be calculated excluding this portion of the walls. The net volume for each thermal zone is listed in Table 3.10

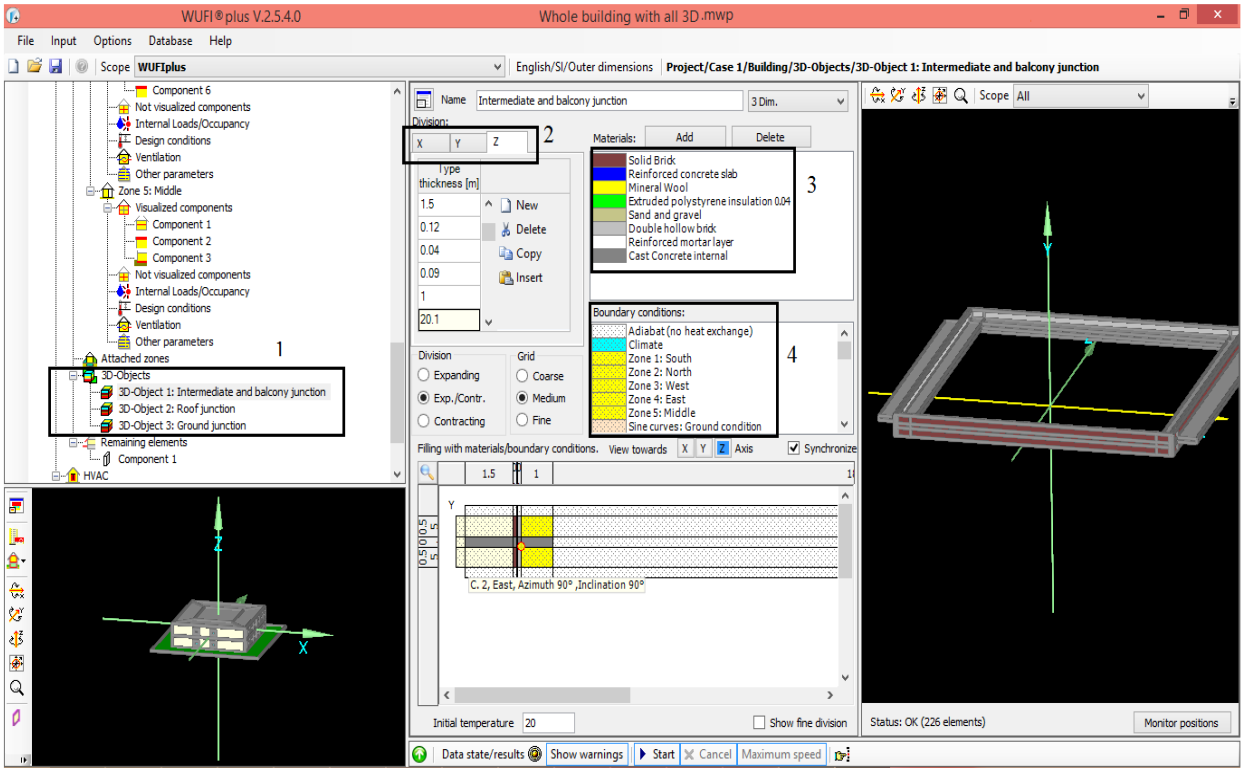

Figure 3.18 Four steps to model 3D thermal bridges in WUFI Plus program

Table 3.10 Net volume of each thermal zones with and without thermal bridges

Thermal zones in the building	Net volume without thermal bridge	Thermal bridge junctions volume	Net volume with thermal bridge	Ratio of thermal bridges
South and north	363.56	39.37	324.19	10.8%
East and west	397.30	41.48	355.82	10.4%
Middle	688.71	0	688.71	0.0%
Total	2210.43	161.70	2048.73	7.3%

3.3 CASE STUDY 2: A HIGH RISE RESIDENTIAL BUILDING

3.3.1 Introduction

A typical multi-unit residential building with a window wall ratio of 52% is chosen as a case study. The building contains a twenty-six storey residential units with a two-level ground portion as commercial space. A typical floor located between five and twenty-six was selected for the whole building energy analysis using WUFI Plus HAM program. Figure 3.19 and 3.20 show the typical floor plan between five to twenty-six storeys and a sketch up of the building, respectively.

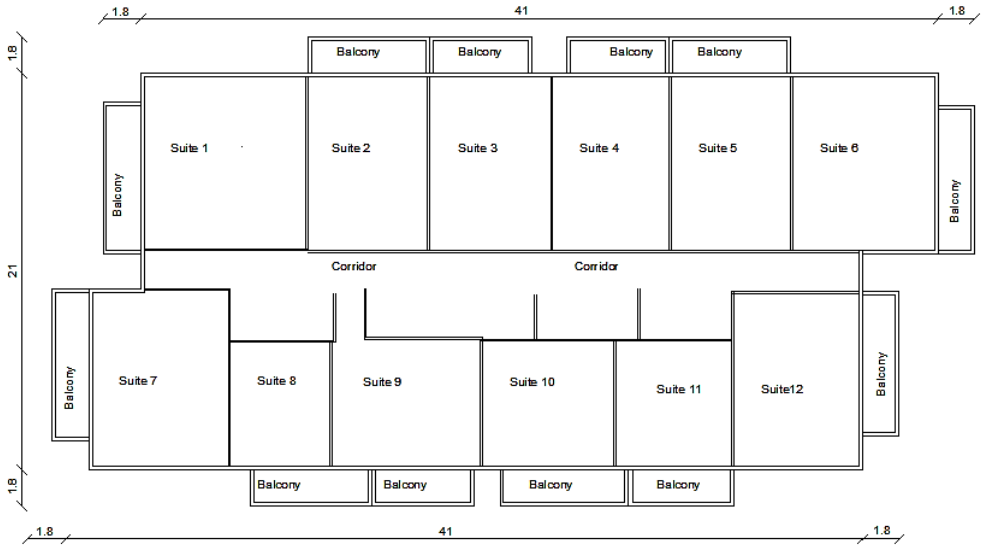

Figure 3.19 A typical floor plan for building of the low-rise residential building. Dimensions are in meters

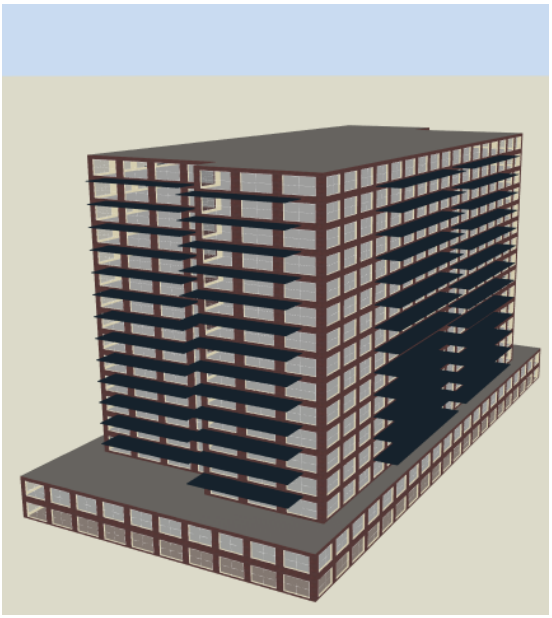

Figure 3.20 Sketch up of the selected building

This building contains two different balcony slab types, namely the spandrel/spandrel balcony slab and sliding door/spandrel balcony. The typical construction details of balcony slab junctions are shown in Figure 3.21 a-d. A hypothetical section is also simulated to represent the cases with well-insulated above and below balcony walls (RSI 3.5), as shown in Figure 3.21e and 3.21f. The effect of balcony thermal break on the energy performance is also investigated by including an insulated balcony separator as thermal break (Figure 3.21). Figure 3.22 shows the distribution of steel reinforcement bars with eight 8mm diameter and four 6 mm diameter for shearing stainless steel at 125mm spacing in the balcony slab and the reinforcement steel is located at 50mm below the balcony surface. Without thermal break, eight 10M steel reinforcement bars with 11.3mm diameter at 125mm spacing are assumed. The typical construction details of both balcony slab junctions are listed in Table 3.11

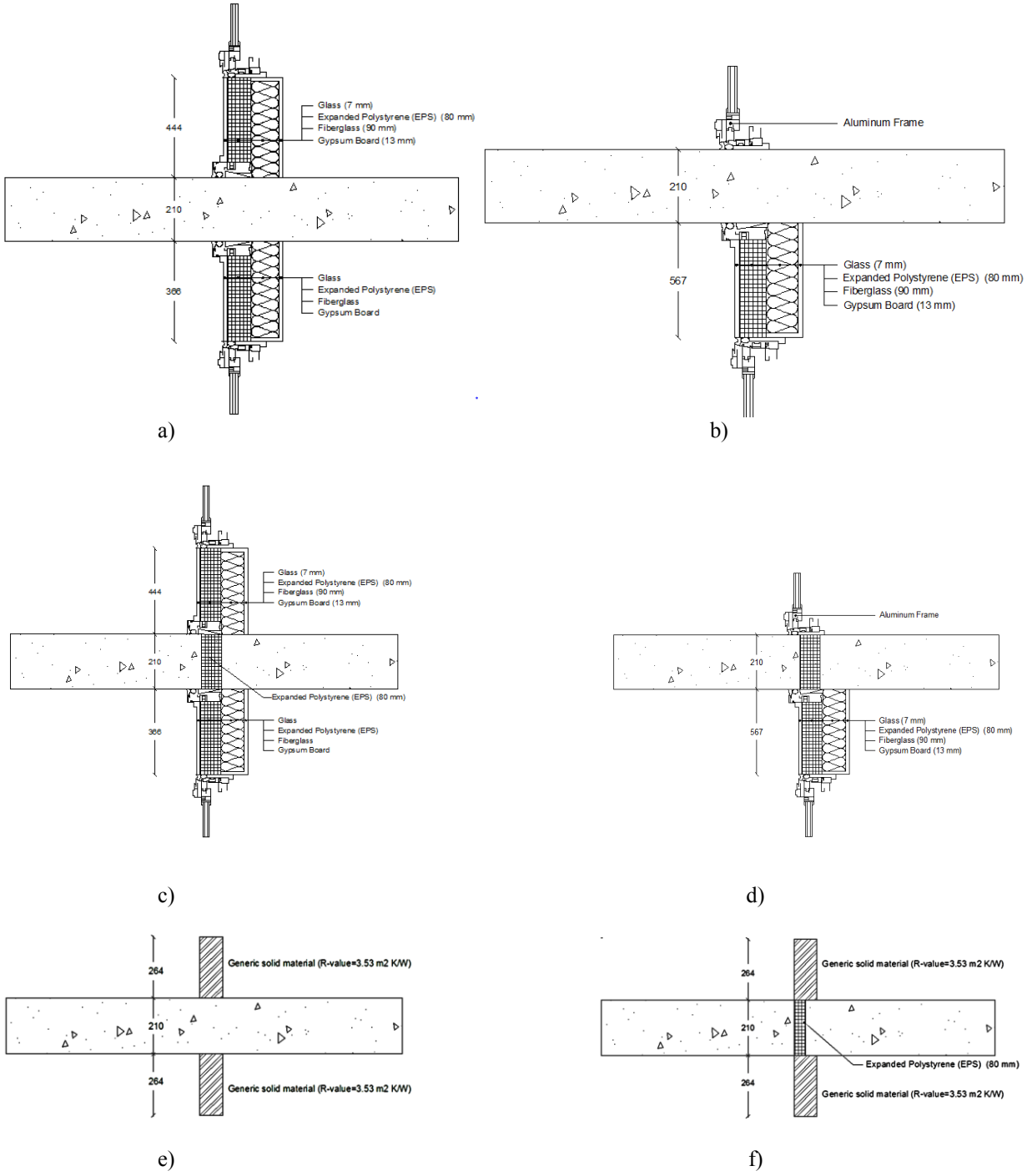

Figure 3.21 Different balcony slabs junctions: a) typical section at spandrel/spandrel balcony without thermal break; b) typical section at sliding-door/spandrel panel balcony without thermal break c) typical section at spandrel/spandrel balcony with thermal break; b) typical section at sliding-door balcony with thermal break; e) hypothetical section with well-insulated generic

spandrel/spandrel balcony without thermal break; f) hypothetical section with well-insulated generic spandrel/spandrel balcony with thermal break. Dimensions are in mm.

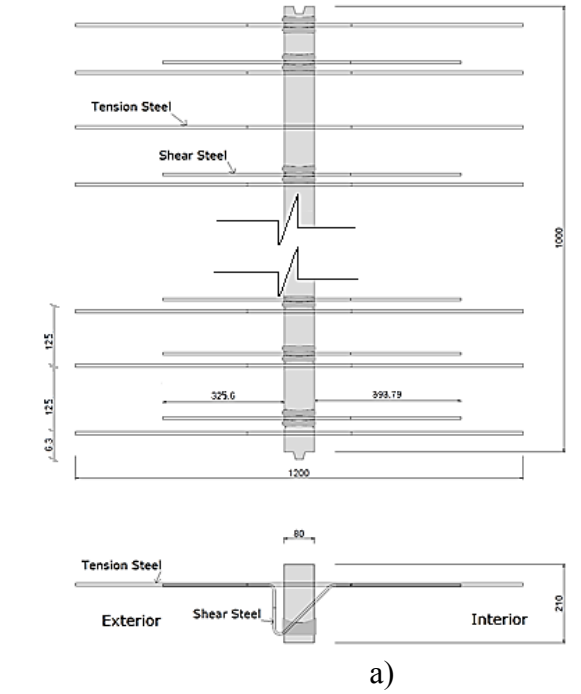

a)

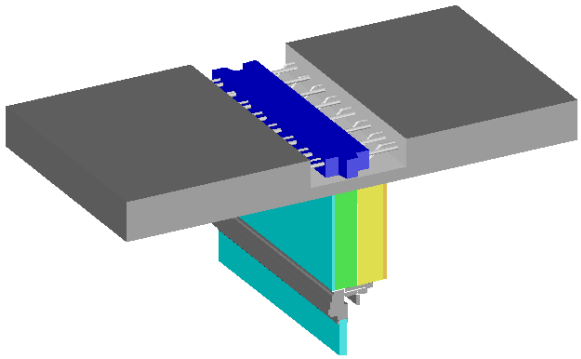

b)

Figure 3.22 a) Plan and section view of the balcony separator; b) 3D model for the balcony thermal break with reinforcement steel

Table 3.11 Thermal and physical properties of the materials (see Fig. 3.21)

Material	K_L (m^2.k/W)	ρ_L (Kg/m^3)	C_L (J/Kg. K)

External glass	1	25	1000
Extruded polystyrene insulation	0.038	25	1500
Fiberglass	0.3	30	840
Gypsum board	0.17	625	870

3.3.2 Modelling of thermal bridges

The balcony slabs are implemented in WUFI Plus programs with and without thermal break using steady state method and dynamic method to find the impact of those thermal bridges on energy performance under three different climates. To simulate the energy load of high-rise residential building, one typical floor with balcony is modelled without including the heat transfer calculation through the roof and ground floor. The dimensions of window, spandrel/spandrel balcony, sliding-door and the ratio of the different areas that are used to model the whole building are listed in the Table 3.12. The contribution of balcony as thermal bridges to the energy consumption depends on the percentage of these thermal bridges. In the current design the balcony represents 60% of the perimeter (case 1), which is about 4.3% of envelope area. To simulate a worst case, 100% perimeter is assumed, which increases the portion of the balcony to 7.1% of the envelope area (case 2).

Table 3.12 Input dimensions in the WUFI Plus program

Building components		Perimeter (m)	Height (m)	Area (m^2)	Ratio of Area
Total floor		132.58	2.94	389.79	100.00%
Balcony slab	Case 1	78.92	0.21	16.57	4.25%
	Case 2	132.58	0.21	27.84	7.1%
Spandrel/spandrel	Case 1	59.35	1.02	-	-

balcony	Case 2	113.01	1.02	-	-
Sliding door/spandrel balcony	Case 1	19.57	0.77	-	-
	Case 2	19.57	0.77	-	-
Generic/generic balcony	Case 1	78.92	0.74	-	-
	Case 2	132.58	0.74	-	-
Glass sliding door		19.57	2.00	45.98	11.80%
Windows between spandrels		30.49	1.95	59.31	15.22%
Windows on spandrel		152.15	0.64	97.57	25.03%
Total Windows		-	-	156.87	40.81%
Total windows and glass doors		-	-	202.86	52.04%

3.3.3 Equivalent U-values

THERM, a 2-dimensional conduction heat-transfer analysis program based on finite-element method developed by Lawrence Berkeley National Laboratory, is used to calculate the effective U-value for thermal bridges under steady-state. The overall U-value obtained from THERM is used as the equivalent U-value for the implementation of thermal bridge junctions in WUFI Plus program. The sub-surfaces with various dimensions that have the same component layers as the 1-D building envelope component are added in WUFI Plus to represent the junctions. In these sub-surfaces, the thickness of insulation is adjusted to achieve the equivalent U-value of junctions that obtained from THERM, while the thickness of other two layers and the physical properties of all three layers are kept the same as the 1-D multi-layer structure.

Each of the two balcony configurations was modeled five times in order to determine their overall thermal transmittance (U-values), accounting for stainless steel reinforcement, with and without the thermal break present. Stainless steel reinforcing bars were accounted for by

modeling sections for each configuration with and without the steel and taking the weighted averages of the U-values based on the steel size and spacing using equations . Without the thermal break, tension steel was modeled with the assumption that 10 M reinforcing bars with an average diameter of 11.3 mm would be used at 125 mm spacing. With the thermal break, both tension and shear steel were modeled, separately. It was assumed that eight 8 mm diameter tension reinforcing bars and four 6 mm diameter shear reinforcing bars would be used in a 1 m width of slab. For each configuration, U-values were found for the balcony taking into account reinforcement steels as thermal bridges, wall section above balcony, and wall section below balcony. Figure 3.23 shows the THERM models generated using the connection details shown in Figure 3.21.

$$U_{av\ without\ break} = \frac{(U_{Con.} * (1000 - 11.3 * 8) + U_{conc.with\ steel\ bar} * 8 * 11.3)}{1000} \quad \text{Equation [3.7]}$$

$$U_{av\ without\ break} = \frac{(U_{in.Con} * (1000 - 8 * 8 - 4 * 6) + U_{in.con\ with\ Ten.} * 8 * 8}{1000} + \frac{U_{in.con\ with\ shear\ steel} * 4 * 6}{1000} \quad \text{Equation [3.8]}$$

The exterior boundary condition was specified as -18°C and ho = 30W/m2K. The interior boundary conditions were specified as 22°C and hi = 8.3W/m2K as per CSA A440.2 (CAN/SA A440.2-09, 2009). The vertical face of the slab on the interior was specified as an adiabatic surface. Each section was modeled with a balcony slab length of 1.8 m on the exterior, and the floor slab was continued for 1 m on the inside of the wall assemblies. The effective U-values of each section for the two balcony configurations are listed in Table 3.13.

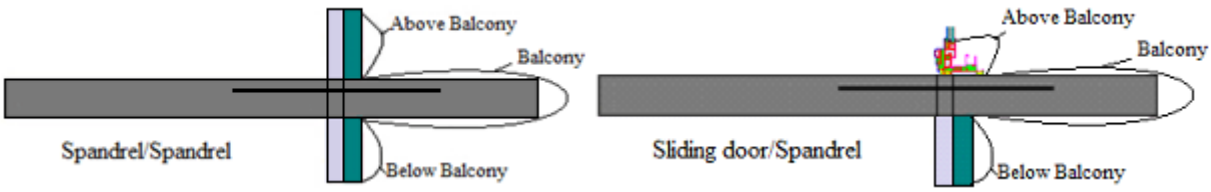

Figure 3.23 THERM models of wall configuration with U-value locations specified

Table 3.13 U-Values for different junctions of the model

Location	Spandrel/ Spandrel U- value (W/m^2 K)		Sliding door/ Spandrel U- value (W/m^2 K)		Generic/Generic balcony U- value (W/m^2 K)	
	without thermal break	with thermal break	without thermal break	with thermal break	without thermal break	with thermal break
Above-balcony	1.82	1.61	7.25	6.44	0.40	0.27
Height of sub-surface(m)	0.44		0.21		0.265	
Balcony slab	3.38	1.24	3.71	0.98	4.60	0.68
Height of sub-surface(m)	0.21					
Below-balcony	1.62	1.24	1.90	1.72	0.40	0.27
Height of sub-surface(m)	0.37		0.57		0.265	

The overall U-value of windows is 1.34 W/m^2.K and the overall U-value of sliding door is 1.34 W/m^2.K. Thermal bridges of windows and connection between windows and opaque walls are taken into account by the effective overall thermal transmittance of fenestration and modeled using THERM. The U-value for the spandrel slab edge without balcony is 1.14 W/m^2.K.

3.3.4 Direct 3D modelling in WUFI Plus

The same steps in section 3.2.6 are used to represent the two different balcony junctions as shown in Figure 3.24. The total surfaces of balcony slab junctions represent around 4% of the total surfaces of the building envelope.

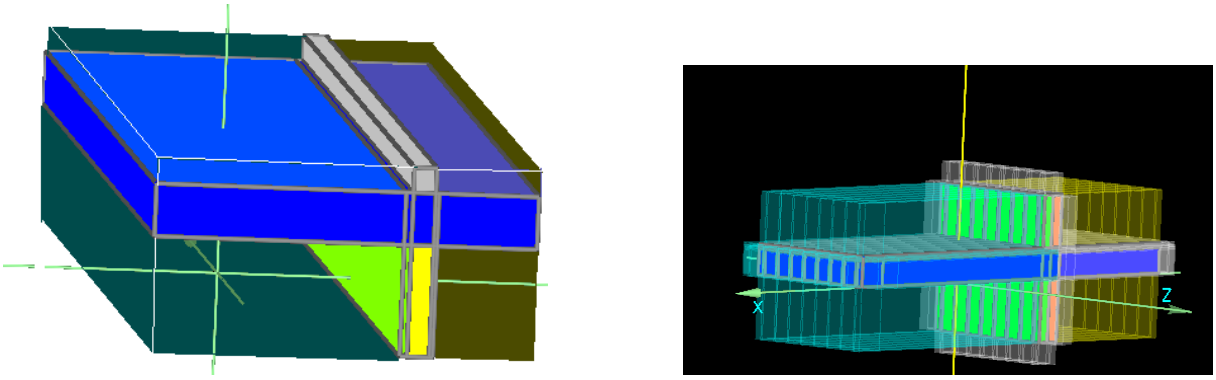

a) b)

Figure 3.24 3D models of wall configuration with the boundary conditions: a) sliding-door/spandrel balcony; b) spandrel/spandrel balcony

3.3.5 Climatic conditions

Three Canadian cities, Toronto, Edmonton and Vancouver, located in Canada Building Energy Code Climate zone 5, 7 and 4, respectively, are chosen for the whole building energy simulations. These climates were discussed in more details in section 3.2.2

These thermal bridge junctions shown in Figure 3 are simulated with two insulation levels. The insulation level is at the level of the existing building envelopes and the high insulation level meets the requirements by the latest National Energy Code of Canada for Buildings (NECB, 2011) for climate zone 7, i.e. Edmonton, and for climate zone 5, i.e. Toronto and Vancouver. The higher insulation level in building envelope is achieved by increasing the insulation thickness, therefore, in 3D direct modeling the higher insulation level is represented by using generic materials with thermal resistances to imitate well insulated walls above and below the balcony slab.

3.4 CASE STUDY 3: A HIGH RISE WOOD BUILDING

3.4.1 Introduction

A hypothetical twenty-storey multi-unit residential building with Cross-laminated Timber (CLT) construction was designed for Vancouver, Canada. Any floor located between two and twenty is a typical floor that will be selected for the whole building energy analysis using WUFI Plus as shown in Figure 3.25.

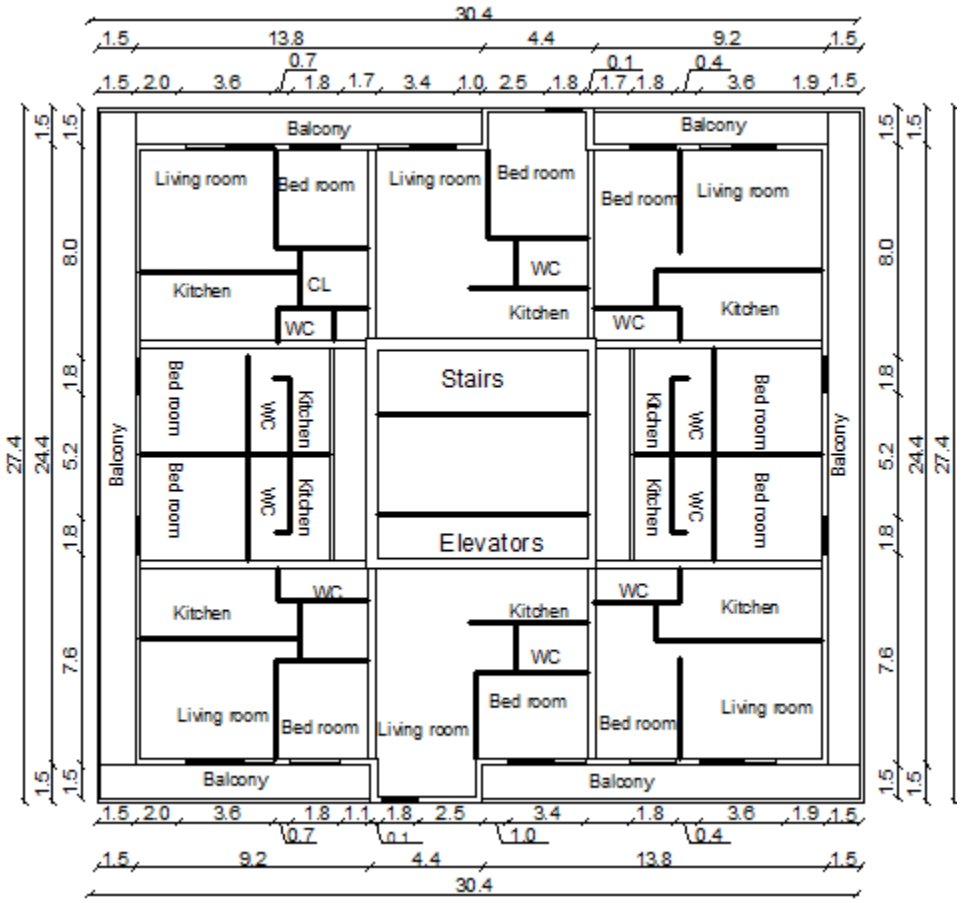

Figure 3.25 A typical floor plan for building

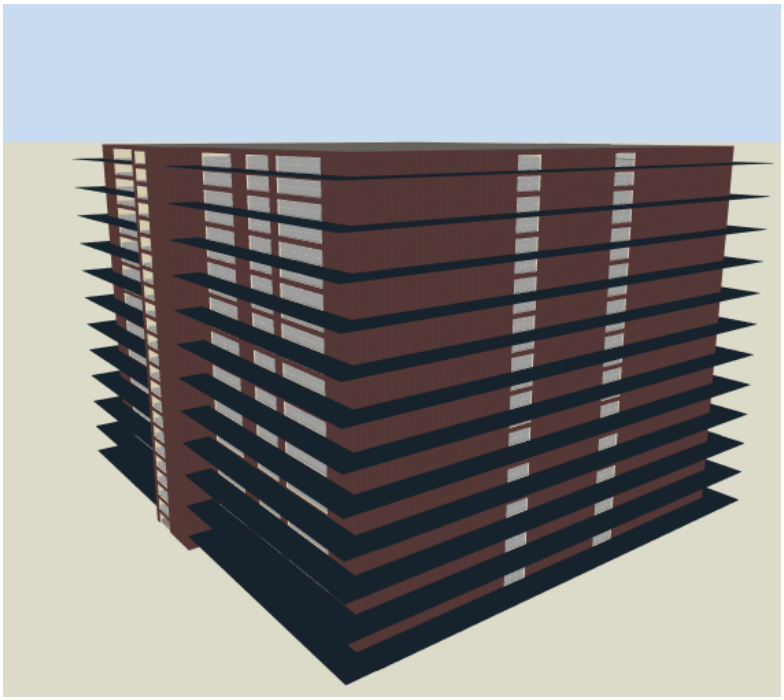

Figure 3.26 Sketch up of the selected building

CLT is a large-scale, prefabricated, solid engineered wood panel. Lightweight yet very strong, with superior acoustic, fire, seismic, and thermal performance, CLT is also fast and easy to install, generating almost no waste onsite. CLT also offers design flexibility and low environmental impacts. For these reasons, CLT is proving to be a highly advantageous alternative to conventional materials like concrete, masonry, or steel, especially in high residential and commercial construction. This advanced product was developed at 1990 in Switzerland (Gagnon and Pirvu, 2011). CLT is manufactured from multi-layered wood; toward each layer is the opposite of the direction of the next layer as shown in Figure 3.27. The best feature of this construction type is the realization of the continuous insulation concept, either through the wall itself or through the various junctions except the balcony slab. To investigate the effect of thermal mass on the dynamic simulation, the concrete construction is chosen to compare with the same dimensions of CLT construction.

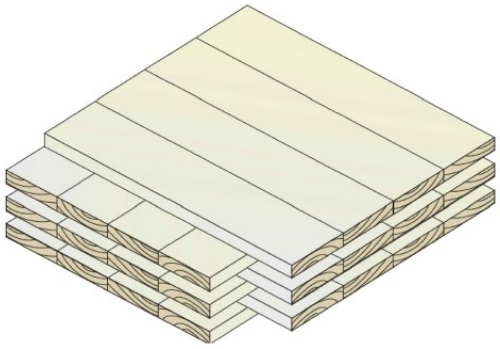

Figure 3.27 Cross laminated timber (CLT) (Gagnon and Pirvu, 2011)

This building has a typical two balcony junctions, namely external-wall/external-wall balcony and sliding door/external-wall balcony, as shown in Figure 3.28.

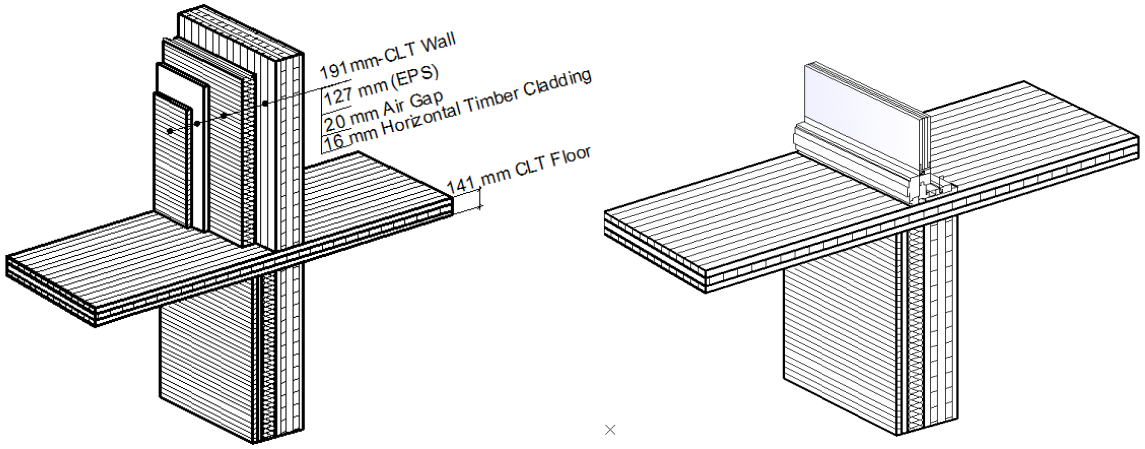

a) b)

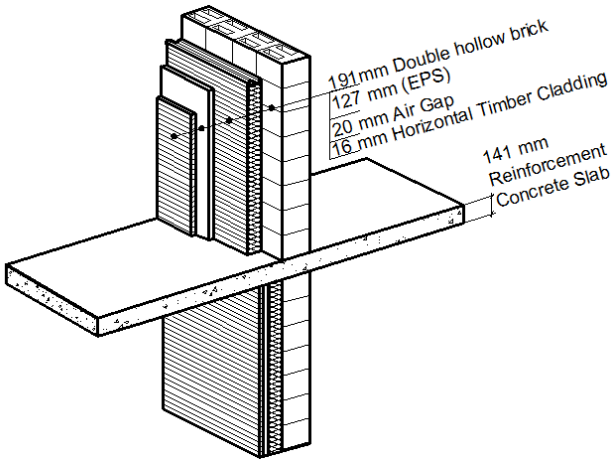

c)

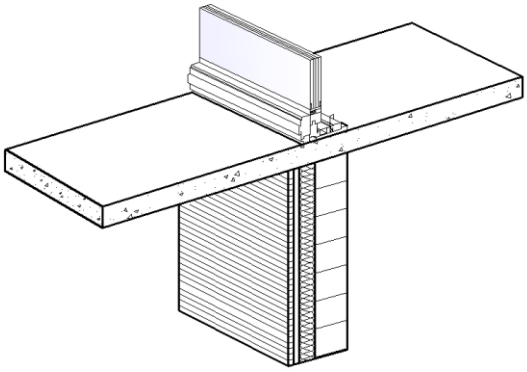

d)

Figure 3.28 Typical Sections at balcony. a) CLT wall/CLT wall balcony; b) sliding door/CLT balcony; c) concrete wall/concrete wall balcony; d) sliding door/ concrete wall balcony

Table 3.14 Thermal and physical properties of the materials in the thermal bridges

Material	K (m^2.k/W)	ρ (Kg/m^3)	C (J/Kg. K)
CLT	0.120	500.0	1880
Extruded polystyrene insulation	0.036	28.0	1220
Air gap	0.130	1.3	1000
Double Hollow Brick	0.212	630.0	1000
Reinforced Concrete Slab	1.220	1090.0	1000
Horizontal timber cladding	0.12	700	2500
Aluminum frame	200	2700	900

Figure 3.29 shows the whole building with two typical floors and external walls, but without including the heat transfer calculation through the roof and ground floors to simulate the energy load of high-rise building. Each floor is divided into five thermal zones, namely south, north,

east, west and middle. The balcony that extends on the total floor parameter is divided into two parts, the sliding-door/external wall balcony with length is 39.3 meters and external wall/external wall balcony with length is 64.3 m. The steady state equivalent U-value method and 3D dynamic modelling method are used to find the impact of those thermal bridges on the energy performance of building.

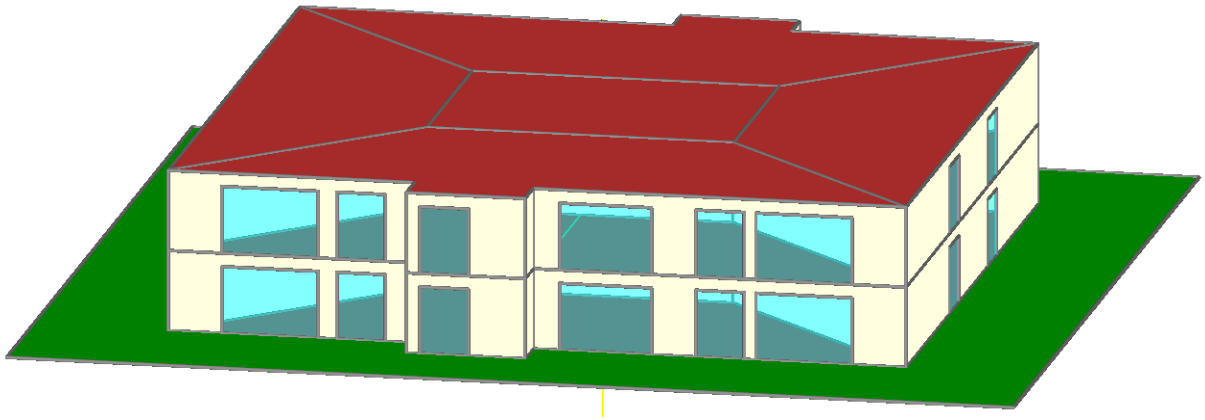

Figure 3.29 High-rise building model in WUFI Plus program

3.4.2 Equivalent U-values

The U-values of the two balcony junctions with CLT construction or concrete construction are calculated using THERM program with the exterior boundary condition T_o =-18°C and h_o = 30W/m^{2}K and the interior boundary conditions T_i =20°C and h_i = 8.3W/m^{2}K. The overall U-values of the 2D junctions are listed in Table 3.15. And again the effective U-values obtained from THERM are used to determine the insulation thickness in the equivalent U-value method to represent these thermal bridge junctions in the different sub-surfaces that are added in WUFI Plus.

Table 3.15 The U-Values for different junctions

wall configuration	CLT construction U- value (W/m^2K)	Concrete construction U- value (W/m^2K)
1D-wall	0.18	0.2
External wall/External wall balcony	0.2	0.45
Reduction	0.02	0.25
Reduction %	10%	56%
1D-wall	0.18	0.2
Sliding door/ External wall	1.58	2.49
Reduction	1.4	2.29
Reduction %	89%	92%

3.4.3 Direct 3D modelling in WUFI Plus

The same steps in section 3.2.6 are used to represent the two different balcony junctions as. The total surfaces of balcony slab junctions represent around 4% of the total surfaces of the building envelope.

4 RESULTS AND DISCUSSIONS

4.1 CASE STUDY 1: A LOW-RISE RESIDENTIAL BUILDING

In the whole building energy simulations, the heating set point is 20 ^{o}C with a night setback temperature of 18^{o}C (22:00–06:00) and the cooling set point is 25 ^{o}C with a night setback temperature of 27 ^{o}C (22:00–06:00). A natural ventilation rate of 0.5ACH and an infiltration rate of 0.1ACH are assumed. Each floor is divided into five thermal zones, four perimeter zones according to the orientation, i.e. south, north, east, west, and one core zone for the corridor. These four perimeter zones include four apartments. Each apartment is assumed with 2 adults and 2 children. The effect of thermal bridges on the energy performance is evaluated by the annual heating and cooling loads.

4.1.1 Verification of WUFI Plus

WUFI Plus program was validated for modeling the 3D thermal bridges under steady-state conditions according to DIN EN ISO 10211 (EN ISO 10211, 2007 and Antretter et al., 2013). In this study, simulation results obtained from WUFI Plus are compared with that obtained from the DesignBuilder (DesignBuilder software, 2009) for the equivalent wall and equivalent U-value methods. The difference between WUFI Plus and DesignBuilder ranges from 0.2% to 2.7% in the annual heating and cooling loads, as shown in Table 4.1. The results obtained from DesignBuilder are used as the reference.

Table 4.1 Annual heating and cooling loads obtained from DesignBuilder and the percentage difference between the DesignBuilder and WUFI Plus.

Methods	Cold Climate (Quebec city)								Hot Climate (Phoenix)			
	Low insulation level				High insulation level							
	heating load (kWhx10^3)	diff.	cooling load (kWhx10^3)	diff.	heating load (kWhx10^3)	diff.	cooling load (kWhx10^3)	diff.	heating load (kWhx10^3)	diff.	cooling load (kWhx10^3)	diff.
Eq. wall method	141.7	-1.6%	1.8	2.2%	81.5	1.2%	5.0	1.6%	3.5	0.3%	68.7	0.4%
Eq. U-value	137.6	-0.7%	2.2	0.6%	78.9	1.7%	5.3	2.0%	3.2	1.8%	66.1	0.2%
Without TB	132.2	-0.5%	2.2	0.4%	70.7	1.1%	5.6	2.7%	2.7	1.8%	64.7	0.3%

4.1.2 Annual heating and cooling loads

Table 4.2 shows the annual heating and cooling loads for the building under four scenarios: 1) direct 3D modeling; 2) equivalent wall method; 3) equivalent U-value method; and 4) without thermal bridges. The comparison among these four scenarios in terms of percentage differences in annual heating and cooling loads is shown in Figure 4.1 for the cold climate.

Table 4.2 Annual heating and cooling loads of the low-rise building under different simulation scenarios.

Implementation Methods	Quebec city				Toronto		Vancouver	
	Low insulation level		High insulation level					
	heating load (kWh×10^3)	cooling load	heating load (kWh×10^3)	cooling load	heating load (kWh×10^3)	cooling load	heating load (kWh×10^3)	cooling load

		($kWh \times 10^3$)		($kWh \times 10^3$)		($kWh \times 10^3$)		($kWh \times 10^3$)
3D Modeling	156.80	1.71	83.60	4.79	60.0	7.77	41.5	5.27
Equivalent wall	144.00	1.78	80.60	5.29	57.7	7.93	39.6	5.58
Equivalent U-value	138.60	2.16	77.40	4.92	55.4	8.10	37.8	5.27
Without TB	132.90	2.25	69.80	5.43	49.6	8.60	33.4	5.82

Table 4.3 Annual heating and cooling loads of the low-rise building under different simulation scenarios.

Implementation Methods	Hot Climate (Phoenix)	
	heating load ($kWh \times 10^3$)	cooling load ($kWh \times 10^3$)
3D Modeling	3.57	77.60
Equivalent wall	3.47	68.40
Equivalent U-value	3.30	66.21
Without TB	2.75	64.43

For Quebec City climate with low-insulation level, the implementation of junctions through 3D dynamic modeling results in an increase of annual heating load by 18% and a reduction of annual cooling load by 24% compared to the case without thermal bridges. The annual heating load modeled using the 3D dynamic method is 9% and 13% higher than that modelled using the equivalent wall method and equivalent U-value method, respectively. The annual cooling load modeled using the 3D dynamic method is 4% and 21% lower than that modelled using the equivalent wall method and equivalent U-value method, respectively.

For Quebec City climate with high insulation level, the implementation of junctions through 3D dynamic model results in an increase of the annual heating load by 20% and a reduction of the annual cooling load by 12% compared to the case without thermal bridges. The annual heating load modeled using the 3D dynamic method is 4% and 8% higher than that modelled using the equivalent wall method and equivalent U-value method, respectively. The annual cooling load modeled using the 3D dynamic method is 3% and 9% lower than that modelled using the equivalent wall method and equivalent U-value method, respectively.

These results show that at the low insulation level, the dynamic analysis of thermal bridges has relatively greater impact on the cooling energy demand although the annual cooling load is less

than 2% of the annual space heating load; and the equivalent wall method performs better modeling the cooling load than modeling heating load when compared to the 3D dynamic analysis. With the increase of thermal insulation level, the effect of thermal bridges on the annual heating load increases, while their effect on the annual cooling load decreases. On the other hand, the difference among the three modeling approaches decreases, especially for the cooling load. The dynamic effect of thermal bridges is reduced with higher insulation level. This may be explained by the structural factors shown in Tables 3.6-3.9 for the equivalent wall method. At a higher insulation level, φ_{ie}, it is clear that the structure factor indicating the responses of the structure to exterior excitation decreases.

For Toronto climate, the presence of junctions through 3D dynamic modeling results in an increase of annual heating load by 21% and a reduction of annual cooling load by 9.7% compared to the case without thermal bridges. The annual heating load modeled using the 3D dynamic method is 4.1% and 8.4% higher than that modelled using the equivalent wall method and equivalent U-value method, respectively. The annual cooling load modeled using the 3D dynamic method is 2% and 4.1% lower than that modelled using the equivalent wall method and equivalent U-value method, respectively.

For Vancouver climate, the implementation of junctions through 3D dynamic model results in an increase of the annual heating load by 24.3% and a reduction of the annual cooling load by 9.5% compared to the case without thermal bridges. The annual heating load modeled using the 3D dynamic method is 5% and 10% higher than that modelled using the equivalent wall method and equivalent U-value method, respectively. The annual cooling load modeled using the 3D dynamic method is 0.1% and 5.6% lower than that modelled using the equivalent wall method and equivalent U-value method, respectively.

The annual heating and cooling loads for different simulation scenarios are listed in Table 4.2. Although the absolute annual space heating load increase due to the four junctions as thermal bridges (when compared with the case without taking into account thermal bridges) is higher for colder climate (13.8MWh in Quebec City v.s. 8.1 MWh in Vancouver), the percentage increase of the thermal bridge contribution is smaller for colder climate (19.8% in Quebec City v.s. 24.3% in Vancouver) because of the higher spacing heating load in Quebec City. In

addition, the dynamic analysis of thermal bridges has relatively greater impact on the coldest climate; and the equivalent wall method performs better than modeling the equivalent U-value method.

Table 4.4 Difference in annual heating loads among the three thermal bridge modeling methods, for the cold climate with high insulation level

	Quebec City	Toronto	Vancouver
comparison between the Scenarios	Annual heating difference (KWh $x10^3$)	Annual heating difference (KWh $x10^3$)	Annual heating difference (KWh $x10^3$)
3D/O	13.8	10.4	8.1
3D/Eq. wall	3.0	2.3	1.9
3D/Eq.U-value	6.2	4.6	3.7
Eq.wall/Eq.U-value	3.2	2.3	1.8

For the hot climate, as shown in Figure 4.2, the implementation of junctions through 3D dynamic modeling increases the annual heating load by 30% and increases the annual cooling load by 20% compared to the case without thermal bridges. The annual heating load modeled using the 3D dynamic method is 3% and 8% higher than that modelled using the equivalent wall method and equivalent U-value method, respectively. The annual space heating load is less than 5% of the annual cooling load. Therefore, it is more important to look at the effect on annual space cooling load. The annual cooling load modeled using the 3D dynamic method is 14% and 17% higher than that modelled using the equivalent wall method and equivalent U-value method, respectively. These results indicate that the equivalent wall method performs better than the equivalent U-value method. However, both methods may considerably underestimate the cooling loads for hot climate.

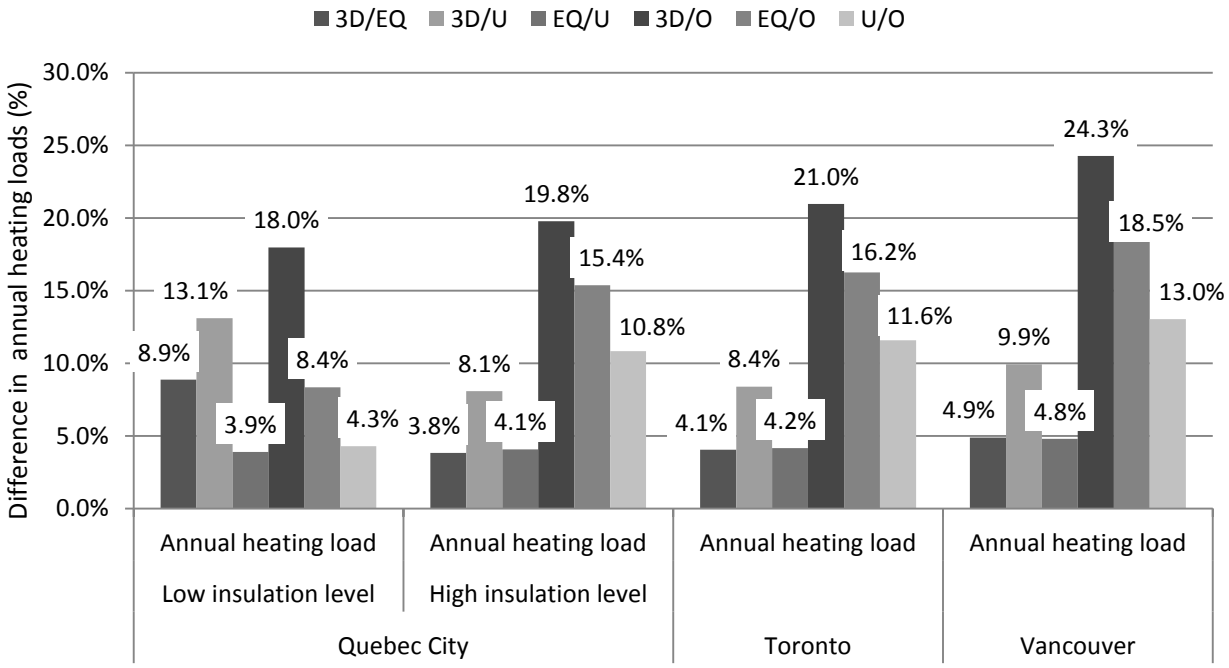

Figure 4.1a Percentage difference in annual heating loads among the three thermal bridge modeling methods for the cold climate.

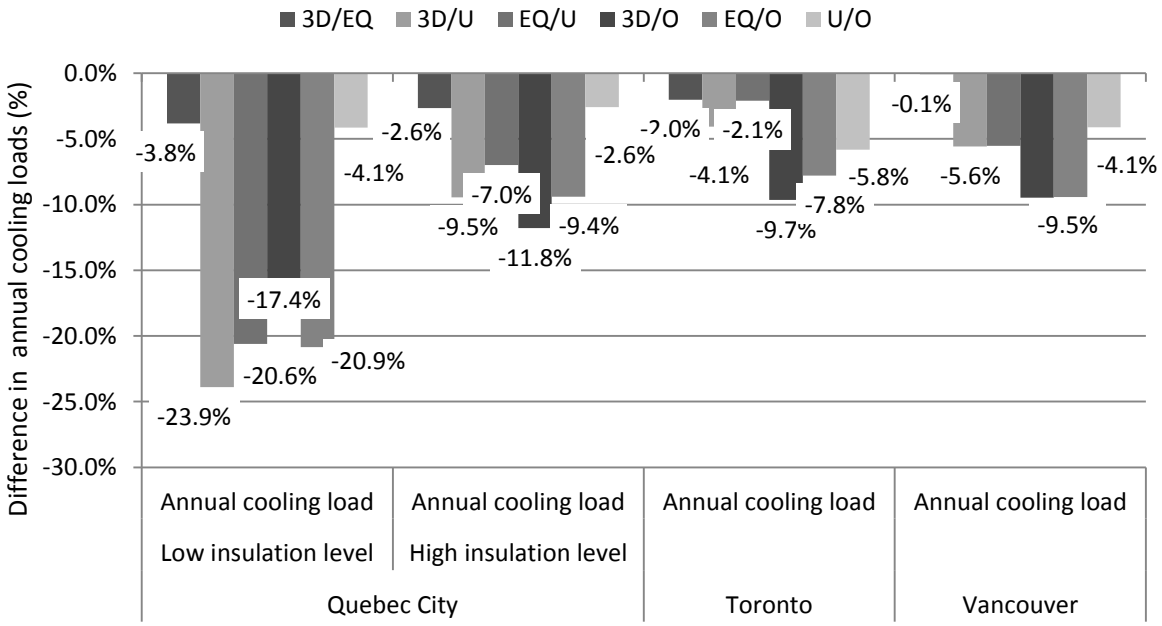

Figure 4.1b Percentage difference in annual cooling loads among the three thermal bridge modeling methods for the cold climate.

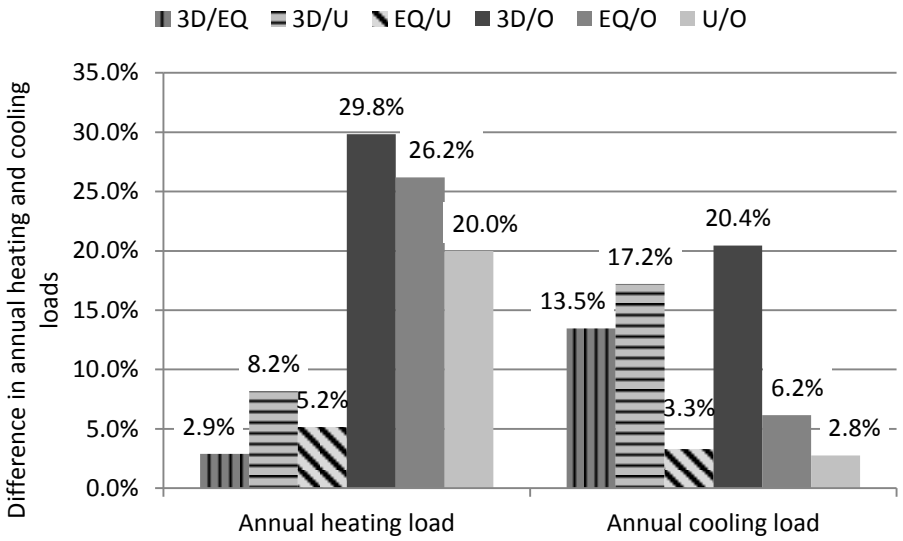

Figure 4.2 Percentage difference in annual heating and cooling loads among the three thermal bridge modeling methods for the hot climate.

4.1.3 Surface Temperature and condensation risk

To investigate the effect of thermal bridges on the surface temperature and the condensation risk, the four different junctions are simulated as 3D modelling under dynamic and steady state condition for Quebec City climate with two insulation levels. For dynamic condition the temperature was measured for each hour per year, while in the steady state condition the mean temperature for each month was selected from Environment Canada, "Canadian climate normals 1981-2010," Québec, Jean-Lesage station, Québec (Canadian climate normal, 2014). Figure 4.3 and 4.4 show the dynamic and steady state conditions that were defined in WUFI Plus program, respectively.

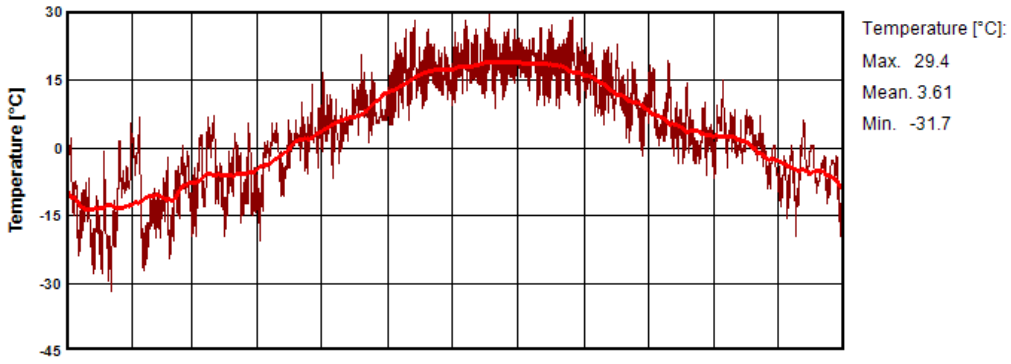

Figure 4.3 Quebec City climate under dynamic condition

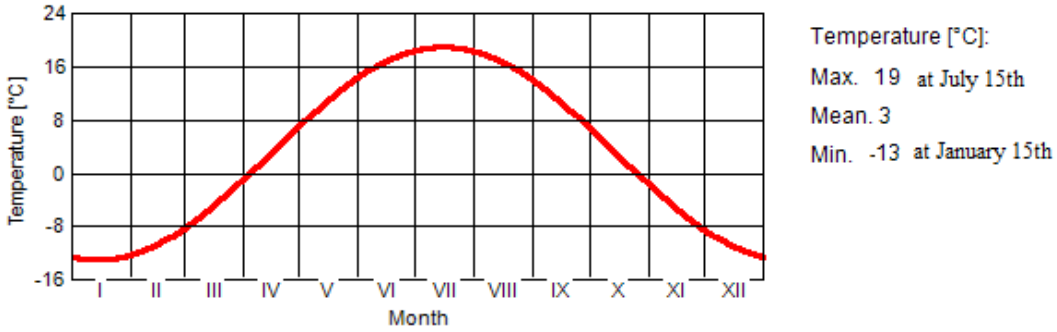

Figure 4.4 Quebec City climate under steady state condition

The condensation risks that result for each junction are listed in Table 4.3. To estimate the condensation risk, the surface temperature at the meeting point of external wall and slab and the interior dew point are calculated under dynamic and steady state conditions as show in Figure 4.5.

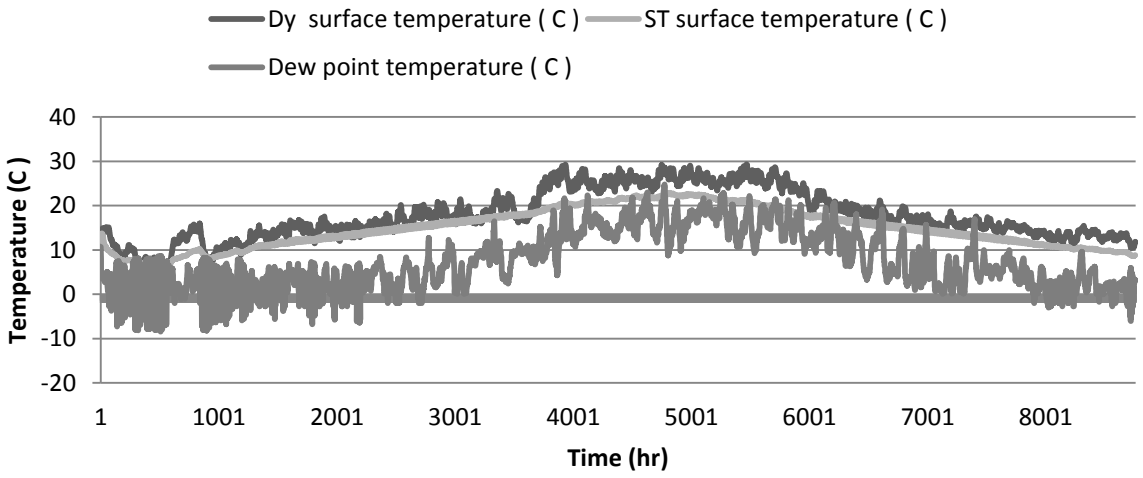

DY: Dynamic simulation; ST: Steady state simulation

Figure 4.5 Surface temperature at balcony junction and interior dew point temperature

Table 4.5 Condensation risk results for the each junction

	Condensation risk ratio					
	High insulation level			Low insulation level		
Junction	DY* simulation	ST* simulation	Difference (ST-DY)	DY* simulation	ST* simulation	Difference (ST-DY)
Balcony junction	0.2%	1.4%	1.2%	2.2%	7.6%	5.4%
Intermediate junction	0.4%	9.2%	8.8%	7.5%	18.1%	10.6%
Roof junction	0.4%	7.7%	7.3%	1.1%	10.8%	9.7%
Ground	0.1%	0.3%	0.2%	0.2%	0.5%	0.3%

junction

*DY and ST are a shortcut to the dynamic and steady state, respectively

These results indicate that the dynamic condition increases the surface temperature and reduces the condensation risk compared with steady state condition. Also, they show that with increasing of insulation level, the condensation risk decreases. For example, the results show that the balcony junction that modelled under dynamic condition increases the condensation risk at interior surface by 0.2% and 2.2% with high and low insulation level, respectively, while under steady state condition increases by 1.4% and 7.6% with high and low insulation level, respectively.

4.2 CASE STUDY 2: A HIGH RISE RESIDENTIAL BUILDING

In the whole building energy simulations, the heating set point is 22 ^{o}C with a night setback temperature of 18 ^{o}C (22:00-6:00) and the cooling set point is 25 ^{o}C with a night setback temperature of 27 ^{o}C (22:00-6:00). A natural ventilation rate of 0.5ACH and an infiltration rate of 0.1ACH are assumed. Each floor is divided into five thermal zones, four perimeter zones according to the orientation, i.e. south, north, east, west, and one core zone for the corridor. These four perimeter zones include twelve apartments with occupancy of 0.04 people/m^2 assumed. The effect of thermal bridges on the energy performance is evaluated by the annual heating and cooling loads.

4.2.1 Verification of WUFI Plus

WUFI Plus program was validated for modeling the 3D thermal bridges under steady-state conditions according to DIN EN ISO 10211 (EN ISO 10211, 2007) by Antretter et. al (Antretter et al., 2013), as mentioned in section 4.1.1. In this study, simulation results obtained from WUFI Plus are compared with that obtained from the DesignBuilder for the equivalent U-value method and the case without accounting thermal bridges. As an example, the difference between WUFI Plus and DesignBuilder are ranges from 1.1% to 2.4% in the annual heating and cooling loads for Toronto, as shown Table 4.6. The results obtained from DesignBuilder are used as the reference.

Table 4.6 Annual heating and cooling loads obtained from DesignBuilder and the percentage difference between the DesignBuilder and WUFI Plus for Toronto.

Methods	Without thermal break				With thermal break			
	Heating load ($kWhx10^3$)	Diff.	Cooling load ($kWhx10^3$)	Diff.	Heating load ($kWhx10^3$)	Diff.	Cooling load ($kWhx10^3$)	Diff
Eq. U-value	66.4	1.1%	8.1	2.8%	64.1	2.2%	97.6	2.4%
Without TB	56.4	1.3%	10.7	2.3%	56.4	1.3%	10.7	2.3%

4.2.2 Annual heating and cooling loads

The annual space heating and cooling loads for the high-rise building are simulated for three Canadian cities under three scenarios: 1) direct 3D modeling with and without thermal break; 2) equivalent U-value method with and without thermal break; and 3) without thermal bridges. The results are listed in Tables 4.7-4.10. Figures 4.6-4.11 show the comparison among these three scenarios in terms of percentage differences in annual heating and cooling loads for the three Canadian cities.

Table 4.7 Annual heating and cooling loads of one typical floor of the high-rise building as designed (balcony slab ratio of 60%).

		Edmonton		Toronto		Vancouver	
Implementation Methods		Annual heating load (kWh $\times 10^3$)	Annual cooling load (kWh $\times 10^3$)	Annual heating load (kWh $\times 10^3$)	Annual cooling load (kWh $\times 10^3$)	Annual heating load (kWh $\times 10^3$)	Annual cooling load (kWh $\times 10^3$)
3D Modeling	without thermal break	90.4	2.8	67.7	7.9	49.4	5.2
	with thermal break	85.7	3.1	63.8	8.2	46.3	5.5
Eq. U-value	without thermal	88.5	4.1	65.7	9.2	47.7	6.9

	break						
	with thermal break	84.7	4.4	62.7	9.5	45.3	7.2
Without thermal bridge		75.53	75.5	5.2	55.6	10.4	39.8

Table 4.8 Annual heating and cooling loads of one typical floor in this high-rise building as designed with assumed balcony slab ratio of 100%.

		Edmonton		Toronto		Vancouver	
Implementation Methods		Annual heating load (kWh $\times 10^3$)	Annual cooling load (kWh $\times 10^3$)	Annual heating load (kWh $\times 10^3$)	Annual cooling load (kWh $\times 10^3$)	Annual heating load (kWh $\times 10^3$)	Annual cooling load (kWh $\times 10^3$)
3D Modeling	without thermal break	93.0	2.7	69.1	7.4	50.8	4.7
	with thermal	87.8	3.0	65.1	7.9	47.6	5.0

	break						
Eq. U-value	without thermal break	89.7	4.7	66.4	9.2	48.5	6.6
	with thermal break	85.4	5.1	63.0	9.7	45.8	6.9
Without thermal bridge		75.53	75.5	5.2	55.6	10.4	39.8

Table 4.9 Annual heating and cooling loads of one typical floor of the high-rise building with hypothetical generic spandrel balcony and high insulation level and balcony slab ratio of 60%.

	Edmonton		Toronto		Vancouver	
Implementation Methods	Annual heating load (kWh $\times 10^3$)	Annual cooling load (kWh $\times 10^3$)	Annual heating load (kWh $\times 10^3$)	Annual cooling load (kWh $\times 10^3$)	Annual heating load (kWh $\times 10^3$)	Annual cooling load (kWh $\times 10^3$)

3D Modeling	without thermal break	60.1	5.1	44.7	9.5	31.1	7.0
	with thermal break	51.8	6.0	38.5	10.4	26.3	7.7
Eq. U-value	without thermal break	57.6	8.1	42.0	12.2	28.9	10.1
	with thermal break	51.2	8.9	37.5	12.9	25.3	10.8
Without thermal bridge		50.49	50.5	9.8	35.6	14.5	24.1

Table 4.10 Annual heating and cooling loads of one typical floor of the high-rise building with hypothetical spandrel balcony and high insulation level and a balcony slab ratio of 100%.

		Edmonton		Toronto		Vancouver	
Implementation Methods		Annual heating load (kWh $\times 10^3$)	Annual cooling load (kWh $\times 10^3$)	Annual heating load (kWh $\times 10^3$)	Annual cooling load (kWh $\times 10^3$)	Annual heating load (kWh $\times 10^3$)	Annual cooling load (kWh $\times 10^3$)
3D Modeling	without thermal break	62.7	4.2	46.7	8.6	32.8	6.3
	with thermal break	52.3	5.2	38.7	9.8	26.6	7.4
Eq. U-value	without thermal break	60.1	7.7	43.8	12.4	30.2	9.7
	with thermal break	51.7	8.9	37.8	13.4	25.6	11.0

Without thermal bridge	50.49	50.5	9.8	35.6	14.5	24.1

For Edmonton, a city located in the coldest climatic zone among the three cities, the presence of thermal bridge i.e. balcony slab increases the annual heating load by 19.6%, while reduces the cooling load by 46.2% compared to the case without accounting for thermal bridges when the 3D dynamic method is used. The annual cooling load is only 2.9% of the annual space heating loads. The implementation of thermal break in the balcony slabs reduces the annual heating load by 5.2%, while increases the annual cooling load by 10.8% when the 3D dynamic modeling method is used. The annual heating load modeled using the 3D dynamic method is 2.1% higher, while the annual cooling load is 31.8% lower than that modelled using the equivalent U-value method, respectively. With the application of thermal break in the balcony, the difference between 3D dynamic method and the equivalent U-value method is slightly reduced to 1.2% for the annual heating load and 29.1% for the cooling load, respectively. With the increase in the amount of thermal bridges, i.e. when the balcony slab ratio is increased to 100% perimeter, the effect of thermal bridges on the heating load and on the effectiveness of implementing thermal break is slightly increased. The inclusion of balcony slab as thermal bridges in the modeling increases the annual heating load by 23.1% compared to the case without thermal bridges and the implementation of thermal break in the balcony slabs reduces the annual heating load by 5.6% when the 3D dynamic modeling method is used. The difference between 3D dynamic method and the equivalent U-value method slightly increases. The annual heating load modelled using the 3D dynamic method is 3.7% higher, while the annual cooling load is 41.8% lower than that modelled using the equivalent U-value method, respectively. With the application of thermal break in the balcony, the difference between 3D dynamic method and the equivalent U-value method is slightly reduced to 2.9% for the annual heating load and 40.7% for the cooling load, respectively.

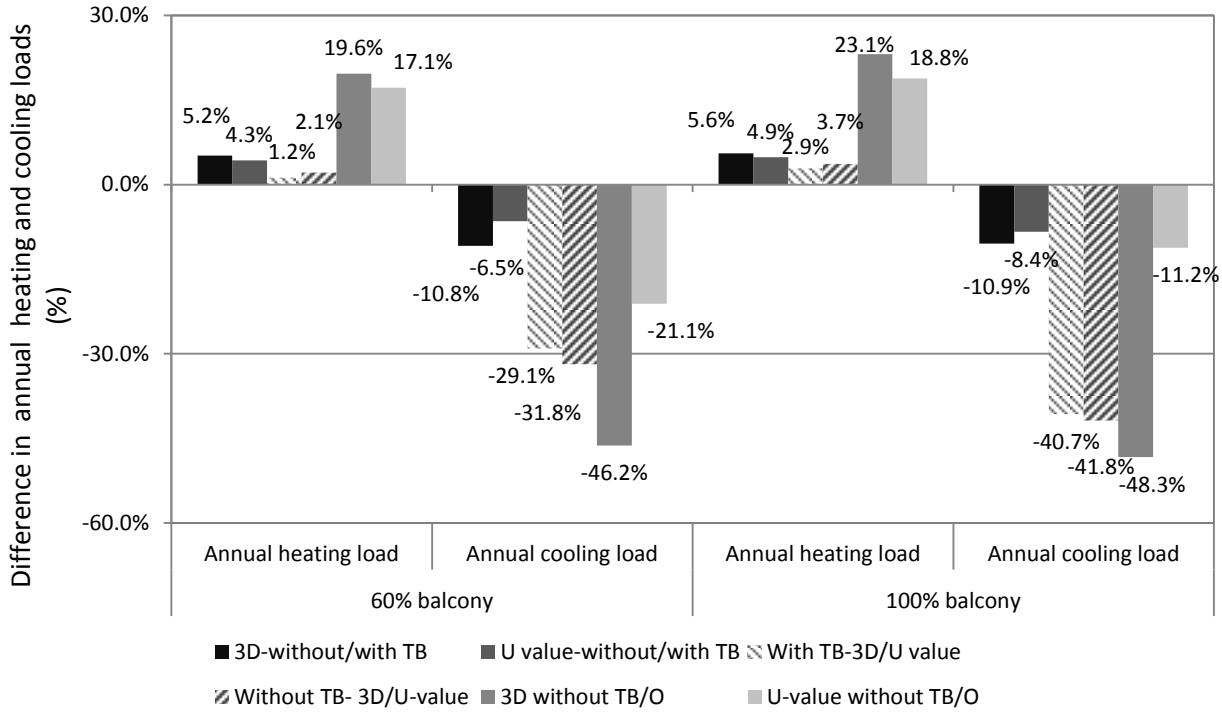

*TB-Thermal break, and O- no balcony thermal bridge included

Figure 4.6 Percentage difference in annual heating loads between the two thermal bridge modeling methods for Edmonton (as-designed balcony)

When a hypothetical well-insulated spandrel walls assumed below and above the balcony, the effect of thermal bridges on the heating load and on the effectiveness of implementing thermal break is increased. The inclusion of balcony slab as thermal bridges in the modeling increases the annual heating load by 23.2% compared to the case without thermal bridges and the implementation of thermal break in the balcony slabs reduces the annual heating load by 13.9 when the 3D dynamic modeling method is used. The difference between 3D dynamic method and the equivalent U-value method increases. The annual heating load modelled using the 3D dynamic method is 4.4% higher, while the annual cooling load is 36.6% lower than that modelled using the equivalent U-value method, respectively. With higher amount of thermal bridges, i.e. when the balcony slab ratio is increased to 100% perimeter, the effect of thermal bridges and the effectiveness of thermal break in balcony slab becomes more significant. The inclusion of balcony slab as thermal bridges in the modeling increases the annual heating load by 28.5% compared to the case without thermal bridges and the implementation of thermal

break in the balcony slabs reduces the annual heating load by 16.6% when the 3D dynamic modeling method is used. The annual heating load modelled using the 3D dynamic method is 4.4% higher than that modelled using the equivalent U-value method. The implementation of thermal breaks in the balcony reduces this difference to 1.0% for a balcony slab ratio of 60% and the same result for a balcony slab ratio of 100%. These results indicate that it is more important to reduce thermal bridging for well-insulated envelopes.

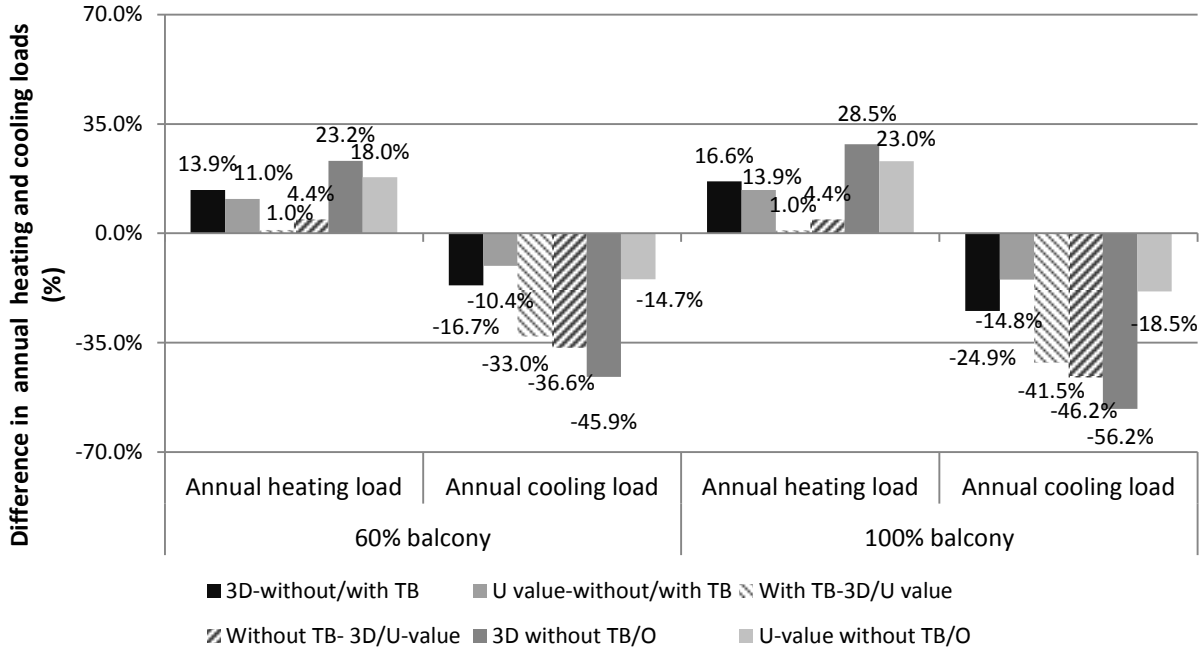

*TB-Thermal break, and O- no balcony thermal bridge included

Figure 4.7 Percentage difference in annual heating loads between the two thermal bridge modeling methods for Edmonton (hypothetical generic balcony)

Similar results are observed for Toronto and Vancouver. For Toronto, a city located in the 2nd coldest climatic zone among the three cities, the presence of thermal bridge increases the annual heating load by 21.7%, while reduces the cooling load by 24.8% compared to the case without thermal bridges when the 3D dynamic method is used. The annual cooling load is 11.8% of the annual space heating load. The implementation of thermal break in the balcony slabs reduces the annual heating load by 5.7%, while increases the annual cooling load by 5.0% when the 3D dynamic modeling method is used. The annual heating load modeled using the 3D dynamic

method is 3.1% higher, while the annual cooling load is 14.6% lower than that modelled using the equivalent U-value method, respectively. With the application of thermal break in the balcony, the difference between 3D dynamic method and the equivalent U-value method is slightly reduced to 1.8% for the annual heating load and 13.4% for the cooling load, respectively. When the balcony slab ratio is increased to 100% perimeter, the inclusion of balcony slab as thermal bridges in the modeling increases the annual heating load by 24.1% compared to the case without thermal bridges and the implementation of thermal break in the balcony slabs reduces the annual heating load by 5.7% when the 3D dynamic modeling method is used. The annual heating load modelled using the 3D dynamic method is 4.0% higher, while the annual cooling load is 19.2% lower than that modelled using the equivalent U-value method, respectively. With the application of thermal break in the balcony, the difference between 3D dynamic method and the equivalent U-value method is slightly reduced to 3.4% for the annual heating load and 18.5% for the cooling load, respectively.

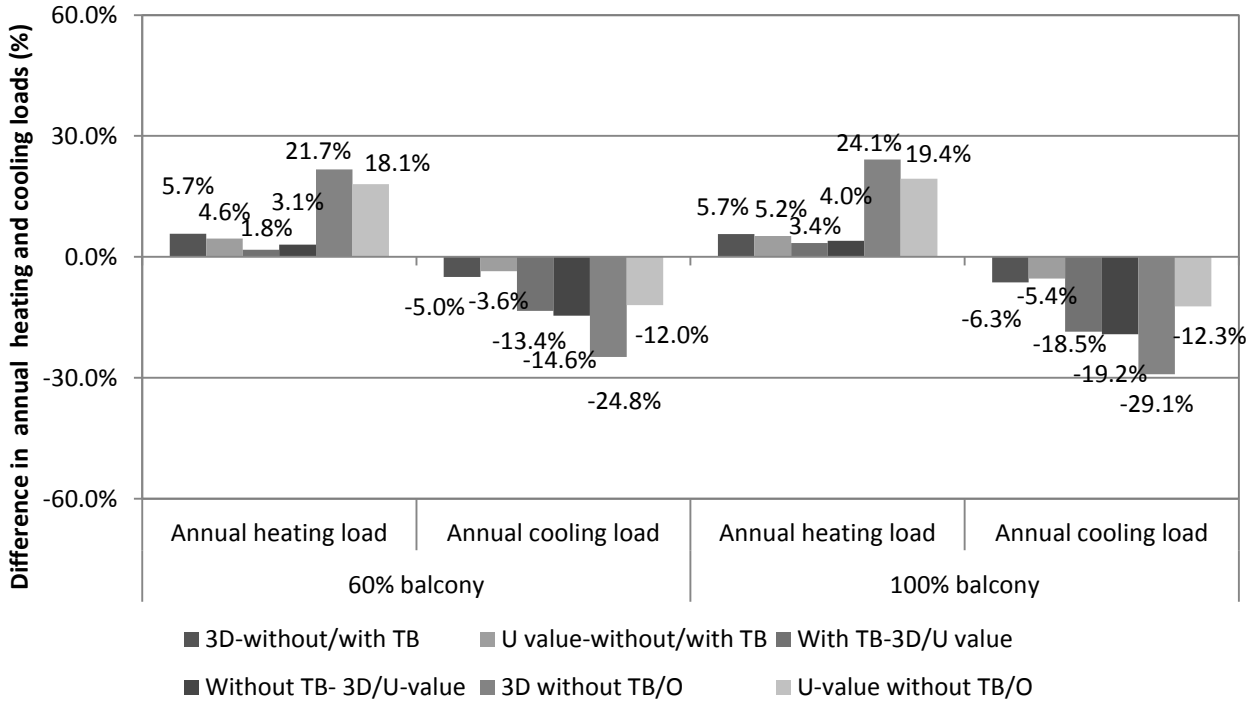

*TB-Thermal break, and O- no balcony thermal bridge included

Figure 4.8 Percentage difference in annual heating and loads between the two thermal bridge modeling methods for Toronto (as-designed balcony)

When a hypothetical well-insulated spandrel walls are assumed below and above the balcony, the inclusion of balcony slab as thermal bridges in the modeling increases the annual heating load by 25.3% compared to the case without thermal bridges and the implementation of thermal break in the balcony slabs reduces the annual heating load by 14.1% when the 3D dynamic modeling method is used. The annual heating load modelled using the 3D dynamic method is 6.3% higher, while the annual cooling load is 22.1% lower than that modelled using the equivalent U-value method, respectively. When the balcony slab ratio is increased to 100% perimeter, the inclusion of balcony slab as thermal bridges in the modeling increases the annual heating load by 31.0% compared to the case without thermal bridges and the implementation of thermal break in the balcony slabs reduces the annual heating load by 17.0% when the 3D dynamic modeling method is used. The annual heating load modelled using the 3D dynamic method is 6.6% higher than that modelled using the equivalent U-value method. The implementation of thermal breaks in the balcony reduces this difference to 2.6% for a balcony slab ratio of 60% and 100%. These results indicate that it is more important to reduce thermal bridging for well-insulated envelopes.

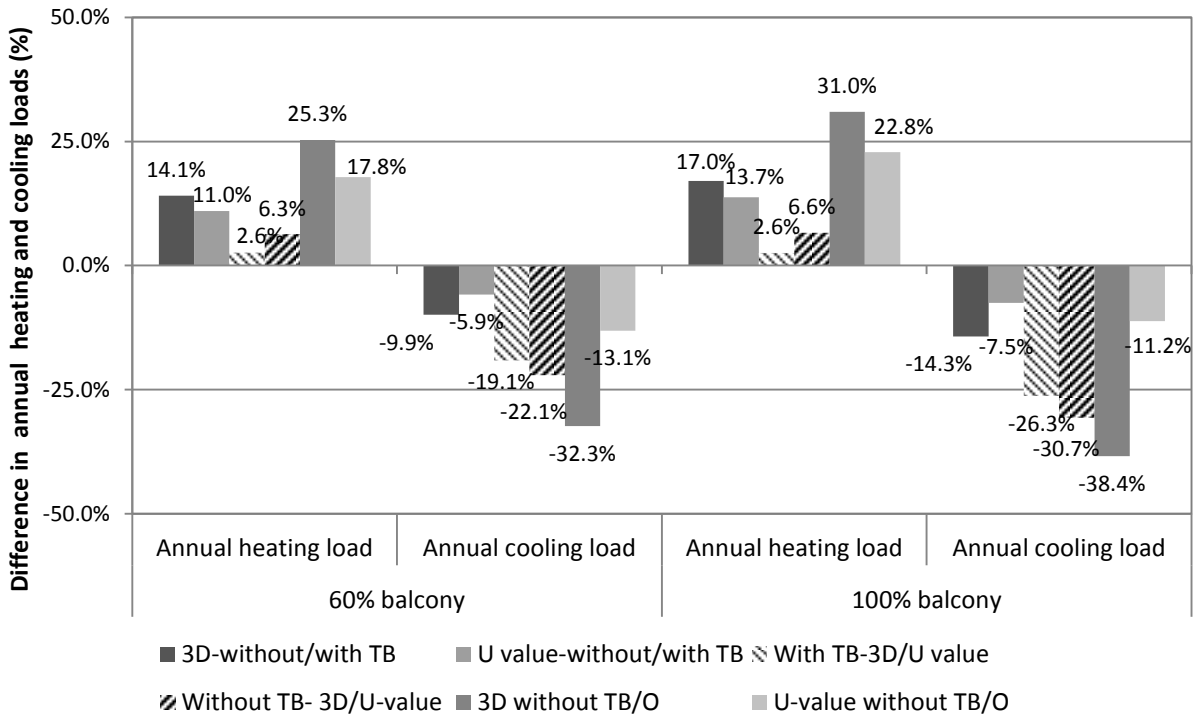

*TB-Thermal break, and O- no balcony thermal bridge included

Figure 4.9 Percentage difference in annual heating and loads between the two thermal bridge modeling methods for Toronto (hypothetical generic balcony)

For Vancouver, a city located in the mildest climatic zone among the three cities, the presence of thermal bridge increases the annual heating load by 24.3%, while reduces the cooling load by 32.9% compared to the case without thermal bridges when the 3D dynamic method is used. The annual cooling load is 10.1% of the annual space heating load. The implementation of thermal break in the balcony slabs reduces the annual heating load by 6.3%, while increases the annual cooling load by 6.7% when the 3D dynamic modeling method is used. The annual heating load modeled using the 3D dynamic method is 3.6% higher, while the annual cooling load is 25.8% lower than that modelled using the equivalent U-value method, respectively. With the application of thermal break in the balcony, the difference between 3D dynamic method and the equivalent U-value method is slightly reduced to 2.1% for the annual heating load and 24.0% for the cooling load, respectively.

When the balcony slab ratio is increased to 100% perimeter, the inclusion of balcony slab as thermal bridges in the modeling increases the annual heating load by 27.8% compared to the case without thermal bridges and the implementation of thermal break in the balcony slabs reduces the annual heating load by 6.3% when the 3D dynamic modeling method is used. The annual heating load modelled using the 3D dynamic method is 4.7% higher, while the annual cooling load is 28.7% lower than that modelled using the equivalent U-value method, respectively. With the application of thermal break in the balcony, the difference between 3D dynamic method and the equivalent U-value method is slightly reduced to 4.0% for the annual heating load and 27.0% for the cooling load, respectively.

When a hypothetical well-insulated spandrel walls are assumed below and above the balcony, the inclusion of balcony slab as thermal bridges in the modeling increases the annual heating load by 29.3% compared to the case without thermal bridges and the implementation of thermal break in the balcony slabs reduces the annual heating load by 15.6% when the 3D dynamic modeling method is used. The annual heating load modelled using the 3D dynamic method is7.8% higher, while the annual cooling load is 30.8% lower than that modelled using the equivalent U-value method, respectively. When the balcony slab ratio is increased to 100% perimeter, the inclusion of balcony slab as thermal bridges in the modeling increases the annual heating load by 36.2% compared to the case without thermal bridges and the implementation of thermal break in the balcony slabs reduces the annual heating load by 18.7% when the 3D dynamic modeling method is used. The annual heating load modelled using the 3D dynamic method is 8.5% higher than that modelled using the equivalent U-value method. The implementation of thermal breaks in the balcony reduces this difference to 3.8% for both the balcony slab ratio of 60% and 100%.

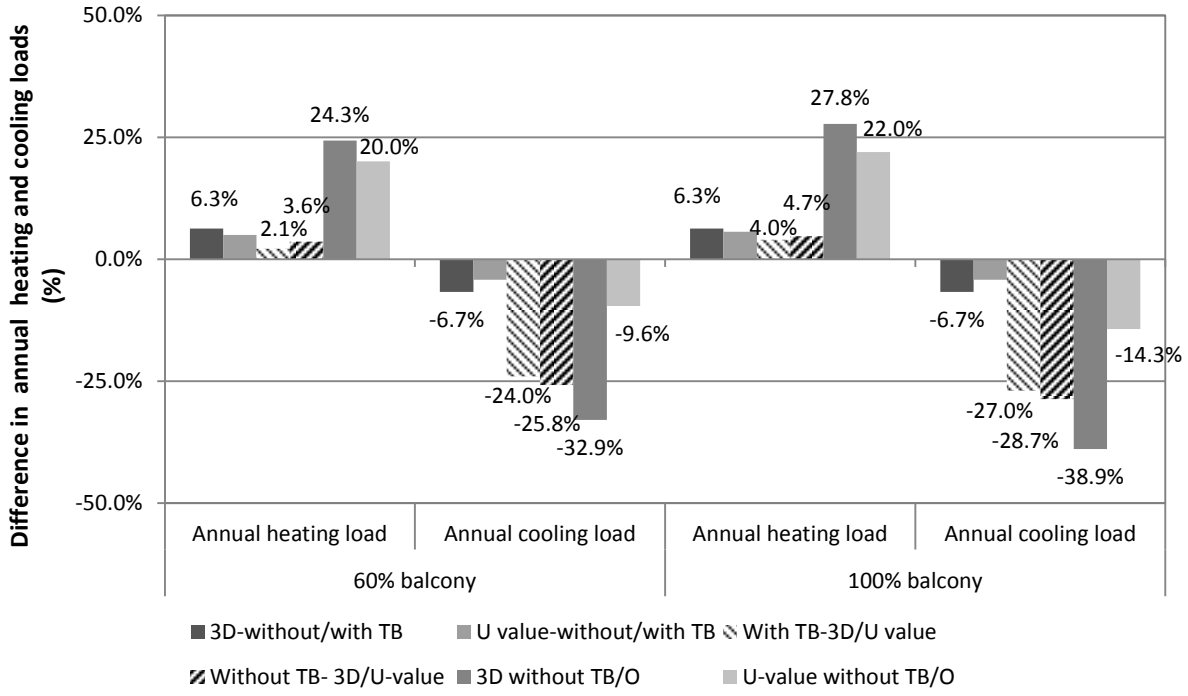

*TB-Thermal break, and O- no balcony thermal bridge included

Figure 4.10 Percentage difference in annual heating and loads between the two thermal bridge modeling methods for Vancouver (as-designed balcony)

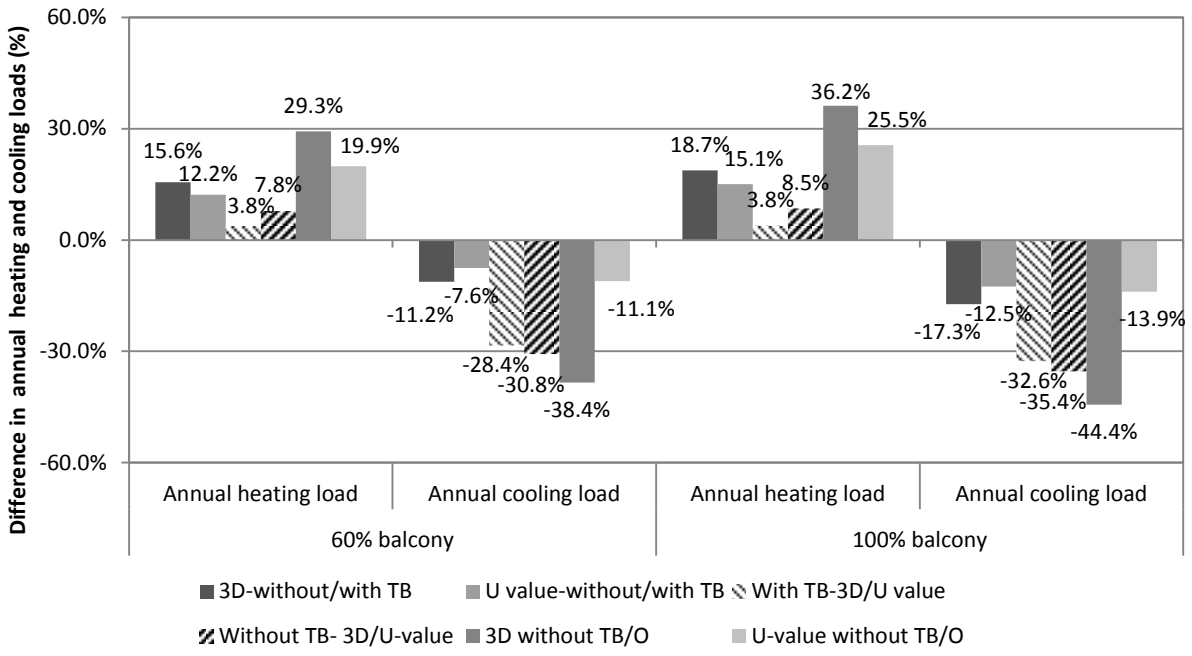

*TB-Thermal break, and O- no balcony thermal bridge included

Figure 4.11 Percentage difference in annual heating and loads between the two thermal bridge modeling methods for Vancouver (hypothetical generic balcony)

As shown in Tables 4.7-4.10, although the increase in annual space heating load due to the balcony slab (the case without thermal breaks compared with the case without thermal bridges) is higher for the colder climate (14.8 MWh in Edmonton v.s. 9.7 MWh in Vancouver), the percentage increase of the thermal bridge contribution is smaller for the colder climate (19.6% in Edmonton v.s. 24.3% in Vancouver) because of the higher spacing heating load in Edmonton. The implementation of thermal break in balcony results in 5.2-6.3% reduction in spacing heating while 5.0-10.8% increase in annual space cooling for these three cities for the building as designed. When well-insulated walls above and below the balcony is assumed, the implementation of thermal break in balcony results in 13.9-15.6% reduction in spacing heating with 60% balcony slab ratio and 16.6-18.7% with 100% balcony slab ratio, while 9.9-16.7% increase in the annual space cooling with 60% balcony slab ratio and 14.3-24.9% with 100% balcony slab ratio for the three cities. The presence of balcony as thermal bridges does help reduce the cooling loads ranging from 46.2% for Edmonton, 32.9% for Vancouver and 24.8% for Toronto. However, the annual cooling load represents a small portion of the annual space

heating load (2.8% for Edmonton, 10.1% for Vancouver and 11.8% for Toronto) given that all three cities are located in cold climate zones.

Typically the annual space heating load modelled by the 3D direct method is higher than that modeled using the equivalent U-value method, however, the difference is insignificant for the as-designed case, ranging from 2.1% to 3.6%. What interesting is that the milder the climate the higher the discrepancy, which is consistent with the observation of the percentage difference in the effect of thermal bridges. As for the cooling load, the modeling approach has a greater impact, ranging from 14.6% to 31.8%. The annual space cooling load modelled by the 3D dynamic method is lower than that using the equivalent U-value method and the colder the climate the greater the discrepancy. With the increase of balcony slab ratio to 100% perimeter, the difference between dynamic modeling and the equivalent U-value method for annual space heating increases to 3.7%-4.7%. With well-insulated walls above and below the balcony assumed, the effect of balcony slab as thermal bridge increases by 23.2-29.3% for 60% balcony slab ratio and 28.5-36.2% for100% balcony slab ratio, respectively, for annual space heating. The difference between dynamic modeling and the equivalent U-value method is 4.4-7.8% for 60% balcony slab ratio and 4.4-8.5% for 100% balcony slab ratio, respectively, for annual space heating. With the improvement of the balcony design, adding thermal breaks, the difference in energy performance as a result of the modeling approaches is reduced

4.3 CASE STUDY 3: HIGH RISE WOOD BUILDING

In the whole building energy simulations, the heating set point is 22 ^{o}C with a night setback temperature at 20^{o}C (22:00–06:00) and the cooling set point is 25^{o}C with a night setback temperature at 27 ^{o}C (22:00–06:00). Each floor is divided into five thermal zones. The effect of thermal bridges on the energy performance is evaluated by the annual heating and cooling loads.

4.3.1 Annual heating and cooling loads

Table 4.11 shows the annual heating and cooling loads for the building under three scenarios, namely direct 3D modeling; equivalent U-value method; and without thermal bridges for two types construction, i.e CLT and concrete construction. The comparison among these three scenarios with two construction types is shown in Figure 4.12.

Table 4.11 Annual heating and cooling loads of the high-rise building under different simulation scenarios.

	CLT construction		Concrete construction	
Implementation Methods	Annual heating load (kWh $\times 10^3$)	Annual cooling load (kWh $\times 10^3$)	Annual heating load (kWh $\times 10^3$)	Annual cooling load (kWh $\times 10^3$)
3D Modeling	28	28.1	31.7	25.4
Eq. U-value	27.1	31.4	29.3	29.36
Without TB	24.8	32.23	25.17	30.8

For the CLT construction, the implementation of balcony junctions through 3D dynamic modeling results in an increase of annual heating load by 11.4% and a reduction of annual cooling load by 14.7% compared to the case without thermal bridges. The annual heating load modeled using the 3D dynamic method is 3.2% higher than that modelled using the equivalent

U-value method, while the annual cooling load modeled is 11.4% lower than that modelled using the equivalent U-value method.

For the concrete construction, the implementation of junctions through 3D dynamic model results in an increase of the annual heating load by 20.6% and a reduction of the annual cooling load by 21.3% compared to the case without thermal bridges. The annual heating load modeled using the 3D dynamic method is 7.6% higher than that modelled using the equivalent U-value method, while the annual cooling load is 15.6% lower than that modelled using the equivalent U-value method.

These results show that the heavyweight construction represented by concrete construction has a greater impact on the annual energy consumption than the lightweight construction; and it increases the heat loss of the whole building. With increasing thermal mass using concrete construction, the dynamic effect of thermal bridges on the annual heating and cooling load increases. For that, the 3D dynamic analysis of thermal bridges is a necessary and critical in the whole building simulation, especially in the heavyweight construction.

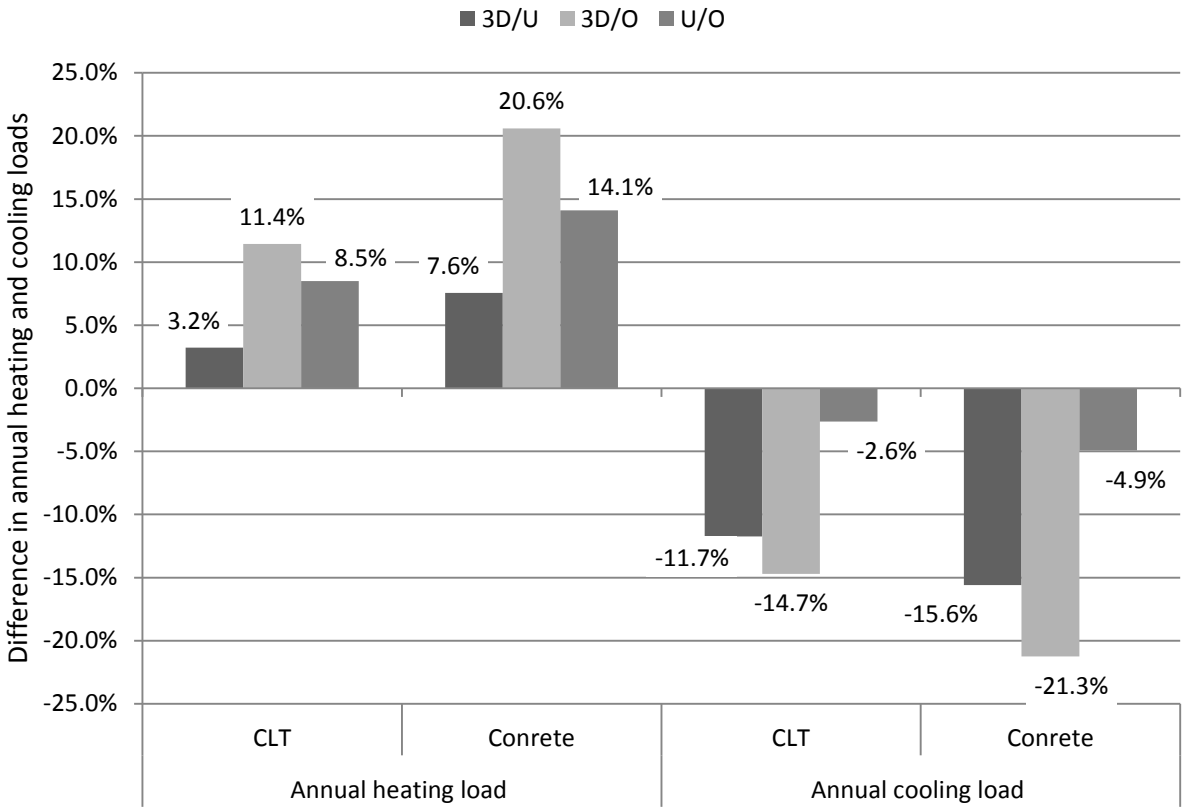

Figure 4.12 Percentage difference in annual heating loads among the three thermal bridge modeling methods for the cold climate.

5 CONCLUSION

The dynamic effect of thermal bridges on energy performance of buildings and surface temperature; and hence condensation risk in building envelope was studied through simulations. The analysis included implementing three thermal bridge modeling methods in whole building energy simulation, namely, 3D dynamic modeling, equivalent wall method (dynamic simulation), and equivalent U-Value method, using WUFI Plus program. These simulations are carried out for three case studies with different insulation levels, construction types and climate conditions.

5.1 CASE STUDY 1: A LOW RISE RESIDENTIAL BUILDING

In this case study, a low-rise residential building was selected to study the dynamic effect of four junction thermal bridges on the annual heating and cooling loads. Also, surface temperature and hence condensation risk in building envelope was studied. The three thermal bridge modeling methods in whole building energy simulation, namely, 3D dynamic modeling, equivalent wall method (dynamic simulation), and equivalent U-Value method, were used to investigate the dynamic effect under three cold climates for two insulation levels and a hot climate of zone for one insulation level.

For the two insulation levels under Quebec City climate, simulation results have shown that:

- The presence of thermal bridges increases the annual heating load by 18%. With the increase of insulation level, the thermal bridging effect increases.

- Compared to the dynamic 3D modeling method, the annual heating load is underestimated by 13% using the equivalent U-value method, and by 9% using the equivalent wall method, respectively.

- With the increase of insulation level, the dynamic effect of thermal bridges decreases. The difference between the U-value method and the dynamic 3D method is reduced to 8% for the annual heating load and to 4% for the annual cooling load, respectively.

- The dynamic effect of thermal bridges has relatively greater impact on the cooling load than that on the heating load. However, the annual cooling load is less than 2% of the annual heating load.

For the three cold climates with high insulation levels, simulation results have shown that:

- The presence of thermal bridges in the colder climate increase the annual space heating load more than that in the mildest climate (18 MWh in Quebec City v.s. 8 MWh in Vancouver). However, the percentage increase of the thermal bridge contribution is smaller for colder climate (19.8% in Quebec City v.s. 24.3% in Vancouver with high insulation level) because of the higher annual space heating load in Quebec City.
- The dynamic effect of thermal bridges increases with the drop of temperature in winter-season. The difference between the U-value method and the dynamic 3D method is reduced from 6 MWh in Quebec City to 4 MWh in Vancouver for the annual heating load of the case model. However, the percentage increase of the thermal bridge contribution is smaller for colder climate (8.1% in Quebec City v.s. 9.9% in Vancouver with high insulation level) because of the higher annual space heating load in Quebec City.

- Equivalent wall method performs better than the equivalent U-value method in three cold climates, especially in Vancouver climate.

For the hot climate, simulation results have shown that:

- The presence of thermal bridges increases the annual heating load by 30% and the annual cooling load by 20%. The annual heating load is only 5% of the annual cooling load.
- Compared to the dynamic 3D modeling method, the equivalent U-value method underestimates the annual cooling and heating loads by 17% and 8%, respectively; while the equivalent wall method underestimates the annual cooling and heating loads by 14% and 3%, respectively.

- Equivalent wall method performs better than the equivalent U-value method; however, both methods considerably underestimate the annual cooling loads in the hot climate.

5.2 CASE STUDY 2: A HIGH RISE RESIDENTIAL BUILDING

The dynamic effect of balcony slab as thermal bridges on the energy performance of a high-rise residential building is studied through simulations. Two modeling approaches, namely, 3D dynamic modeling and the equivalent U-Value method, are used in implementing thermal bridges into a whole building HAM modeling program WUFI Plus. The evaluation is carried out for three Canadian cities representing three cold climatic zones with two balcony slab ratios, i.e. 60% and 100% and two wall insulation levels, as designed and better-insulated. Simulation results show that:

- The presence of thermal bridges increase the annual heating load by 19.6-24.3% for the three cities studied for the building as designed. When the portion of thermal bridge increases, i.e. the slab balcony ratio is increased to 100% perimeter, the presence of thermal bridges increases the annual space heating load by 23.1-27.8%. With the improvement of the building envelope i.e. well-insulated walls above and below balcony slab, the effect of thermal bridges increases. The presence of thermal bridges increases the annual space heating load by 23.2-29.3% with 60% balcony slab ratio and 28.5-36.2% balcony slab ratio, respectively.
- Compared to the dynamic 3D modeling method, the annual heating load is underestimated by 2.1-3.6% using the equivalent U-value method depending on the climatic zones for the building as designed. The milder the climate, the greater the discrepancy between these two approaches. When the balcony slab ratio is increased to 100% perimeter, the difference is increased to 3.7-4.7%. When well-insulated walls above and below balcony slab assumed, the difference between these two methods increases to 4.4-7.8% with 60% balcony slab ratio and 4.4-8.5% with 100% balcony slab ratio.
- The implementation of the thermal break in the balcony slab reduces the annual heating load by 5.2-6.3% using the 3D dynamic method for the building as designed. The effectiveness increases when the building envelope is better insulated. With well-insulated walls above and below balcony, the implementation of thermal breaks reduces the annual heating load by 13.9-15.6% for 60% balcony slab ratio and 16.6-18.7% for 100% balcony slab ratio, respectively using the 3D dynamic method. The difference

between these two approaches is reduced to 1.0-3.8% with the inclusion of thermal break in the balcony slab.

- The presence of thermal bridges reduces the annual cooling load by 24.8-46.2%; consequently, the implementation of thermal break in the balcony slab increases the annual cooling load by 5.0-10.8% using the 3D dynamic method. Compared to the dynamic 3D modeling method, the equivalent U-value method overestimates the annual cooling load by 14.6-32.0%. With the addition of thermal break, the difference between these two approaches, i.e. the dynamic effect of thermal bridges is reduced. The dynamic effect of thermal bridges has relatively greater impact on the cooling load than that on the heating load. However, the annual cooling load is less than 2.9-11.8% of the annual heating load for the as designed case and 7.1 to 20.9% for the well-insulated case for the three Canadian cities.

In conclusion, the dynamic effect of balcony slab as thermal bridges is insignificant for the case study building due to the small percentage of balcony, 4.3% of the total exterior envelope, for the building as designed. For buildings with a higher portion of thermal bridges and better-insulated building envelopes, the impact of thermal bridges and the difference in energy performance as a result is greater. The difference between 3D dynamic modeling and the equivalent U-value is up to 8.5% for the case with better-insulated walls and 100% balcony slab ratio for annual space heating load. With the improvement of the balcony design, adding thermal breaks, the difference in energy performance as a result of the modeling approaches is reduced. It is interesting to observed that the dynamic effect is more significant (in term of percentage difference) for milder climates for heating load calculation and more significant for colder climates for cooling load calculation. Therefore, more effort should be placed on designing building envelopes with improved connection details to eliminate thermal bridges and it is equally important for all climates to eliminate thermal bridges.

5.3 CASE STUDY 3: A HIGH RISE WOOD BUILDING

A high-rise residential building that was constructed using CLT construction method was chosen to study the dynamic effect of heavyweight and lightweight constructions on annual

heating and cooling loads of buildings. The 3D dynamic modeling and equivalent U-Value method were used to investigate the dynamic effect under Vancouver climate.

The simulation results have shown that the presence of thermal bridges in heavyweight construction represented by concrete construction increases the annual heating load by 21%, while the same thermal bridges in lightweight construction increases the annual heating load by 11%. With the increase of thermal mass, the dynamic effect of thermal bridges increases. Compared to the dynamic 3D modeling method, the annual heating load using CLT construction is underestimated by 3% using the equivalent U-value method, while using concrete construction is underestimated by 8%.

The simulation results have shown that the presence of thermal bridges in heavyweight construction decreases the annual cooling load by 21%, while the same thermal bridges in lightweight construction decreases the annual cooling load by 15%. With the increase of thermal mass, the dynamic effect of thermal bridges increases. Compared to the dynamic 3D modeling method, the annual heating load using CLT construction is underestimated by 16% using the equivalent U-value method, while using concrete construction is underestimated by 12%. In addition, the dynamic effect of thermal bridges has a relatively greater impact on the cooling load than that on the heating load

5.4 CONTRIBUTIONS

The existence of thermal bridges in building envelopes affects the energy performance of buildings, their durability and occupants' thermal comfort. Typically the effect of thermal bridges on the energy performance is taken into account by implementing an equivalent U-value in 1D whole building energy simulation program. This treatment accounts for the effect of thermal bridges on the overall thermal transmittance, while their thermal inertia effect is ignored. The presence of thermal bridges not only reduces the overall thermal resistance but also changes the dynamic thermal characteristics of the envelope. Therefore, the equivalent U-value method accounting for thermal bridges in whole building energy modeling may lead to errors in predicting energy performance.

This research represents the first time a comprehensive study of the dynamic effect of thermal bridges on the energy performance of residential buildings in cold climate. It is also the first time study on comparing three thermal bridge modeling approaches. The three case study buildings chosen are representative of residential buildings with thermal mass. The parameters studied cover a broad range including typical thermal bridge junctions, level of insulations, climatic conditions, amount of thermal bridges, and light-weight and heavy weight constructions. Therefore, the findings obtained from these three case studies could be generalized for Canadian residential buildings. The simulation results indicate that the higher the thermal mass the greater difference between the dynamic modeling and equivalent U-value method as expected. However, this study enables us to answer the question on how much difference we may expect between the U-value method and the dynamic modeling. The equivalent U-value method can underestimate the annual space heating loads by up to 13% depending on the amount of thermal bridges for typical Canadian climates. With the decrease in the amount of thermal bridges and the improvement of thermal bridge junctions, the difference between equivalent U-value and 3D dynamic modeling decreases. The implementation of thermal break not only reduces the thermal bridging effect but also its thermal inertia effect. Therefore, it is important for architects and engineers to make efforts to improve the building envelope designs to minimize thermal bridges to avoid implementing the complex dynamic modeling in whole building energy simulations. This study also found that the thermal bridge effect is equally important for milder climates such as Vancouver. Generally, for light-weight construction, i.e. wood-frame, even heavy wood structure such as cross-laminated timber structure, the dynamic effect is not significant.

6 REFERENCE

Aguilar, F., Solano, J.P., &, P.G. (2014). Transient modeling of high-inertial thermal bridges in buildings using the equivalent thermal wall method. *Journal of Applied Thermal Engineering,* 67, 370–377.

Al-Sanea, S.A, & Zedan, M.F. (2012), Effect of thermal bridges on transmission loads and thermal resistance of building walls under dynamic conditions. *Journal of Applied Energy*. 98, 584–593

ANSI/ASHRAE/IES Standard 90.1. (2013). "Energy Standard for Buildings Except Low-Rise Residential Buildings". *ASHRAE*, USA.

Antretter, F., Radon, J., & Pazold, D.M. (2013). Coupling of Dynamic Thermal Bridge and Whole-Building Simulation, Conference Proceeding by ASHRAE.

Antretter, F., Sauer, F., Schöpfer, T., & Holm, A. (2011). Validation of a hygrothermal whole building simulation software. Proceedings of Building Simulation 2011: 12th *Conference of International Building Performance Simulation Association*, Sydney, Australia.

ASHRAE 1365 RP. (2011). Thermal Performance of Building Envelope Details for Mid- and High-Rise Buildings. Morrision Hershfield, ASHRAE,USA.

Bates, J.M., Rorek, D.A., & Ballantye, M.H. (1993). Dustmite counts and mite allergens in family homes beforeand after dry extraction carpet cleaning. Indoor Air '93,*Proceedings of the 6th International Conference on AirQualiO*, and Climate, Helsinki, Finland, 33-38

Brown, W.P., & Wilson, A.G. (1963). Thermal Bridges in Buildings. Canadian Building Digests, CBD-44, *National Research Council of Canada, Division of Building Research*, Ottawa

Building Envelope Thermal Bridging Guide: analysis, application and insights. (2014). A technical report by *BC Hydro Power Smart*.

CAN/SA A440.2-09, Fenestration energy performance, Canadian Standard Association, 2009.

Cappellettia, F., Gasparella, A., Romagnoni, P., & , P. (2011). Analysis of the influence of installation thermal bridges on windows performance: The case of clay block walls. *Journal of Energy and Buildings*, 43(6), 1435–1442

Ceylan, H. T., & Myers, G. E. (1980). Long-time Solutions to Heat Conduction Transients with Time-Dependent Inputs. *ASME Journal of Heat Transfer*, 102(1), 115-120.

Corvacho, M. H. (1996). "Pontes térmicas, análise do fenómeno e proposta de soluções", unpublished Ph.D thesis, *Faculdade de Engenharia da Universidade do Porto*, Portugal

Déqué, F., Ollivier, F., & Roux, J.J. (2001). Effect of 2D modelling of thermal bridges on the energy performance of buildings: Numerical application on the Matisse apartment. *Journal of Energy and Buildings*, 33(6), 583–587.

DesignBuilder Software. DesignBuilder 2.1user's manual. 2009. Retrieved from http://www.designbuildersoftware.com/docs/designbuilder/DesignBuilder_2.1_Users-Manual_Ltr.pdf.

EN 673: Glass in building – Determination of thermal transmittance (U value) – Calculation method, CEN, 1997

EN ISO 10077: Thermal performance of windows, doors and shutters – Calculation of thermal transmittance – Part 2: Numerical method for frames (ISO 10077:2012), CEN, 2012

EN ISO 10211: Thermal bridges in building construction – Heat flows and surface temperatures – detailed calculations (ISO 10211:2007), CEN, 2007

EN ISO 10456: Building materials and products - Hygrothermal properties -Tabulated design values and procedures for determining declared and design thermal values (ISO 10456:2007), CEN, 2007

EN ISO 13783: Thermal Performance of Building Components. Dynamic Thermal Characteristics. Calculation Methods, 2007, CEN, 2007

EN ISO 14683. (2007). “Thermal Bridges in Building Construction – Linear Thermal Transmittance Simplified Methods and Default Values”. *ISO International Organization for Standardization.* ICS**:** 91.120.10.

EN ISO 6946: Building components and building elements – Thermal resistance and thermal transmittance – Calculation method (ISO 6946:2007), CEN, 2007

Energy Code of Canada for Buildings NECB. (2011). *National Research Council*, Canada, 2011.

Energy efficiency trends in Canada 1990-2008. (2008). *Natural Recourses Canada NRCan*, Canada.

EnergyPlus. (2003). EnergyPlus articles from the building energy simulation user news. Lawrence Berkeley National Laboratory. Berkeley, California.

EnergyPlus. (2013). EnergyPlus engineering reference: The reference to EnergyPlus calculations. Building Simulation Group. Lawrence Berkeley National Laboratory. Berkeley, California.

Erhorn, H., Erhorn-Kluttig, H., Citterio, M., Cocco, M., Orshoven, D.V., Tilmans, A., & et al. (2010). An effective handling of thermal bridges in the EPBD context, *Final Report of the IEE ASIEPI Work on Thermal Bridges*, 69 pp.

Fraunhofer Institut Bauphysik IBP. (2012). WUFI Plus manual handbook. Retrieved from http://www.wufi-wiki.com/mediawiki/index.php5/Hauptseite

Fraunhofer IBP. 2013. WUFI®Plus, Ver. 2.5.3. Fraunhofer Institute for Building Physics,Valley, Germany.

Gagnon, S., & Pirvu, C. (2011). CLT handbook Canadian Edition. FPInnovations Special Publication SP-528E, Quebec.

Gao, Y., Roux, J.J., Zhao, L.H., & Jiang, Y. (2008). Dynamical building simulation: a low order model for thermal bridges losses. *Journal of Energy and Buildings*, 40(12), 2236-2243.

Ge, H., McClung, V.R., & Zhang, S. (2013). Impact of balcony thermal bridges on the overall thermal performance of multi-unit residential buildings: A case study. *Journal of Energy and Buildings*, 60, 163–173

Gomes, A., Souza, H., &Tribess, A. (2013). Impact of thermal bridging on the performance of buildings using Light Steel Framing in Brazil. *Journal of Applied Thermal Engineering*, 52. 84–89

Gorgolewski, M. (2007). Developing a simplified method of calculating U-values in light steel framing. *Journal of Building and Environment*, 42, 230–236.

Government of Canada, Canadian Climate Normals 1971-2000 Station Data http://climate.weather.gc.ca/climate_normals (retrieved 2014)

Hendricks, D.M. (1985). College of Agriculture, University of Arizona, Technology & Engineering.

Kosny, J., & Desjarlais, A.O. (1994). Influence of architectural details on the overall thermal performance of residential walls systems. *Journal of Thermal Insulation and Building Envelopes,* 18 (1), 53–69.

Kossecka, E., & Kosny, J. (1996). Relations between structural and dynamic thermal characteristics of building walls. Proceedings of 1996 International Symposium of CIB W67 *"Energy and Mass flow in the Life cycle of Buildings"*, Vienna, 4-10 August 1996, 627-632.

Kossecka, E., & Kosny, J. (1997). Equivalent wall as a dynamic model of a complex thermal structure. *Journal of Thermal Insulation and Building Envelopes,* 20, 249-268.

Kossecka, E., & Kosny, J. (2001). Conduction Z-transfer function coefficients for common composite wall assemblies. *Journal of Thermal Performance of the Exterior Envelopes of Buildings* VIII.

Kossecka, E., & Kosny, J. (2002). Influence of insulation configuration on heating and cooling loads in a continuously used building. *Journal of Energy and Buildings,* 34, 321-331.

Kossecka, E., (1998). Relationships between structure factors, response factors and z-transfer function coefficients for multi-layer walls. *ASHRAE Transactions,* 104(1A), 68-77.

Künzel, H.M. 1994. Verfahren zurein-und zweidimensionalen Berechnung des gekoppelten Wärme- und Feuchtetransports in Bauteilen mit einfachen Kennwerten. University Stuttgart.

Lahmidi, H., & Leguillon, F. (2010). Study for the ASIEPI project: Thermal bridges influence on the primary energy consumption. *Summary report of ASIEPI WP4*

Lawrence Berkeley National Laboratory. (2013) . THERM 6.3/ WINDOW 6.3 NFRC Simulation Manual. Retrieved from http://windows.lbl.gov/software/therm/7/index.html

Mahattanatawe, P., Puvanant, C., & Wat, D.M.(2006). The energy performance of the cold-formed steel-frame and wood-frame houses developed for Thailand. *Journal of SimBuild*, 183-190.

Mao, G., & Johannesson , G. Dynamic calculation of thermal bridges. (1997). *Energy Build,* 26, 233–40.

Martin, K., Erkoreka, A., Flores, I., Odriozola, M., & Sala, J.M. (2011). Problems in the calculation of thermal bridges in dynamic conditions. *Journal of Energy and Buildings*, 43, 529-535.

Martin, K., Escudero, C., Erkoreka, A., Flores, I., & Sala, J.M. (2011). Equivalent wall method for dynamic characterisation of thermal bridges. *Journal of Energy and Building*, 55, 704-714.

Ouyang, K., & Haghighat, F. (1991). A Procedure for Calculating Thermal Response Factors of Multi-layered Walls-State Space Method. *Journal of Building and Environment*, 26 (2), 173-177.

Purdy, J., & Beausoleil-Morrison, I. (2001). The significant factors in modelling residential buildings, in: Building SIMULATION, Rio de Janeiro. Anais, *International Building Performance Simulation Association,* 207-214.

Sedlbauer, K., Krus, M., Zillig, W., & Kunzel, H. 2007. Mold Growth Prediction by Computational Simulation. *ASHRAE Conference IAQ 2001* (pp. 185-189). San Francisco: Fraunhofer-Institute for Building Physics

Seem, J.E. 1987. Modeling of Heat Transfer in Buildings, Ph.D. Thesis, University of Wisconsin, Madison, WI.

Straube, J. (2006). Ice Dams. *Journal of Building Science*. Retrieved from http://www.buildingscience.com/documents/digests/bsd-135-ice-dams/?searchterm=ice%20dam

Šubrt, R. (2007). Influence of thermal bridge details on the energy performance of houses with different energy quality. *Czech Republic*.

Theodosiou, T.G., & Papadopoulous, A.M. (2008). The impact of thermal bridges on the energy demand of buildings with double brick wall constructions, *Energy and Buildings* 40 2083-2089.